C. R. Library 4

CENTRAL RESEARCH LIBRARY
DOCUMENT COLLECTION

MARTIN MARIETTA ENERGY SYSTEMS LIBRARIES
3 4456 0350546 4

ORNL-2402
Metallurgy and Ceramics

HIGH-TEMPERATURE MECHANICAL PROPERTIES OF HASTELLOY B AND HASTELLOY W

C. R. Kennedy
D. A. Douglas

OAK RIDGE NATIONAL LABORATORY
operated by
UNION CARBIDE CORPORATION
for the
U.S. ATOMIC ENERGY COMMISSION

CENTRAL RESEARCH LIBRARY
DOCUMENT COLLECTION
LIBRARY LOAN COPY
DO NOT TRANSFER TO ANOTHER PERSON
If you wish someone else to see this document, send in name with document and the library will arrange a loan.

Printed in USA. Price 2.25 cents. Available from the

Office of Technical Services
U. S. Department of Commerce
Washington 25, D. C.

LEGAL NOTICE

This report was prepared as an account of Government sponsored work. Neither the United States, nor the Commission, nor any person acting on behalf of the Commission:

A. Makes any warranty or representation, express or implied, with respect to the accuracy, completeness, or usefulness of the information contained in this report, or that the use of any information, apparatus, method, or process disclosed in this report may not infringe privately owned rights; or

B. Assumes any liabilities with respect to the use of, or for damages resulting from the use of any information, apparatus, method, or process disclosed in this report.

As used in the above, "person acting on behalf of the Commission" includes any employee or contractor of the Commission to the extent that such employee or contractor prepares, handles or distributes, or provides access to, any information pursuant to his employment or contract with the Commission.

ORNL-2402

Contract No. W-7405-eng-26

METALLURGY DIVISION

HIGH-TEMPERATURE MECHANICAL PROPERTIES OF HASTELLOY B AND HASTELLOY W

C. R. Kennedy
D. A. Douglas

DATE ISSUED

NOV 13 1958

OAK RIDGE NATIONAL LABORATORY
Oak Ridge, Tennessee
operated by
UNION CARBIDE CORPORATION
for the
U.S. ATOMIC ENERGY COMMISSION

MARTIN MARIETTA ENERGY SYSTEMS LIBRARIES

3 4456 0350546 4

HIGH-TEMPERATURE MECHANICAL PROPERTIES OF HASTELLOY B AND HASTELLOY W

C. R. Kennedy and D. A. Douglas

INTRODUCTION

Nickel-base compositions alloyed primarily with molybdenum have demonstrated high resistance to corrosion in fused salts. Since such alloys also afford excellent high-temperature strength, they show much promise as structural materials for a circulating-fuel reactor. These alloys also are relatively free from objectionable high cross section elements.

The major factors to be considered in an evaluation of the strength properties of metals for service in circulating-fuel reactors are the high-operating temperatures and corrosive environments encountered in the core and heat exchangers of this high-power-density system. While stress-rupture, creep, and tensile properties are normally the criteria for investigating materials in the temperature range of interest, tests to furnish such information are conventionally accomplished in air. It has, therefore, been necessary to further evaluate these alloys in the environment to which the structural material will be subjected.

Other factors which limit the use of materials are the temperature and load fluctuations causing thermal strains to be introduced into the structure. Unless the material exhibits sufficient ductility so that these thermal strains are absorbed, the structure will fail. Therefore, no evaluation program is complete without obtaining a measure of the alloy's ductility.

PROCEDURE

The two alloys under consideration are commercial air melts of Hastelloy B and W, obtained from the Haynes Stellite Company in the form of 0.060-in. sheet. The compositions furnished by the vendor are given in Table I. The creep specimens were machined according to specifications.[1] After machining, the

---

[1] D. A. Douglas and W. D. Manly, A Laboratory for the High-Temperature Creep Testing of Metals and Alloys in Controlled Environments, ORNL-2053 (September 1956).

TABLE I

COMPOSITION OF HASTELLOY B AND W FURNISHED BY HAYNES STELLITE COMPANY

Alloy	Heat No.	Composition Wt % - Balance Nickel									
		Cr	P	Fe	C	Mn	V	Mo	S	Si	Co
Hast. B	B-1364	0.30	0.003	4.85	0.05	0.87	0.32	27.5	--	0.65	0.34
Hast. W	W-1011	4.71	0.008	5.25	0.03	0.39	0.27	24.30	0.020	0.20	0.82

specimens were solution-annealed in hydrogen at 2100°F for 2 hr; this was the condition in which the majority of the specimens were tested. However, in order to determine the effects of prior aging on the creep properties of Hastelloy B, aging heat treatments of 100 hr at 1300°F and 40 to 70 hr at 1500°F were given certain specimens before testing.

The creep-rupture equipment used for testing in gaseous and liquid environments are described also by Douglas and Manly.[2] The creep-rupture properties of the two alloys in the solution-annealed condition were determined in argon for design purposes and as a basis for comparing the effects of environment. The creep tests were performed in the temperature range of 1300 to 1800°F. Since the compositions and stress-rupture properties of the two alloys are very similar, the majority of the testing to determine the effects of environment was carried out with Hastelloy B. The environments under consideration were argon, sodium, air, hydrogen, Fused Salt No. 30*, and Fused Salt No. 107**.

Metallographic examination was made on all the creep specimens and photomicrographs of representative structures are presented in this report.

---

[2] Ibid.

* ($NaF-ZrF_4-UF_4$, 50-46-4 mole %)

** ($NaF-KF-LiF-UF_4$, 11.2-41-45.3-2.5 mole %)

Hardness versus aging time plots were obtained at the four test temperatures by taking the hardness of the shoulders of the specimens after test. Ductility versus aging time plots were obtained at the four test temperatures by cutting the shoulders of creep specimens into bend specimens and testing at room temperature.

Short-time high-temperature tensile properties of solution-annealed Hastelloy B and W alloys are shown in Figs. 1 and 2 which give the 0.2% offset yield strength, ultimate strength, and final elongation from 1000 to 1800°F.

RESULTS AND DISCUSSION

Creep Data. Creep curves obtained from tests in argon of solution-annealed Hastelloy B and W alloys are given in Figs. 3 through 11. Plots of these data in the form of design curves are presented in Figs. 12 through 20. These graphs are produced by cross-plotting the creep curves on log-stress and log-time coordinates. Stress versus minimum creep rate is logarithmically plotted in Fig. 21 for Hastelloy B at 1500, 1650, and 1800°F. High-stress creep tests of Hastelloy B at 1300°F always ruptured in the first stage of creep; therefore, no minimum creep-rate curve is possible for this temperature. Stress versus creep rate is logarithmically plotted in Fig. 22 for Hastelloy W at 1300, 1400, 1500, 1650, and 1800°F. Since the Hastelloy W strain-rate curves only represent 3 to 4 high-stress test points, the shape of the curves are not well defined.

The temperature dependency of the creep properties is shown in Figs. 23 through 28 where stress to the 1/3 power is plotted versus $\frac{1}{T}$°K. The stress plotted is the one that will produce a designated strain or rupture in a set time at that temperature. Figures 23 and 26, Figs. 24 and 27, Figs. 25 and 28 are 100, 1000, and 2000-hr plots for the two alloys. This type of plot can be used to compare alloys showing the differences in operating temperatures for a given set of design conditions. In Fig. 29 four alloys, Inconel, 316 stainless steel, Hastelloy B, and Hastelloy W, are compared for the design conditions of 1% strain in 1000 hr. Thus it can be seen that Hastelloy B has an approximate 300°F temperature advantage over Inconel.

MICROSTRUCTURES

Hastelloy B. Metallographic examination of creep-test specimens show aging or transformation reactions occurring at all test temperatures. However, the appearance of the precipitating phases varies with temperature. As can be seen in the photomicrographs, Figs. 30 through 32, specimens tested at 1300°F have a considerable quantity of second phase in a Wiedmenstatten pattern. The phase diagram of the nickel-molybdenum binary system, as shown in Fig. 33, indicates that this phase is probably beta. The results of creep tests at this temperature indicate that this precipitation causes a severe loss of ductility. Although the aging reactions for this alloy system are extremely sluggish, strain accelerates the reaction to such an extent that even the short-time, high-strain-rate, stress-rupture tests have only 8% total strain at rupture.

As shown in Figs. 34 to 36, the phase which transforms at 1500°F has an altogether different appearance than the phase present at 1300°F. The appearance of the second phase formed at 1500°F has a marked similarity to the phase identified by E. E. Stansbury, in his work on the nickel-molybdenum phase diagram, as gamma.[3] This phase does not have as severe an effect on the ductility as did the beta phase at 1300°F.

At 1650 and 1800°F the precipitates that form, as shown in Figs. 37 to 42, have not been satisfactorily identified. Some of them are probably carbides; however, the relatively low carbon content precludes all of the precipitate from being of this type. The phase diagram of the binary nickel-molybdenum system would indicate that the alloy should be in the solid solution condition at this temperature but the presence of iron and other residual elements in the metal could easily lead to complex phases stable in this temperature range.

Hastelloy W. In comparison to Hastelloy B, Hastelloy W has 3% less molybdenum and an additional 5% chromium. Shown in Figs. 43 through 45 are

---

[3] D. W. Stoffel and E. E. Stansbury, A Metallographic and X-Ray Study of Nickel Alloys of 20–30 Per Cent Molybdenum, AECU-3105 (December 1955).

photomicrographs of Hastelloy W specimens after creep testing at 1300°F. It is seen that the microstructure closely resembles that of Hastelloy B at the same temperature; however, the relative amount of second phase is much less. Although the modification in alloy content has suppressed the phase transformation, creep-test results show only a very slight increase in elongation at failure. It is again apparent that strain greatly accelerates this transformation.

The transformation or aging reactions that occur at 1400°F, as shown in Figs. 46 and 47, appear quite different from those that occur at 1300°F. There is a notable absence of any phase that can be identified with the Ni-Mo binary diagram. The small particles dispersed through the matrix are quite similar to those found in Hastelloy B at 1650 and 1800°F. Thus it appears that the composition change in Hastelloy W has caused a suppression of the gamma transformation. The creep ductility at this temperature is not affected by these particles and the creep curves have a logarithmic rate indicative of a solid-solution alloy.

There is no pronounced change in the microstructure of Hastelloy W from 1400 to 1800°F, as is shown in Figs. 48 to 52, and the creep ductility at these temperatures does not appear to be greatly affected by the dispersed particles.

EFFECT OF AGING

The aging or transformation reactions of the nickel-base molybdenum alloys are extremely sluggish and complex. The sluggishness of the reactions for Hastelloy B and W alloys is shown in Figs. 53 and 54 as hardness versus aging time at temperatures of 1300, 1500, 1650, and 1800°F. It is also evident that these alloys fail to soften on continued heat treatment at 1300 and 1500°F. The ductility of these alloys, determined by bend testing at room temperature after heat treatment, correlates with the hardness curves. Figures 55 and 56 are plots of bend angle versus aging time at 1300, 1500, 1650, and 1800°F. It is interesting to note that for both alloys there is an immediate loss of ductility at 1650 and 1800°F which is gradually recovered; whereas, at 1300 and 1500°F the loss is more gradual with time and is not recovered. This loss of room-temperature bend ductility caused by the 1650

and 1800°F treatments does not seem to be connected with the beta or gamma phases but rather to the unidentified complex secondary phases that are present. It is also interesting to note that Hastelloy B shows an increase in ductility with time at 1800°F, indicating the second phase may be over-aging. The curves for Hastelloy W at 1300°F, where beta is the second phase, and at 1500°F, where some other phases are stable, overlap, also indicating that these unknown phases may be the dominating factor in room-temperature ductility. However, as stated previously, only the beta transformation has a great effect on the creep ductility and the minor phases show little effect.

The effect of prior aging at 1300°F for 100 hr on the creep properties of Hastelloy B were investigated by creep-rupture testing of aged specimens at 1300, 1500, 1650, and 1800°F at stresses that would produce rupture lives of 100 and 1000 hr for solution-annealed material. Creep curves comparing tests of solution-annealed Hastelloy B to those of aged specimens are shown in Figs. 57, 58, 59, and 60. Specimens given additional aging heat treatments of 40 and 70 hr at 1500°F were tested at 1500°F with a stress of 12,000 psi, producing the creep curves shown in Fig. 58. In general, at all test temperatures, aged specimens have shown a decrease in creep rate and total elongation compared to specimens tested in the solution-annealed condition.

Material aged at 1300°F and then tested at 1300 and 1500°F showed improved creep properties and longer rupture lives as compared to the annealed material. This fact tends to add proof that Hastelloy B has not overaged at these two temperatures and the internal strains produced by the aging reactions have not been relieved. It is apparent that aging is accelerated in tests at 1300°F of solution-annealed material by the small difference in total elongation in tests of annealed and aged specimens. However, 1500°F tests of aged material show that any prior aging that decreases the creep rate will cause the total elongation at rupture also to decrease drastically.

One might predict that there would be little effect of prior aging at 1300°F upon the creep-rupture properties at 1650°F, or higher, because the solution of the beta and gamma phases would allow the internal strains produced by the aging reaction to be relieved. However, the creep curves shown in Figs. 59 and 60 indicate that the prior aging treatment does have a

significant effect upon the creep rate and rupture life of the material. The initial creep rate for the aged material is much lower than that of the solution-annealed material; however, third stage or an accelerated creep rate is initiated much earlier for aged specimens and the result is a shorter rupture life. From the above behavior, it would be considered inadvisable to use this material structurally where the operating temperature would vary from 1300 to 1650°F.

EFFECT OF ENVIRONMENT

Hastelloy B. The effects of various environments upon the creep properties of Hastelloy B sheet were investigated at temperatures from 1300 to 1800°F. Shown in Figs. 61, 62, 63, and 64 are stress-rupture plots of tests run in environments of argon, air, H_2, Na, Fused Salt No. 30, and Fused Salt No. 107. Only those environments which alter the surface of the material appear to affect the creep properties of Hastelloy B. It can be seen from the above figures that only air (Fig. 62) and Fused Salt No. 30 (Figs. 61 to 64) affect the creep properties of the alloy. Air, of course, produces an adherent oxide film under isothermal conditions, and Fused Salt No. 30 can be considered to have created a very thin surface film by a chemical alteration of the surface, as shown in Fig. 65. A comparison of creep curves of tests in argon to those in air or Fused Salt No. 30, shown in Figs. 66 and 67, show that these two environments decrease the creep rate and increase the rupture life.

Hastelloy W. Results described above shown that the Fused Salts Nos. 30 and 107 were either inert or strengthening to nickel-molybdenum alloys with no chromium present. However, Hastelloy W contains approximately 5% chromium which is an element found to be easily leached by the Fused Salts. Shown in Figs. 68, 69, 70, and 71 are stress-rupture plots of Hastelloy W tested from 1300 to 1800°F in argon. Also in the above figures are points obtained from tests in both the Fused Salts. The results strongly indicate that the effect of the 5% chromium is negligible and that Hastelloy W reacts to the environments identically to that of Hastelloy B. The Fused Salt No. 30 again produced a chemical alteration of the surface, as shown in Fig. 72, and strengthened this alloy to approximately the same degree as Hastelloy B.

However, since the environmental effects in both alloys appear to be dependent upon surface reactions, the degree of strengthening will depend on the surface-area-to-volume ratio. Thus, this data must be applied rather judiciously to design problems in recognition of the important role of geometry and section size.

CONCLUSIONS

These two alloys were tested to determine their adaptability for use as structural materials in a circulating-fuel reactor. They were found to have excellent corrosion resistance to the Fused Salts and good high-temperature strength; however, phase transformations occurring within the operating-temperature range of the reactor and causing severe losses of ductility restricts their use. Although the embrittling behavior of these two alloys rendered them unsafe for reactor construction, their other excellent properties do illustrate the advantages of the nickel-molybdenum alloy system. The following general conclusions can be drawn from this test program:

1. Both alloys possess reasonably good high-temperature strength properties.
2. Hastelloy B and W exhibit a severe loss of hot ductility at temperatures where the beta transformation occurs.
3. The change in composition found in Hastelloy W results in a suppression of the beta and gamma transformation.
4. Room-temperature tests indicate that both alloys fail to soften after 4000 hr at 1300 and 1500°F.
5. Room-temperature ductility is apparently affected by the formation of unidentified phases of molybdenum and minor alloying constituents such as iron.
6. Hastelloy B and W are very resistant to corrosion by both Fused Salts Nos. 30 and 107.
7. Air and Fused Salt No. 30 are two environments which strengthen Hastelloy B and W by surface alteration when there is a large surface-to-volume of metal ratio.

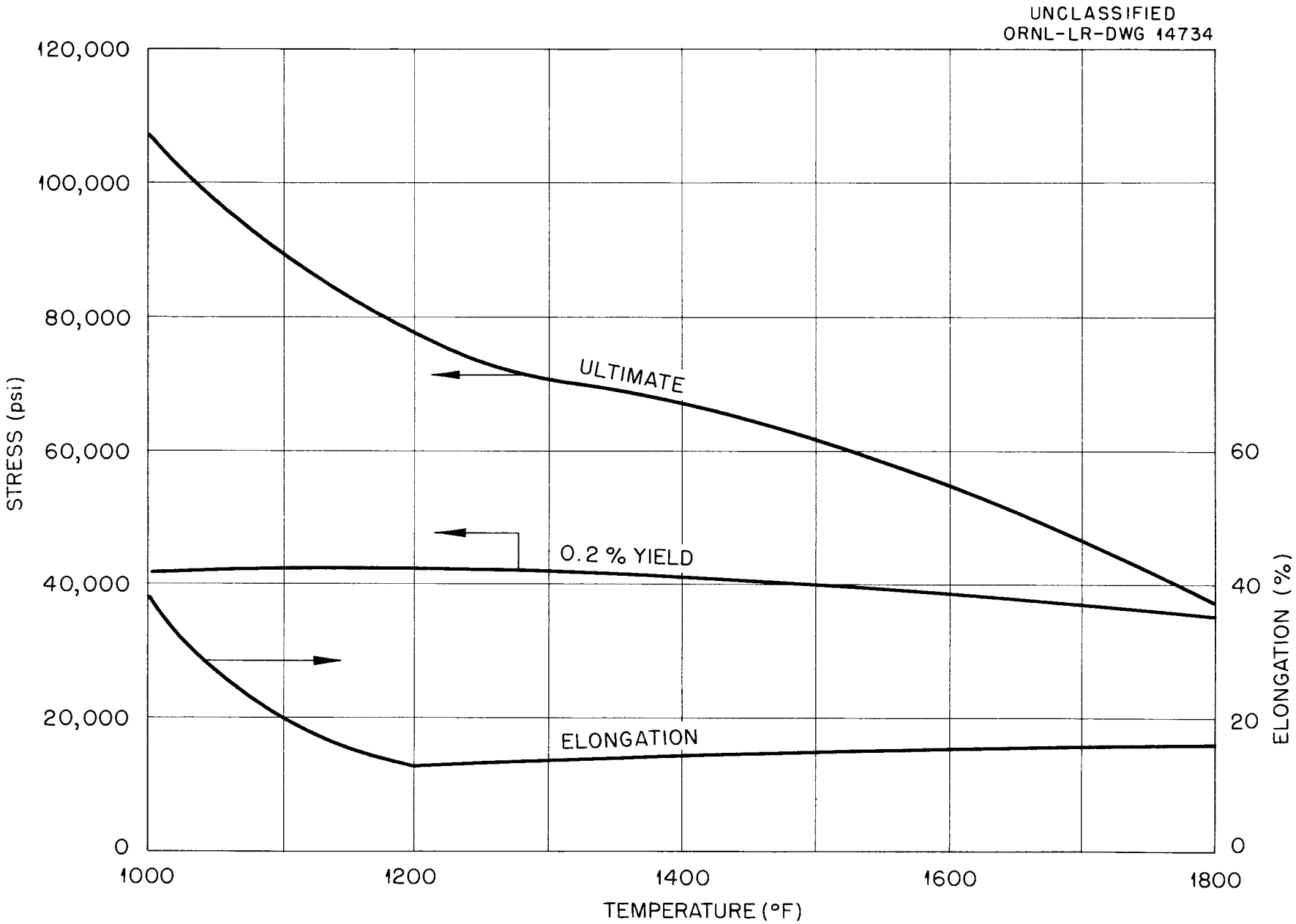

Fig. 1. Short-Time High-Temperature Tensile Properties of Solution-Annealed Hastelloy B.

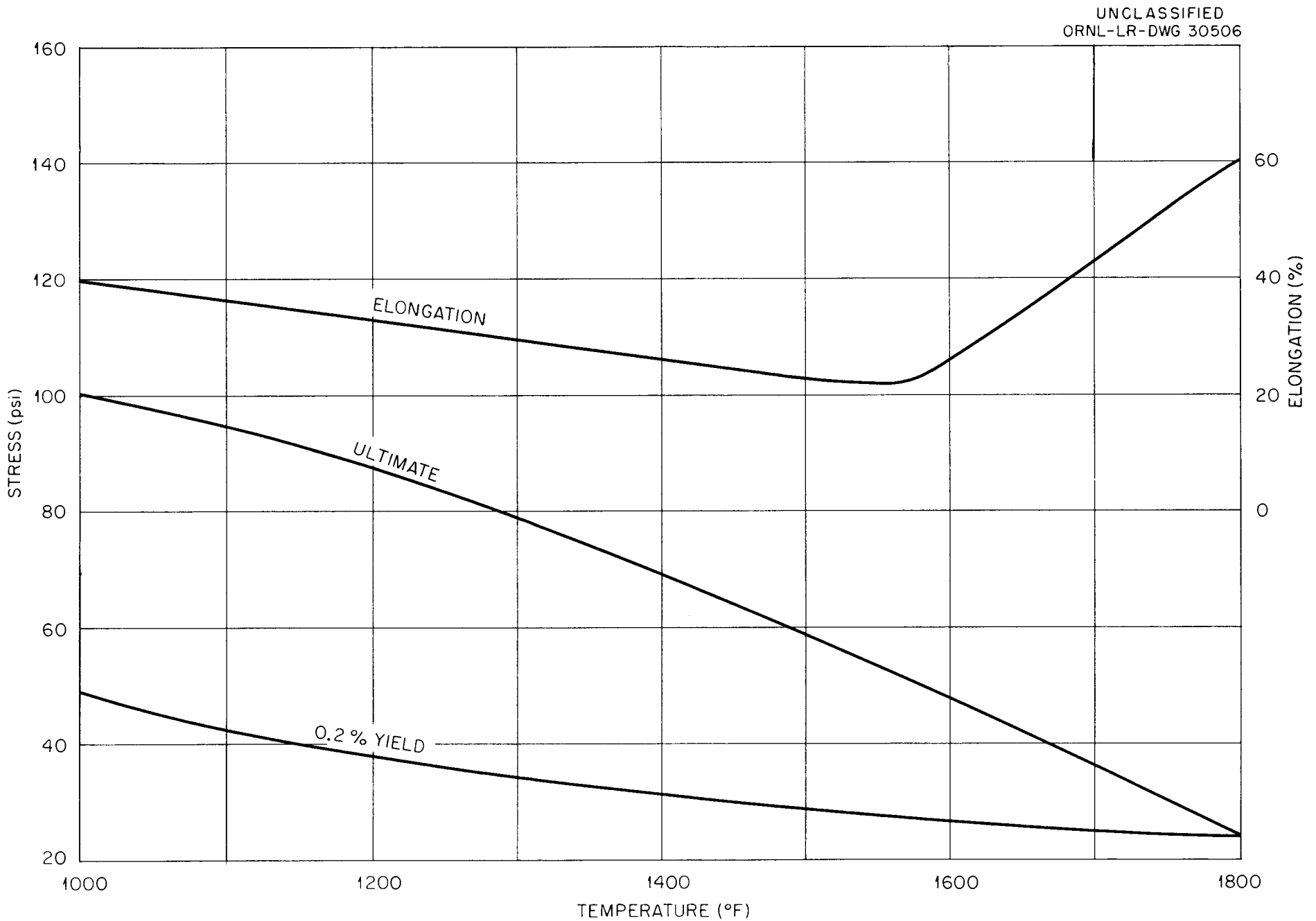

Fig. 2. Short-Time High-Temperature Tensile Properties of Solution-Annealed Hastelloy W.

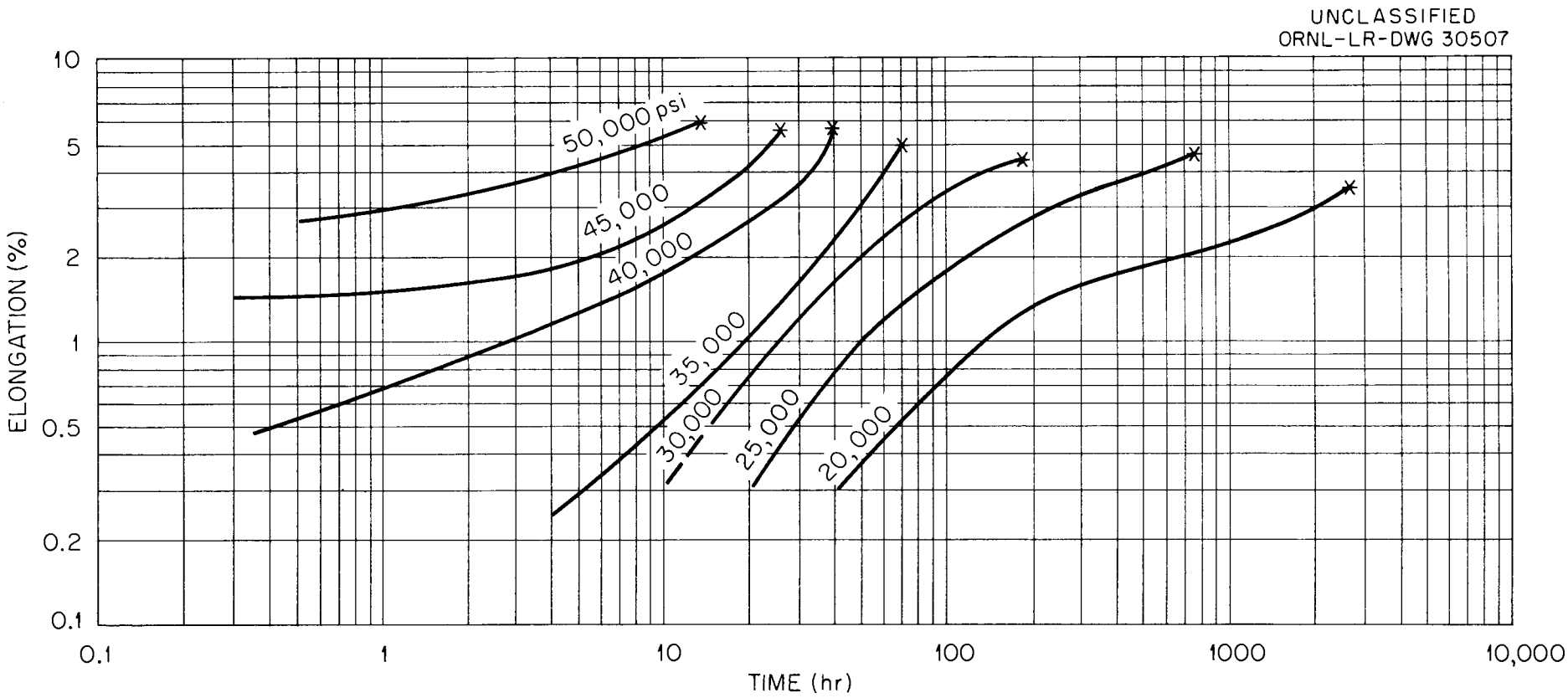

Fig. 3. Creep Curves of Solution-Annealed Hastelloy B Sheet Tested in Argon at 1300°F.

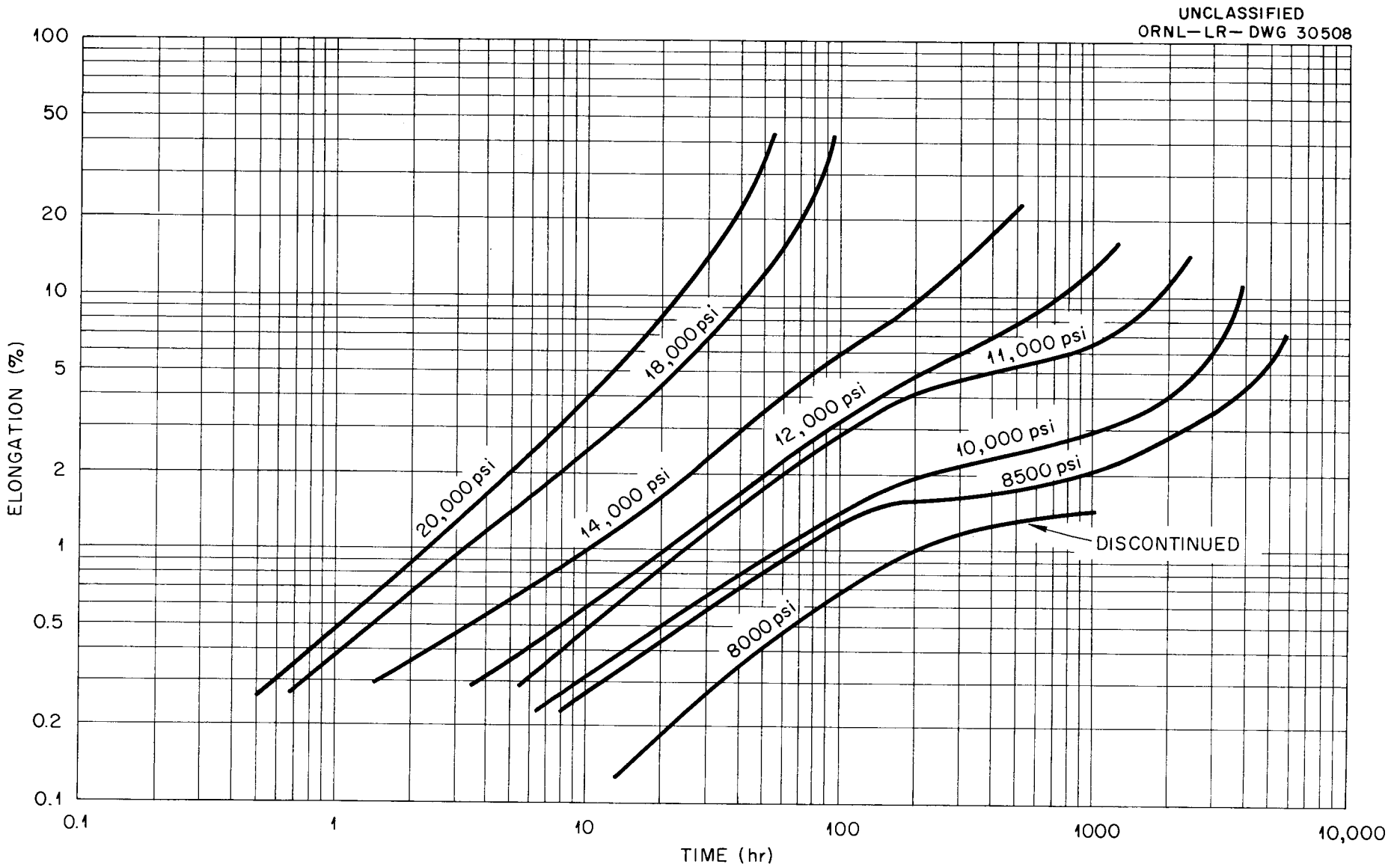

Fig. 4. Creep Curves of Solution-Annealed Hastelloy B Sheet Tested in Argon at 1500°F.

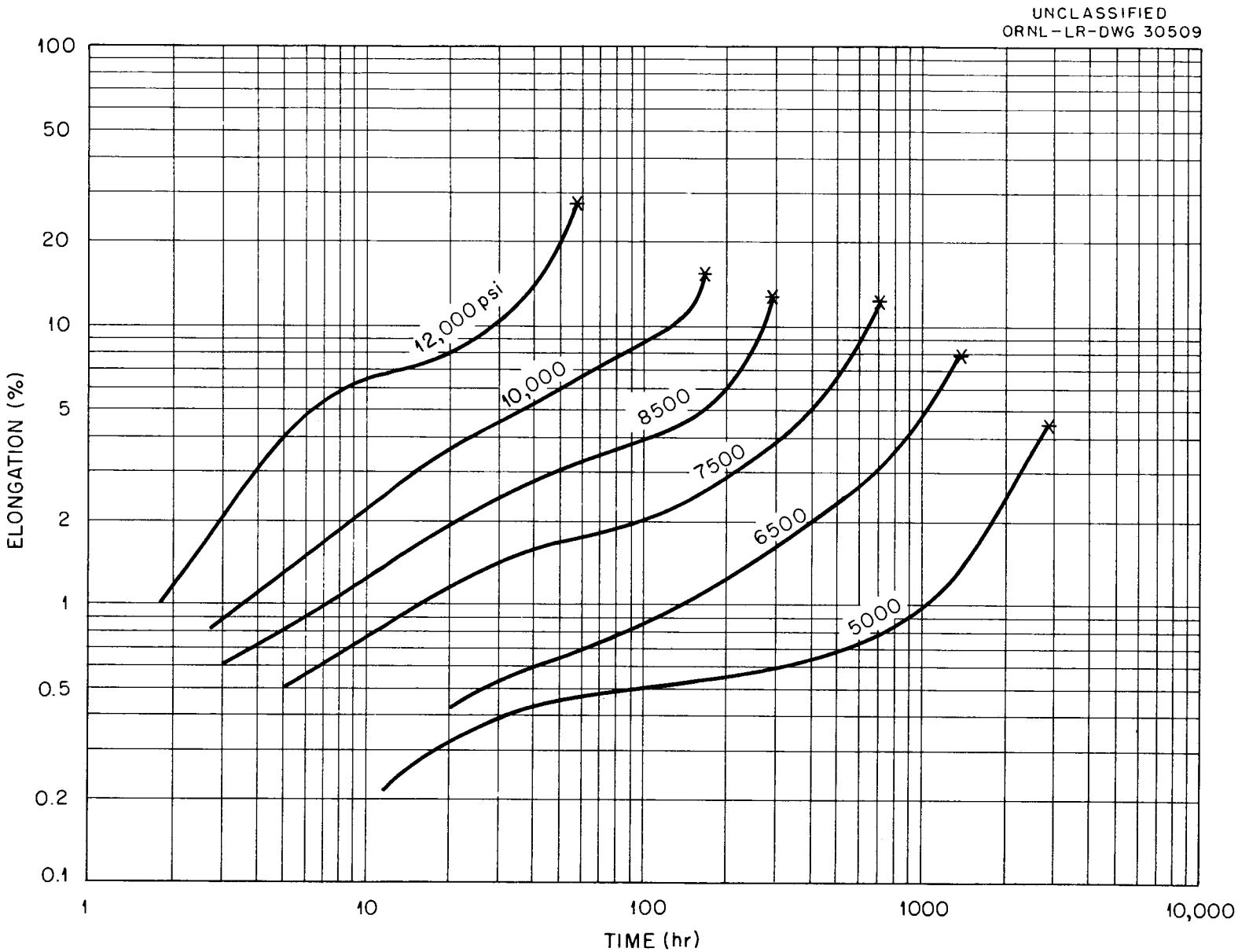

Fig. 5. Creep Curves of Solution-Annealed Hastelloy B Tested in Argon at 1650°F.

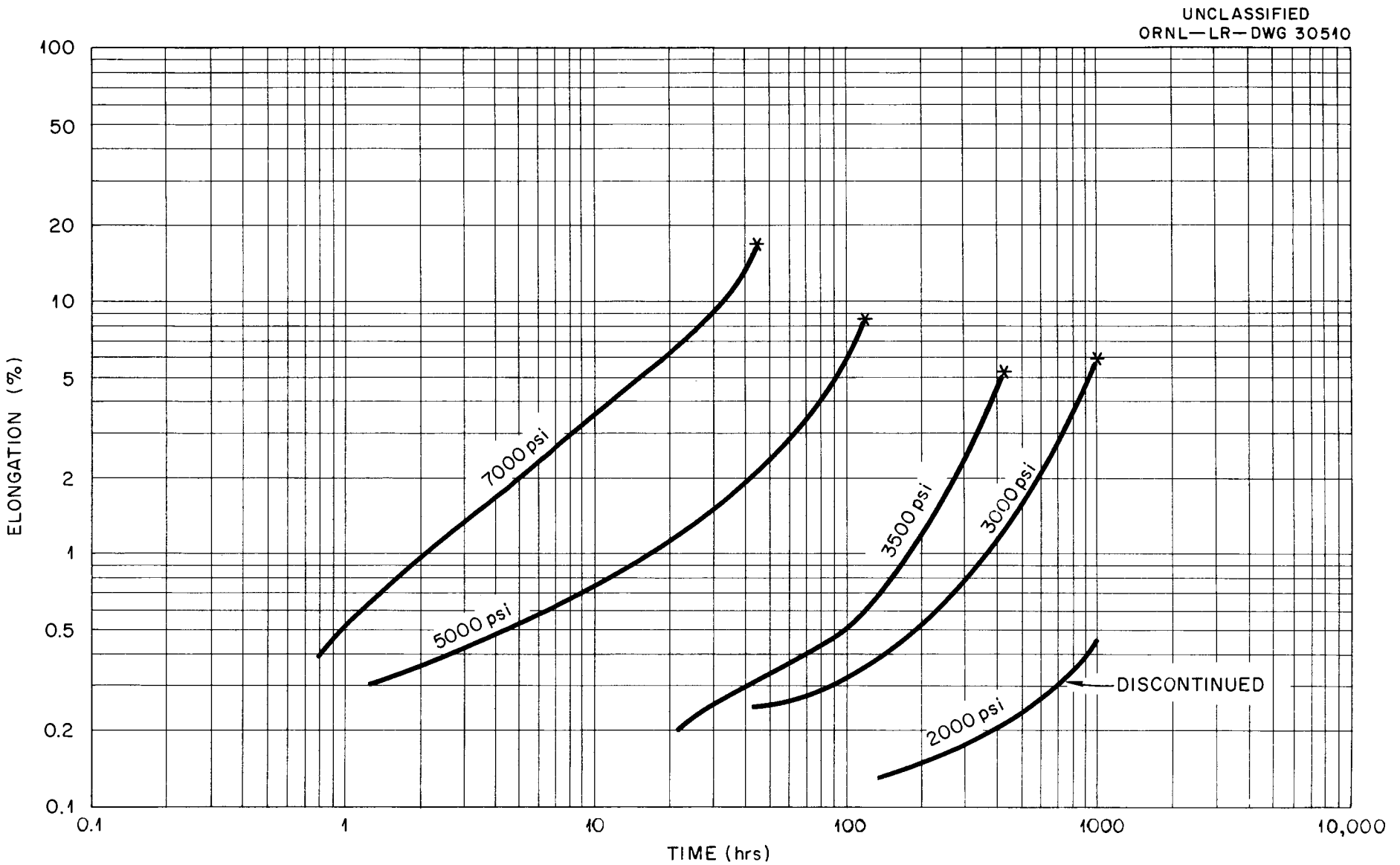

Fig. 6. Creep Curves of Solution-Annealed Hastelloy B Sheet Tested in Argon at 1800°F.

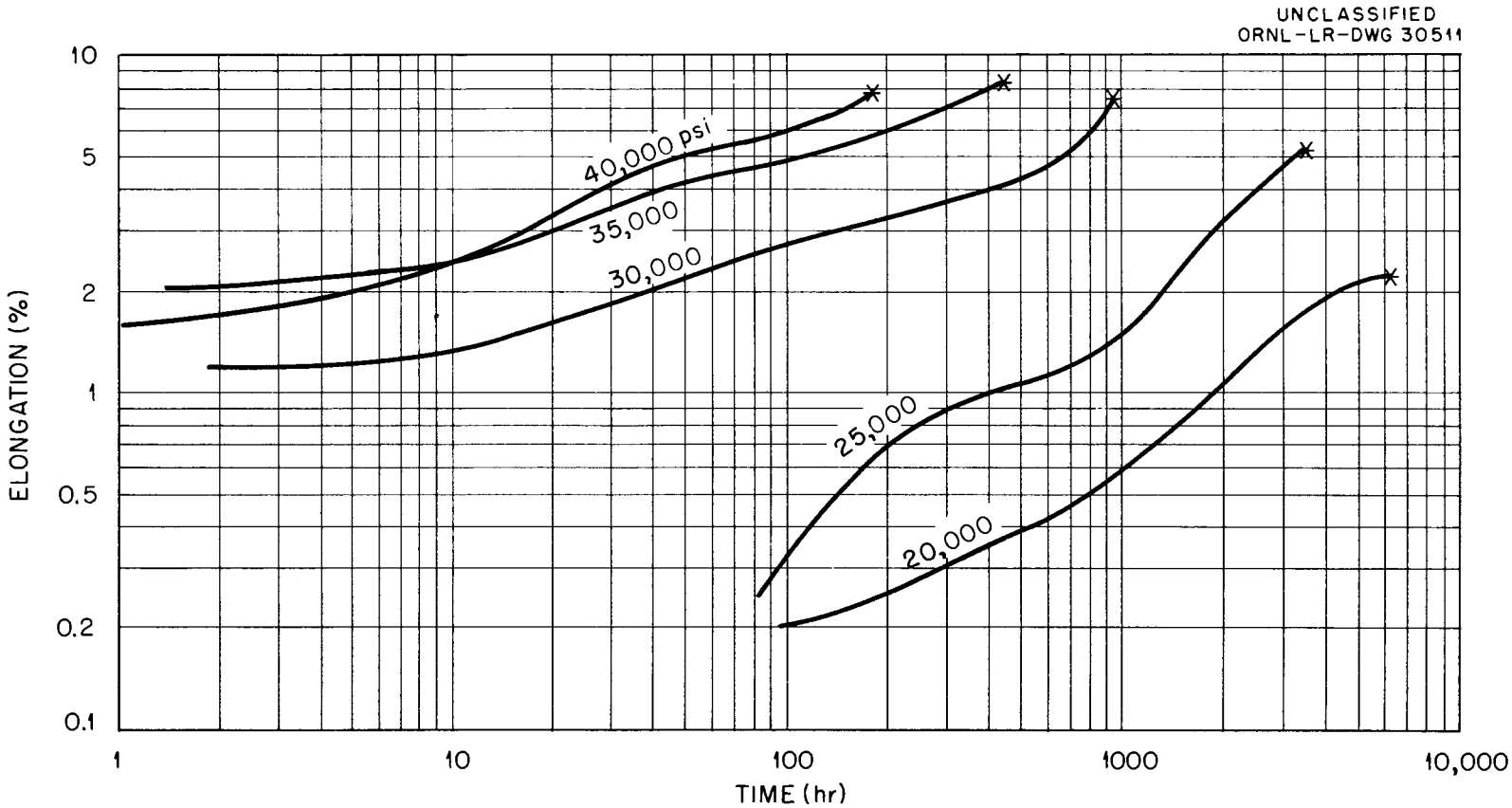

Fig. 7. Creep Curves of Solution-Annealed Hastelloy W Sheet Tested in Argon at 1300°F.

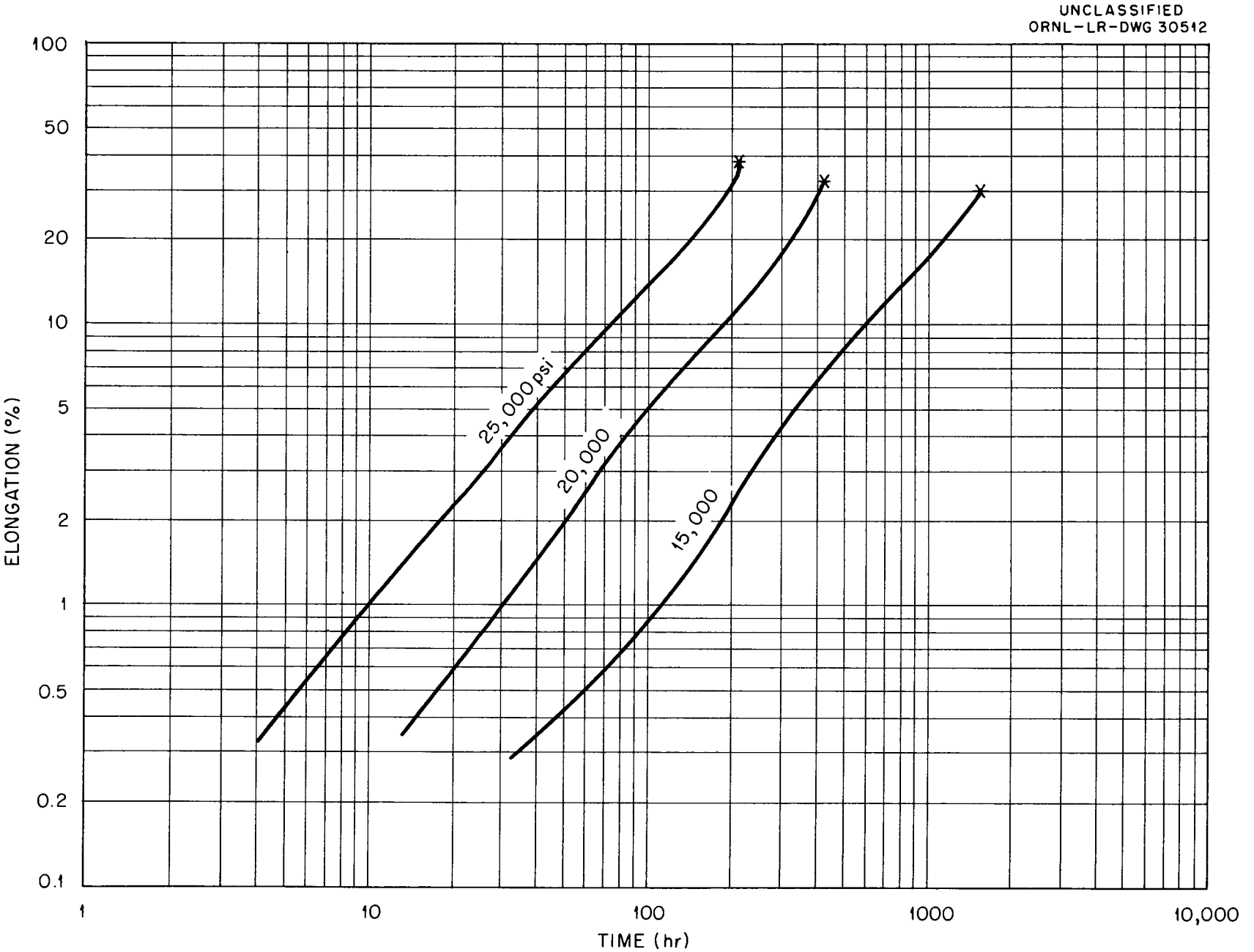

Fig. 8. Creep Curves of Solution-Annealed Hastelloy W Sheet Tested in Argon at 1400°F.

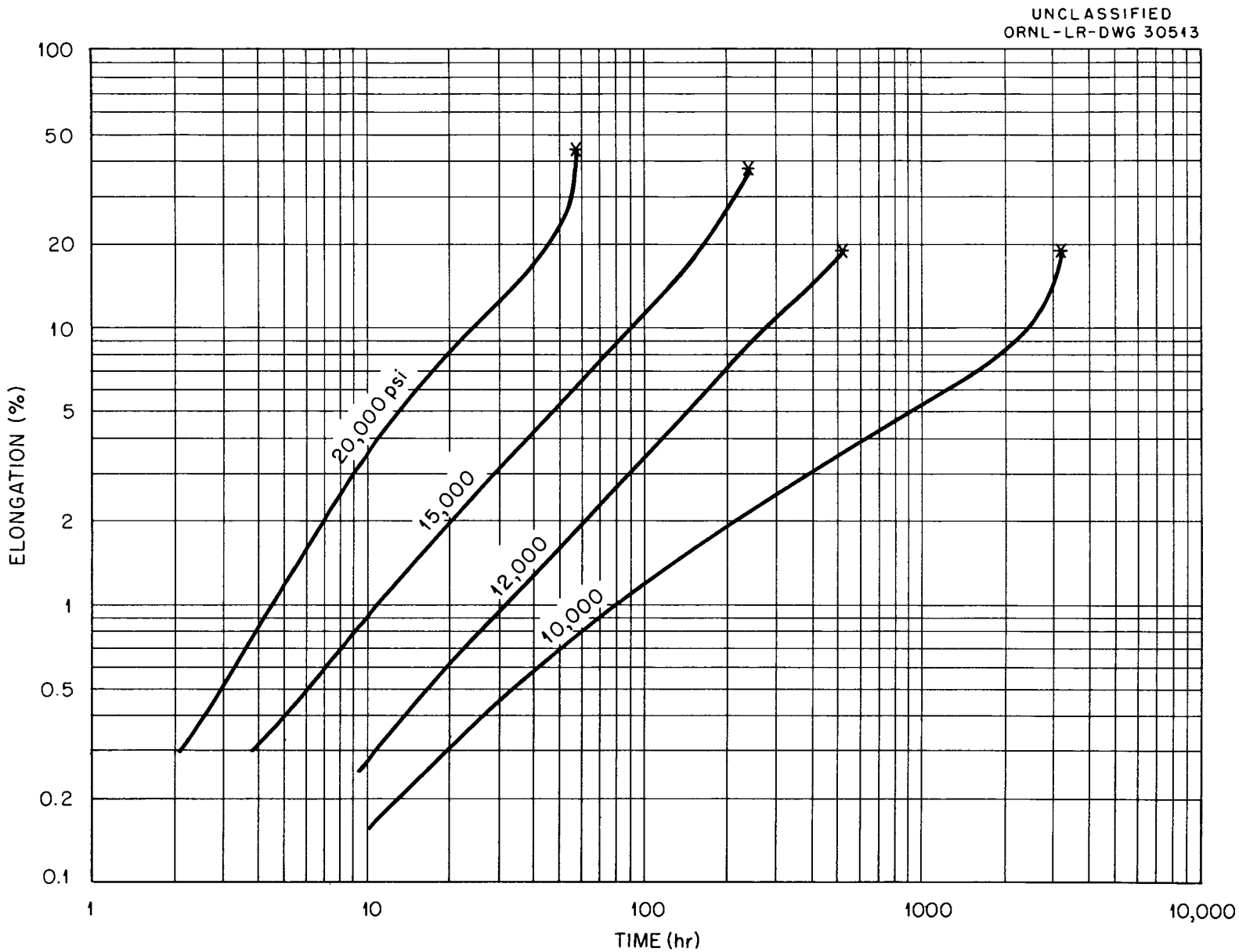

Fig. 9. Creep Curves of Solution-Annealed Hastelloy W Sheet Tested in Argon at 1500°F.

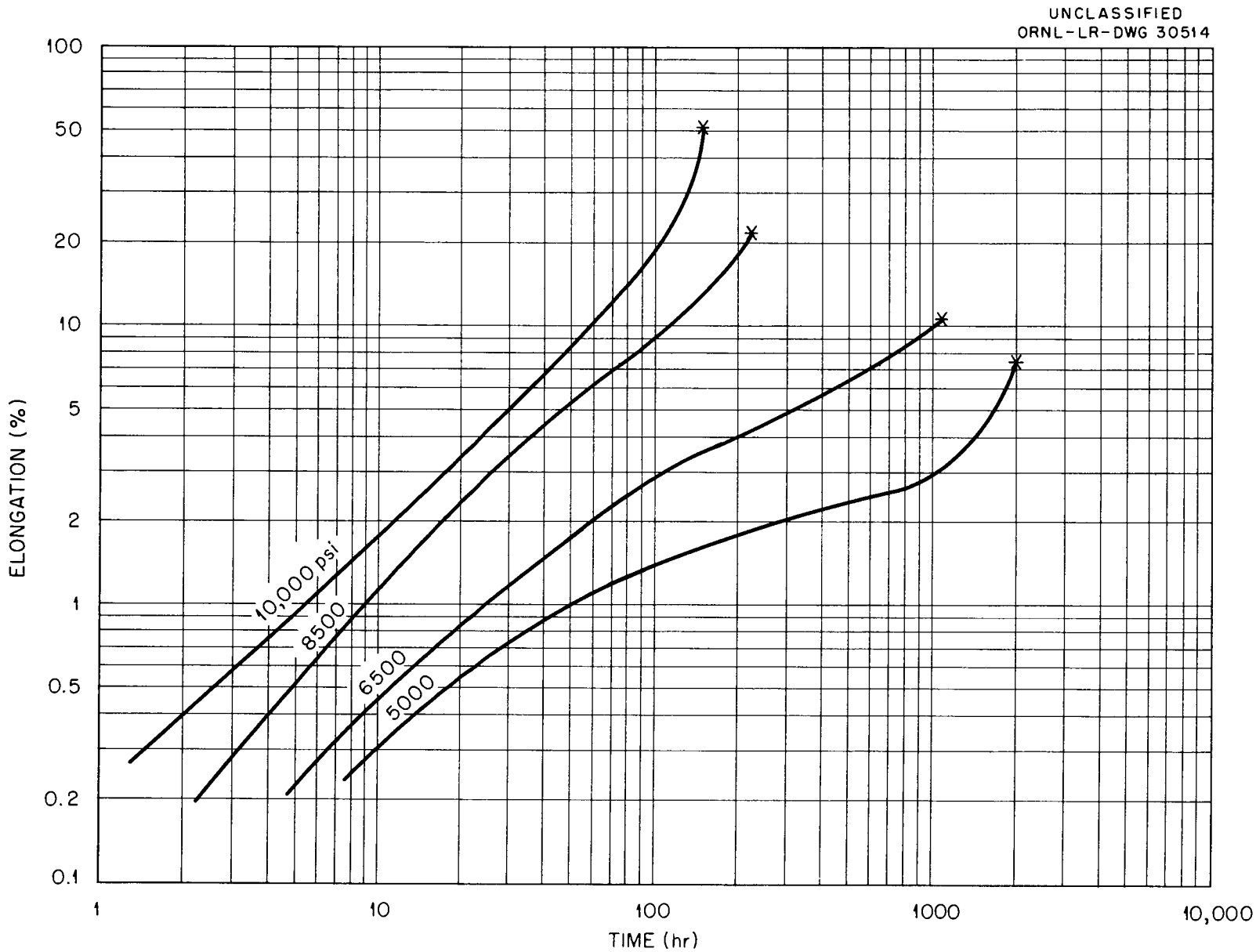

Fig. 10. Creep Curves of Solution-Annealed Hastelloy W Sheet Tested in Argon at 1650°F.

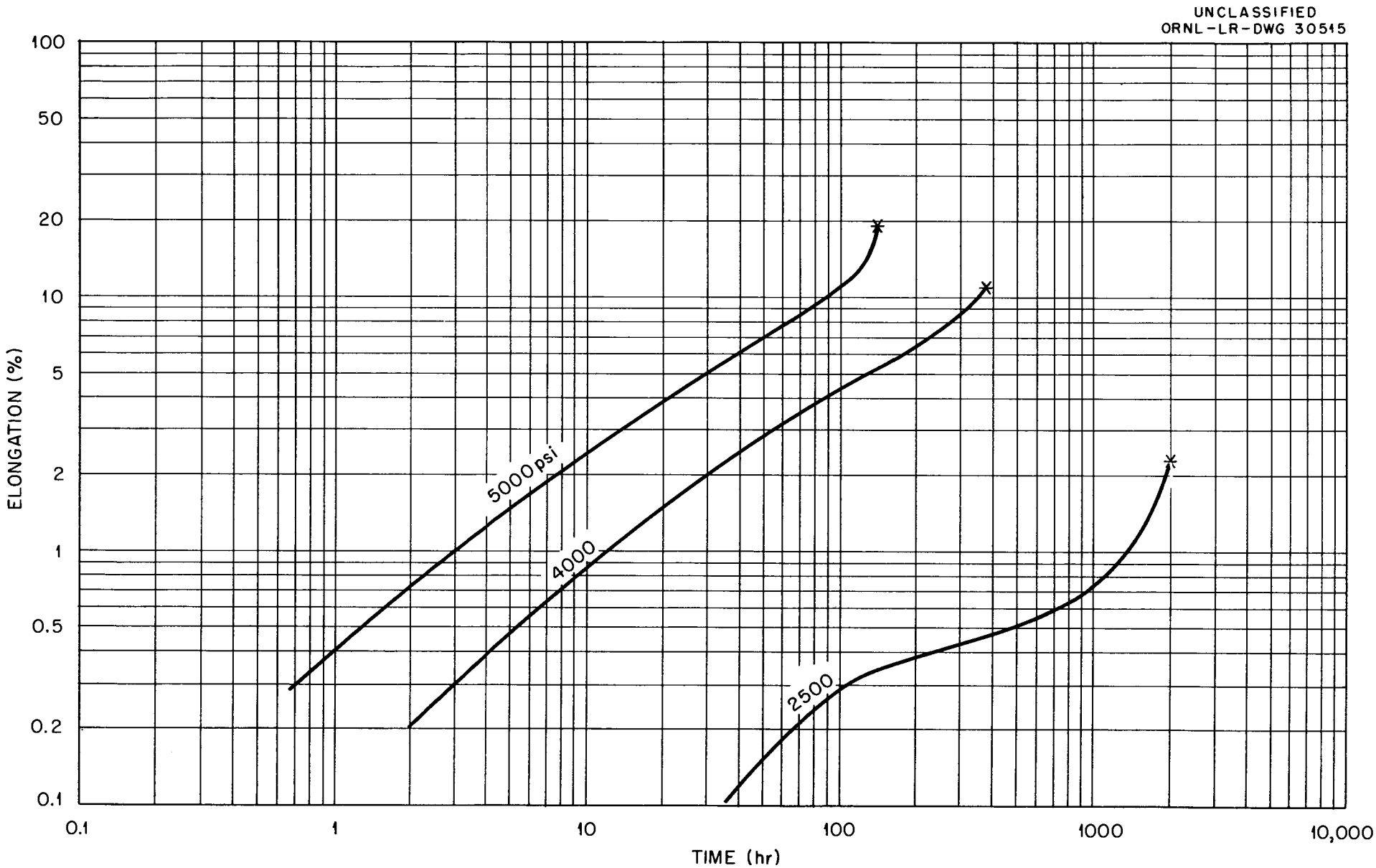

Fig. 11. Creep Curves of Solution-Annealed Hastelloy W Sheet Tested in Argon at 1800°F.

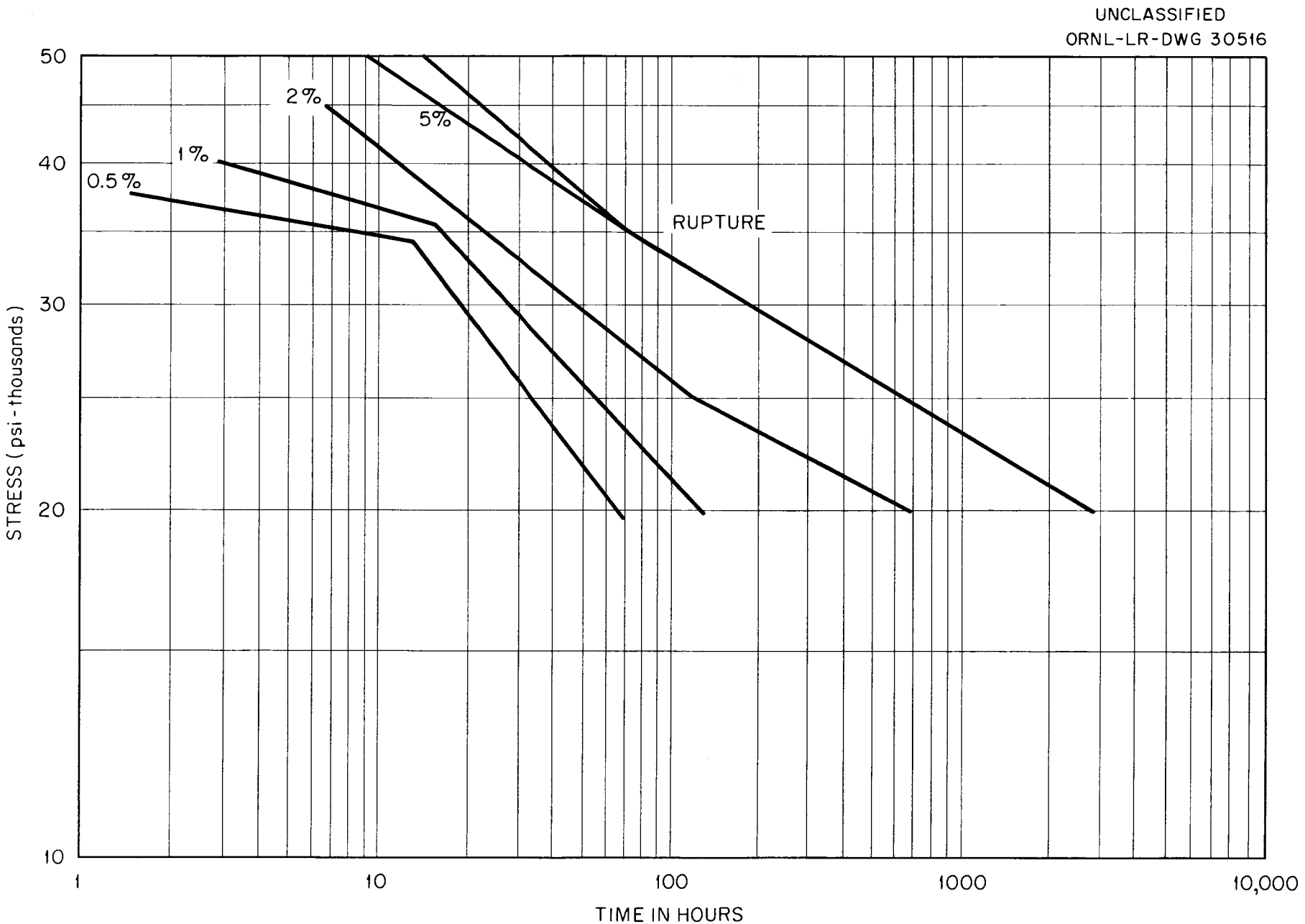

Fig. 12. Design Curves of Solution-Annealed Hastelloy B Sheet Tested in Argon at 1300°F.

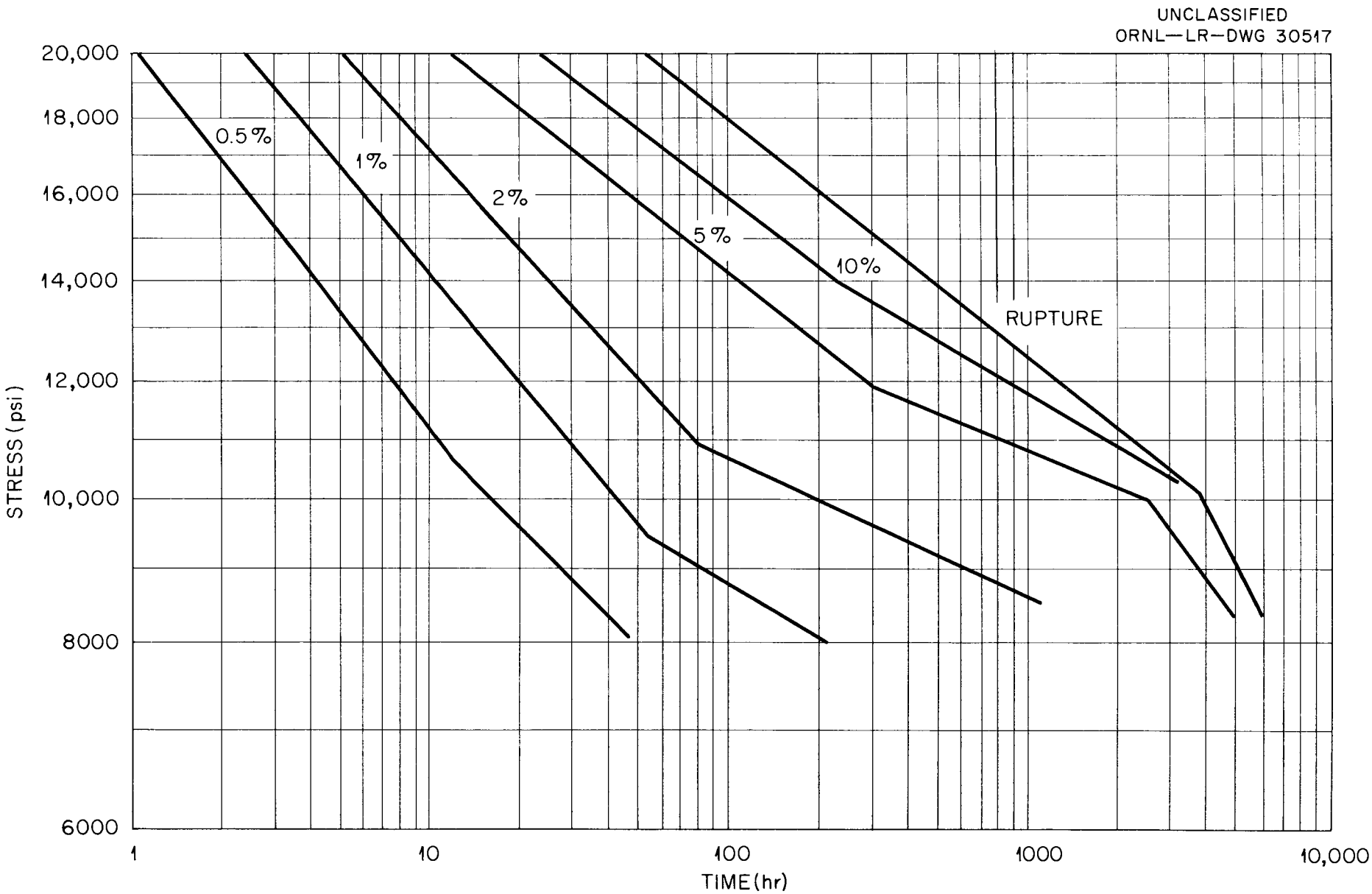

Fig. 13. Design Curves of Solution-Annealed Hastelloy B Sheet Tested in Argon at 1500°F.

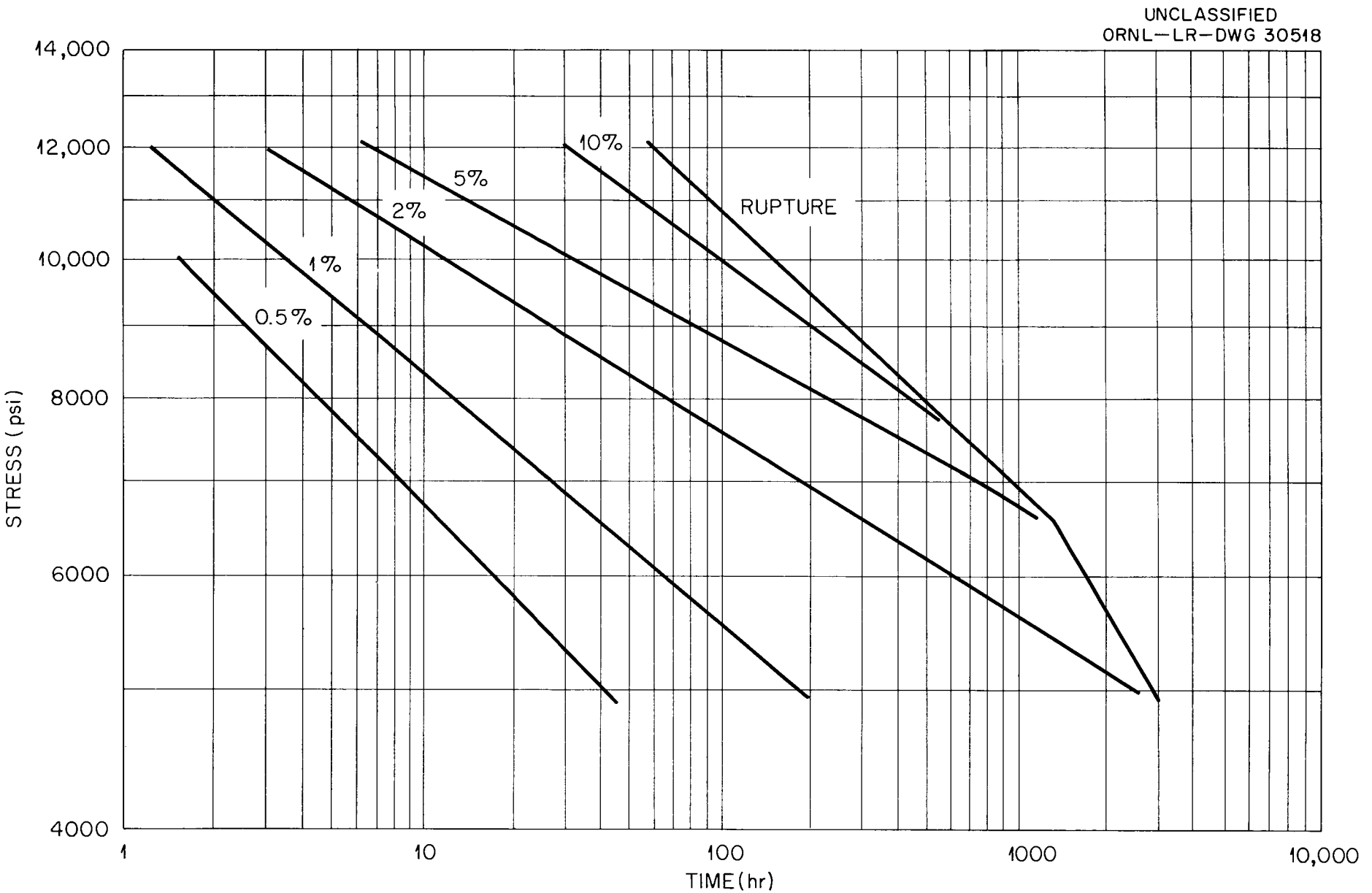

Fig. 14. Design Curves of Solution-Annealed Hastelloy B Sheet Tested in Argon at 1650°F.

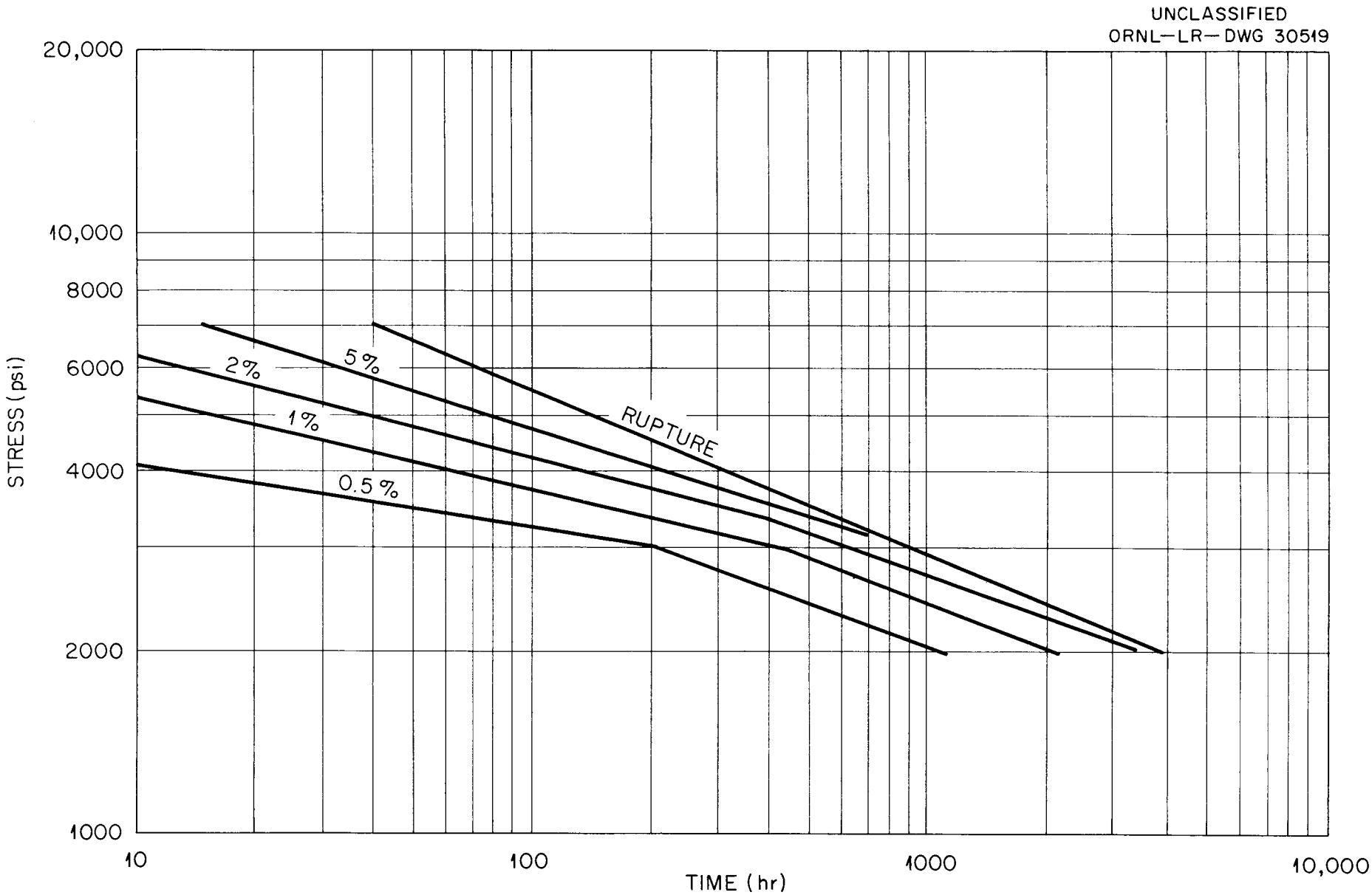

Fig. 15. Design Curves of Solution-Annealed Hastelloy B Sheet Tested in Argon at 1800° F.

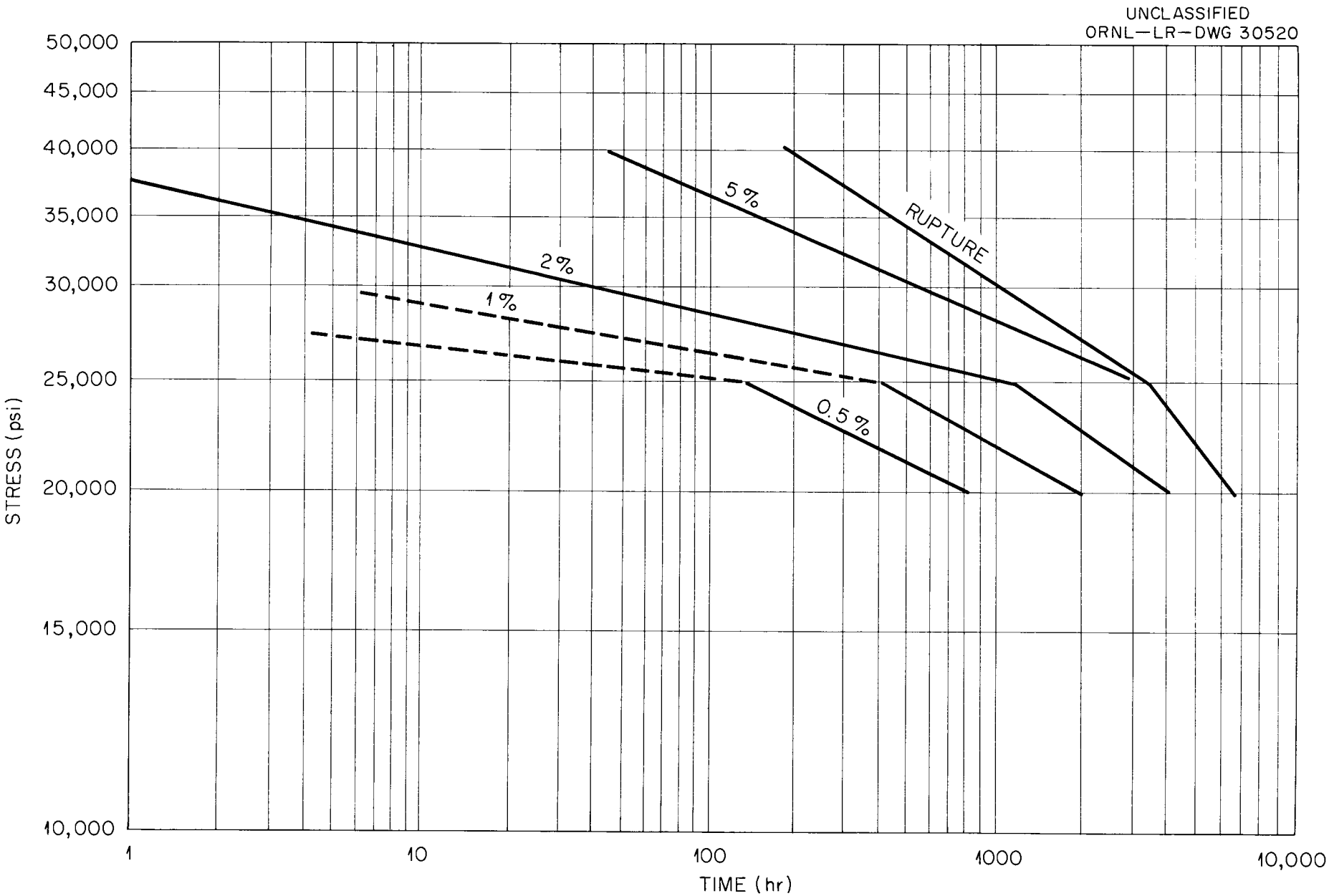

Fig. 16. Design Curves of Solution-Annealed Hastelloy W Sheet Tested in Argon at 1300° F.

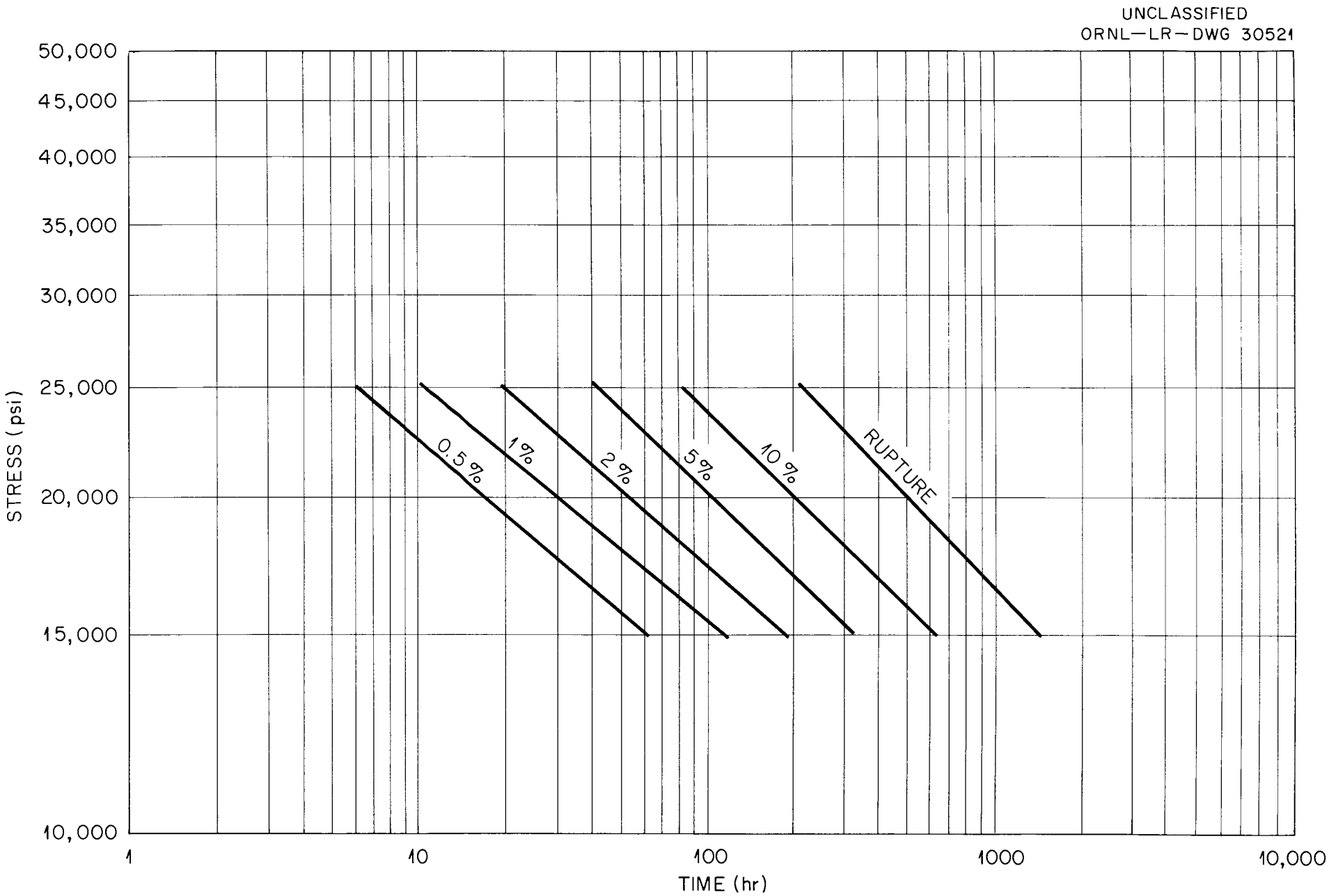

Fig. 17. Design Curves of Solution-Annealed Hastelloy W Sheet Tested in Argon at 1400°F.

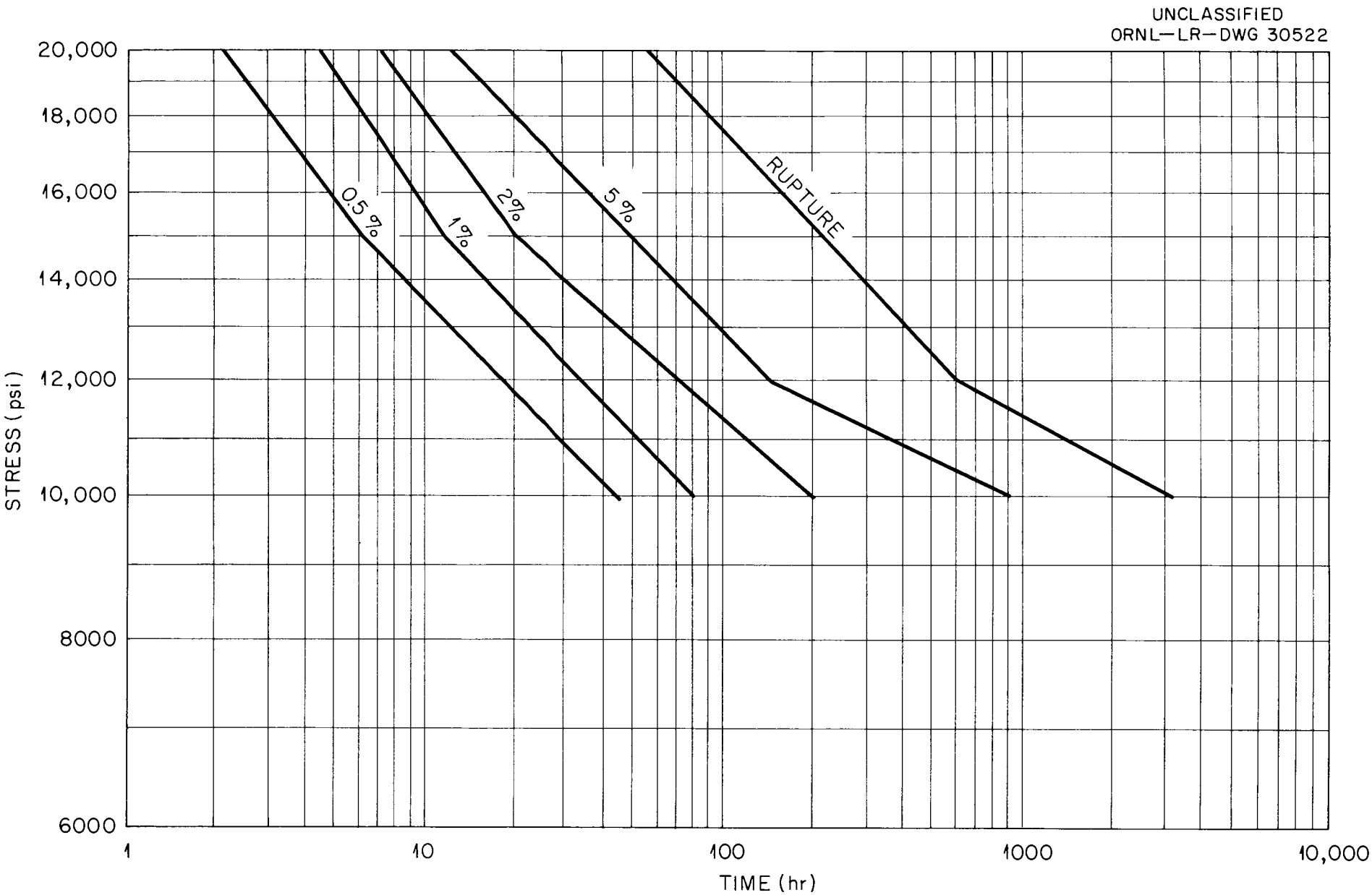

Fig. 18. Design Curves of Solution-Annealed Hastelloy W Sheet Tested in Argon at 1500° F.

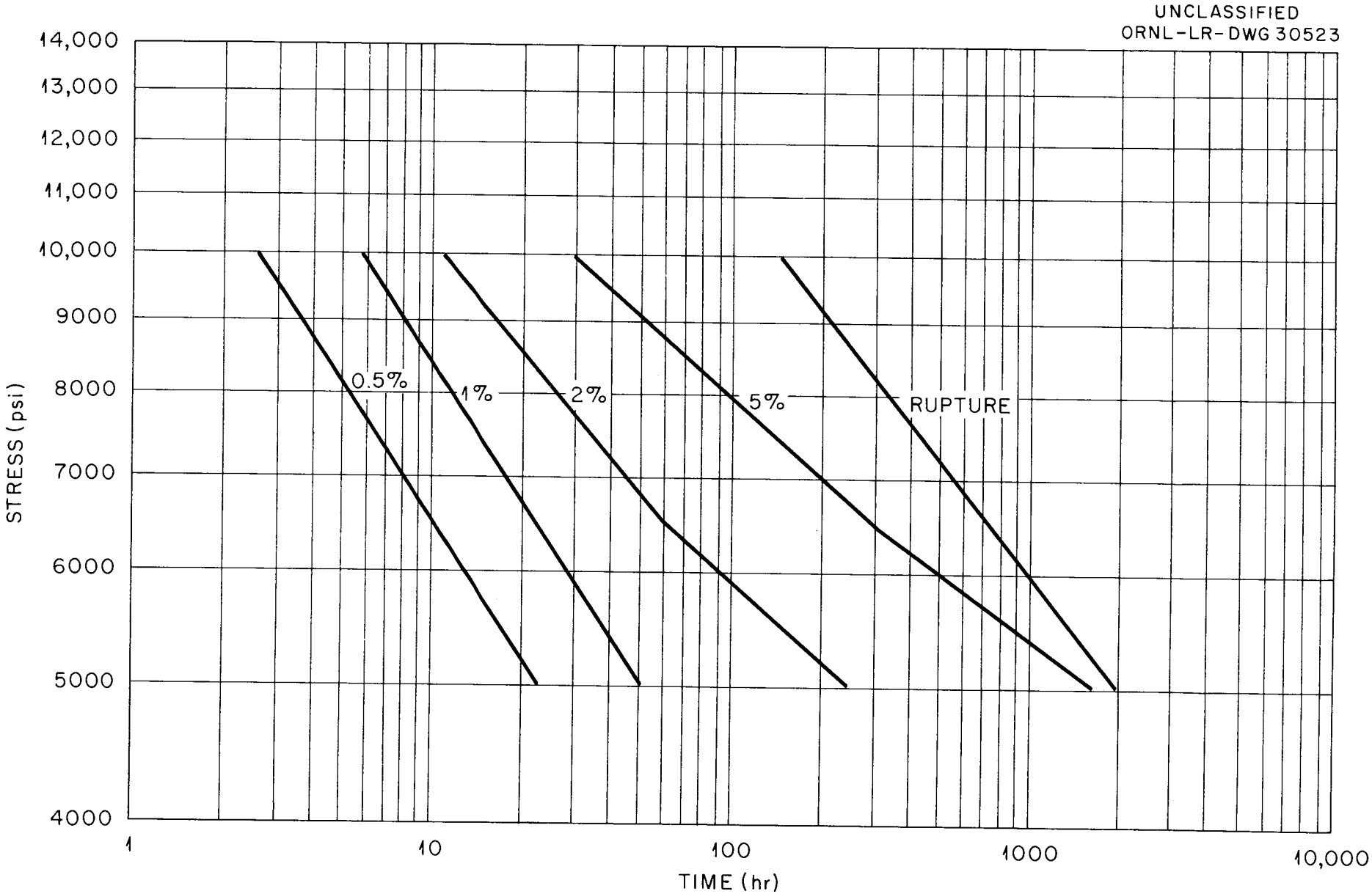

Fig. 19. Design Curves of Solution-Annealed Hastelloy W Sheet Tested in Argon at 1650°F.

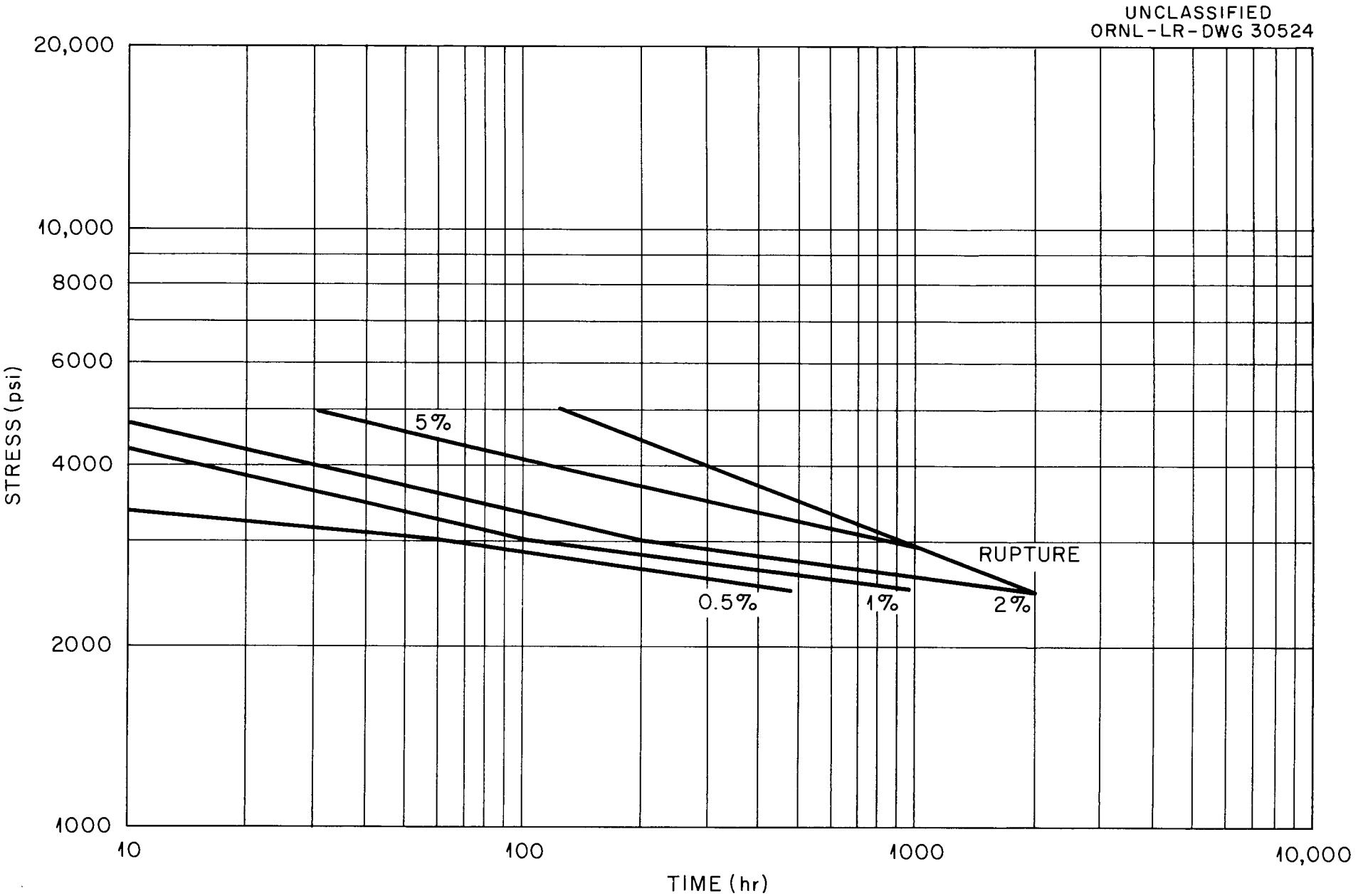

Fig. 20. Design Curves of Solution-Annealed Hastelloy W Sheet Tested in Argon at 1800°F.

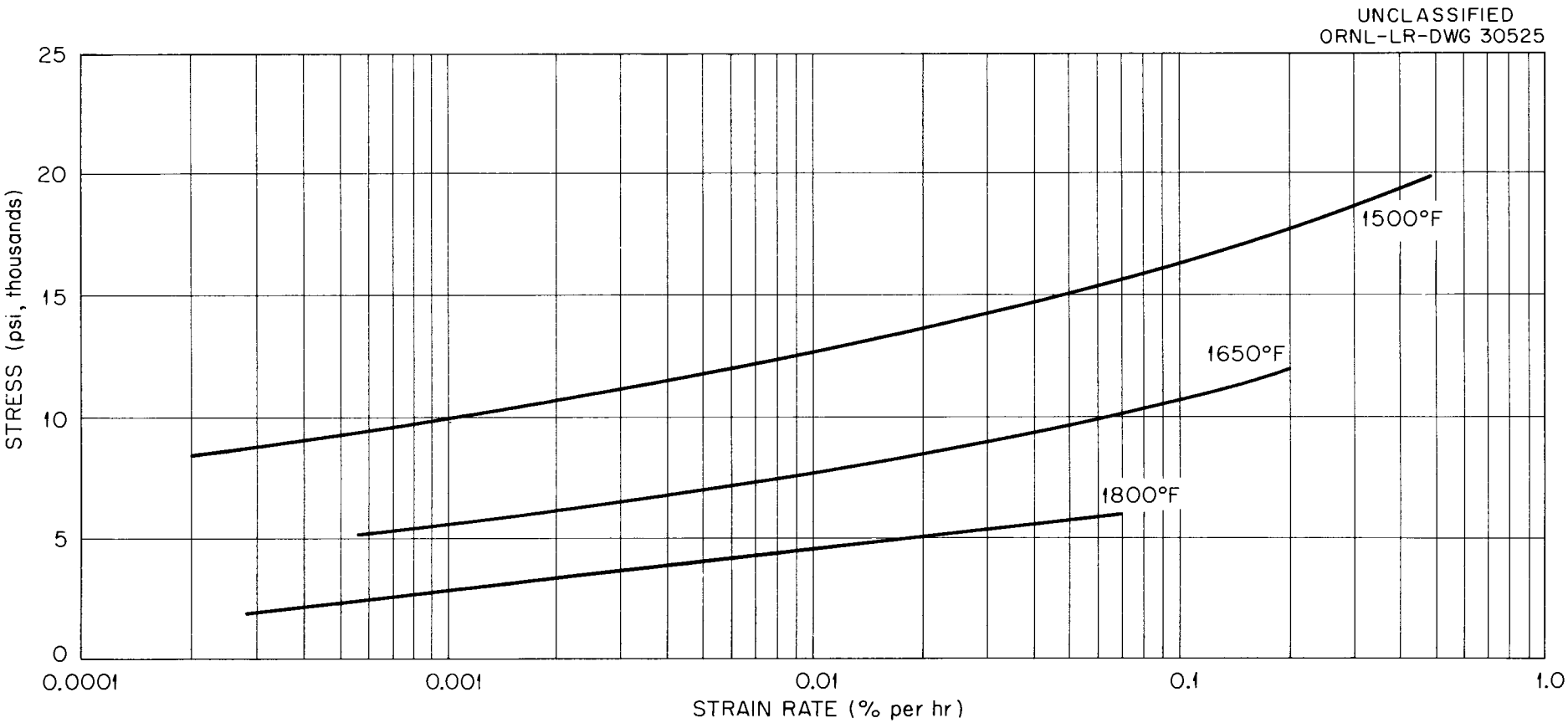

Fig. 21. Plot of Stress vs. log Minimum Creep Rate for Solution-Annealed Hastelloy B Sheet Tested in Argon at 1500, 1650, and 1800°F.

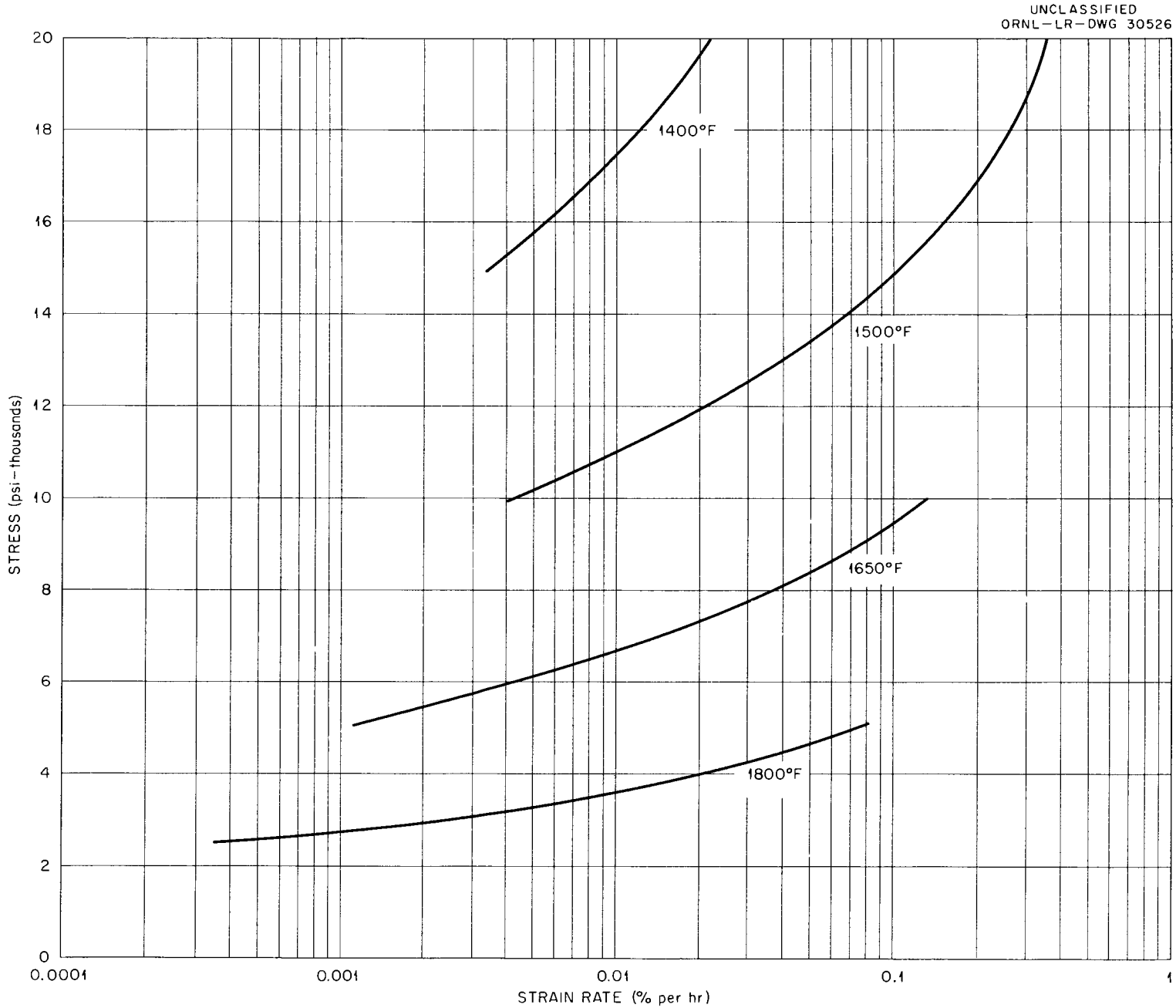

Fig. 22. Plot of Stress vs log Minimum Creep Rate for Solution-Annealed Hastelloy W Sheet Tested in Argon at 1400, 1500, 1650, and 1800°F.

UNCLASSIFIED
ORNL-LR-DWG 30527

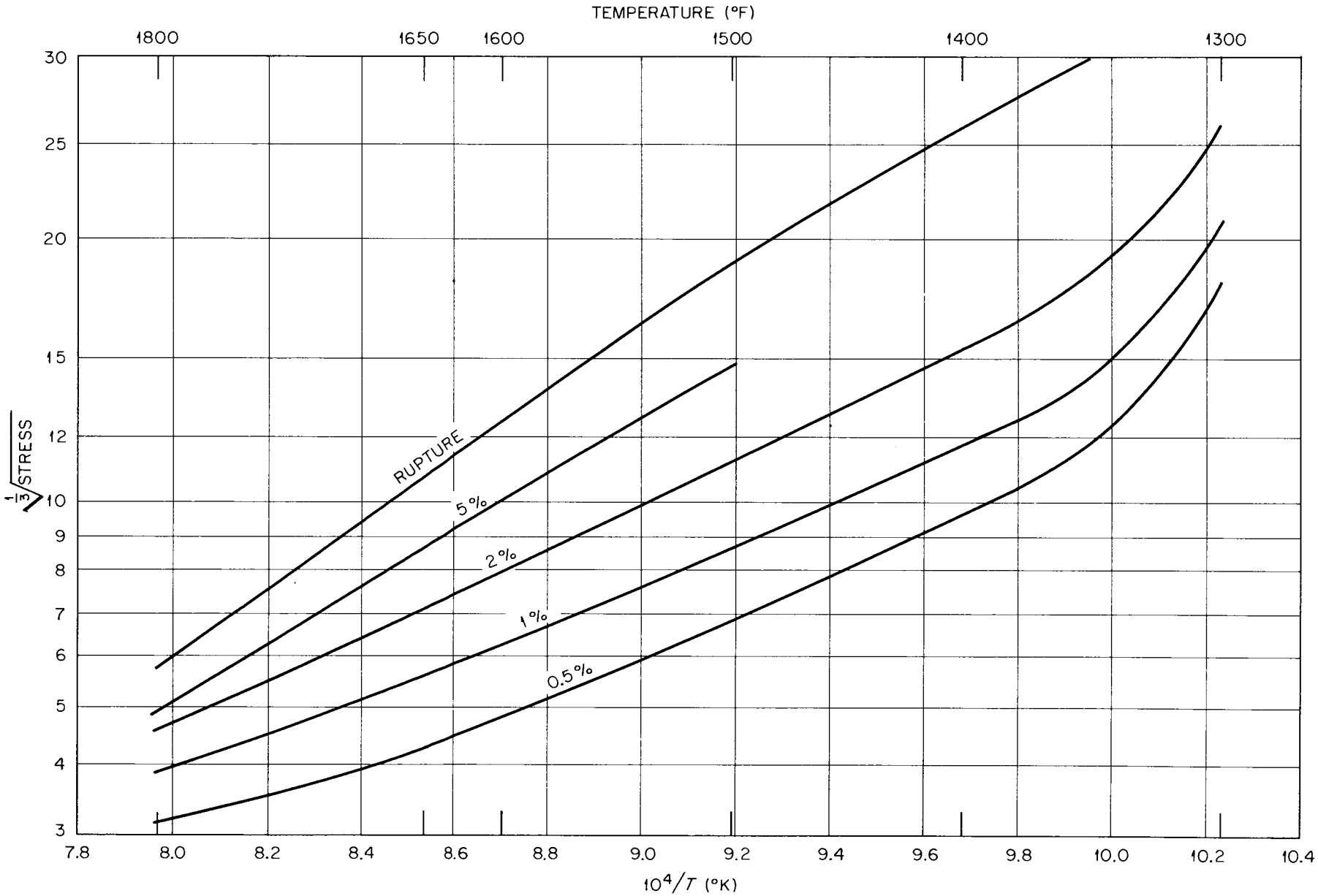

Fig. 23. 100 hr Isochronous Curves of Solution-Annealed Hastelloy B Sheet Tested in Argon.

UNCLASSIFIED
ORNL-LR-DWG 30528

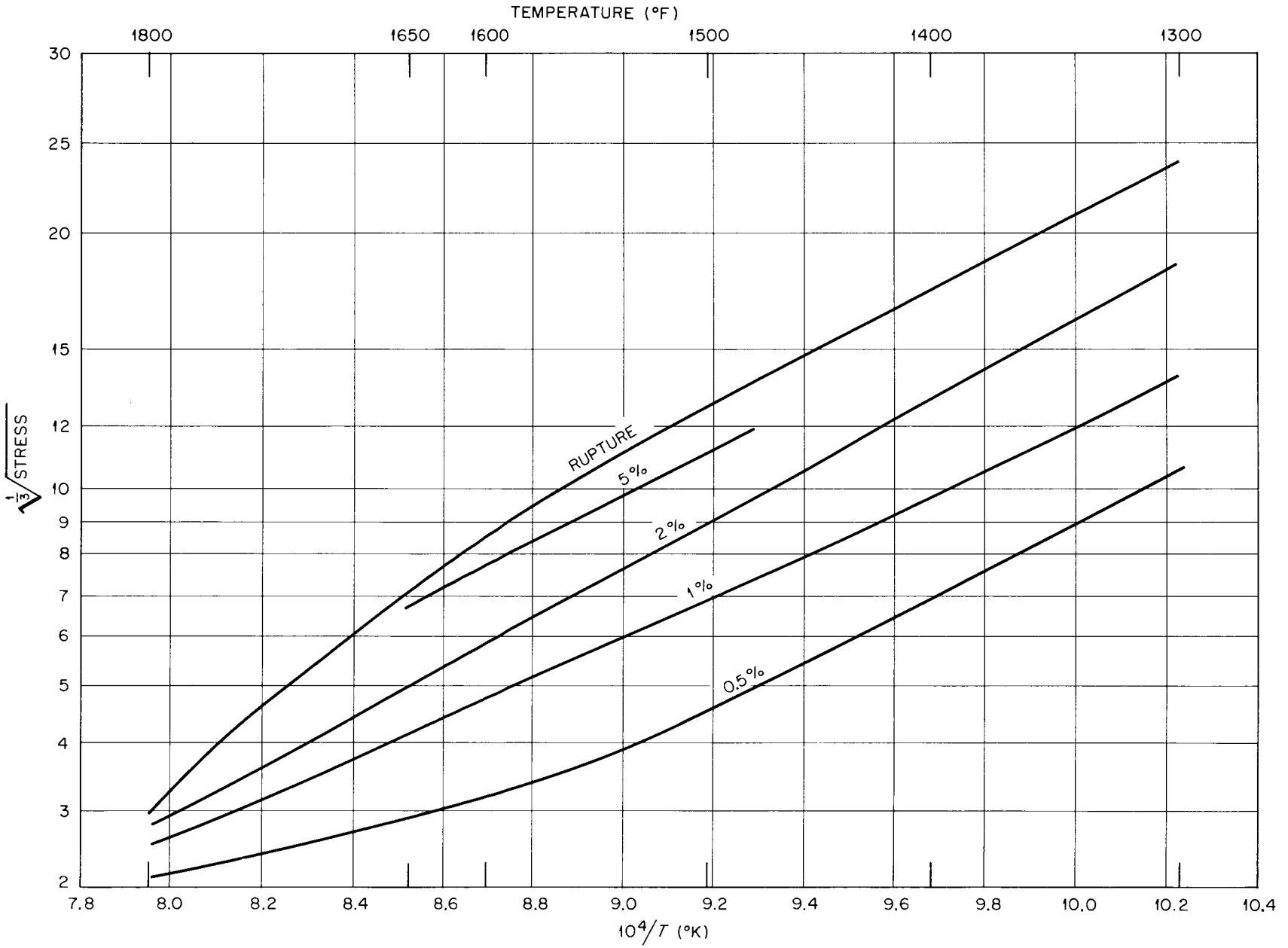

Fig. 24. 1000hr Isochronous Curves of Solution – Annealed Hastelloy B Sheet Tested in Argon.

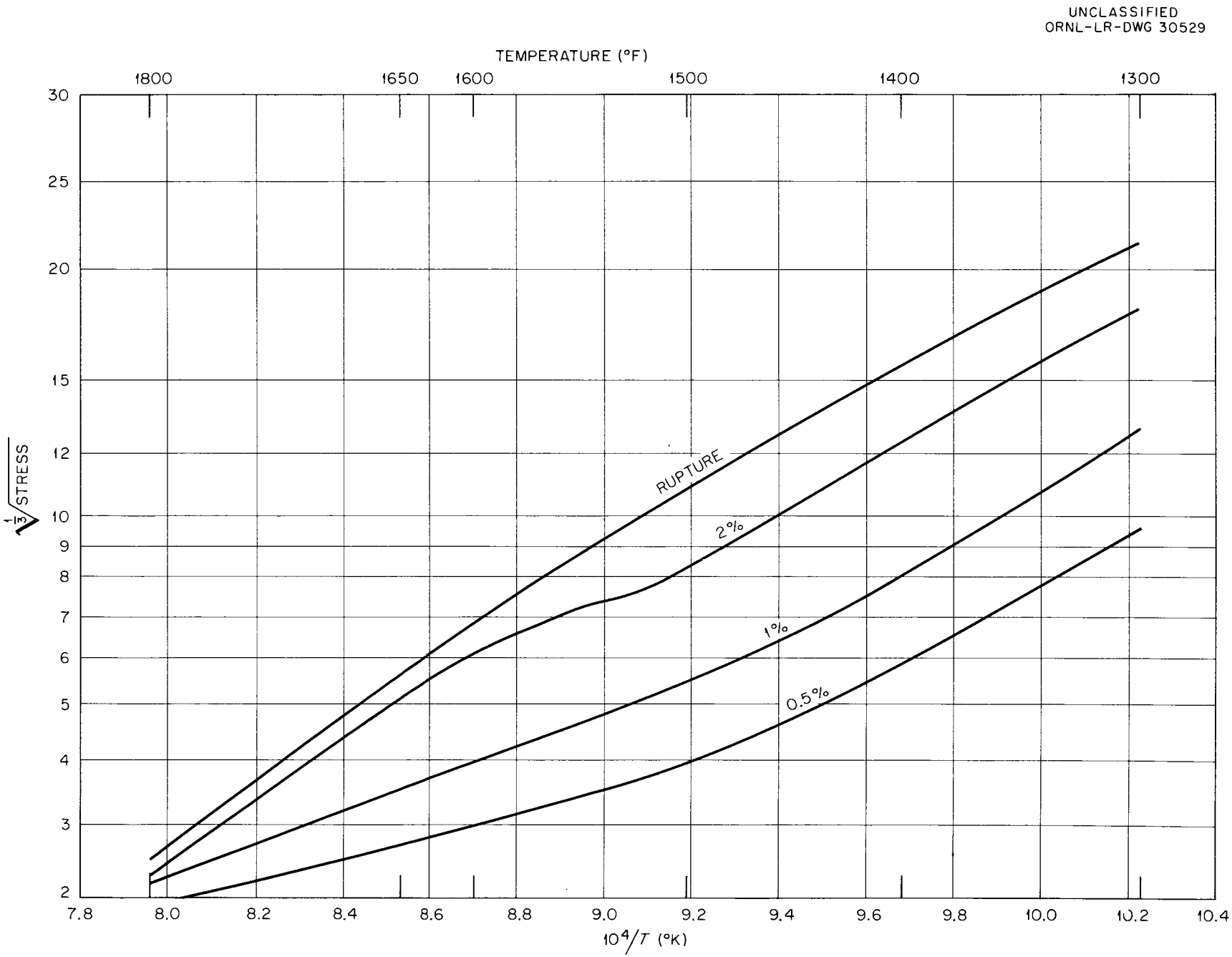

Fig. 25. 2000 hr Isochronous Curves of Solution-Annealed Hastelloy B Sheet Tested in Argon.

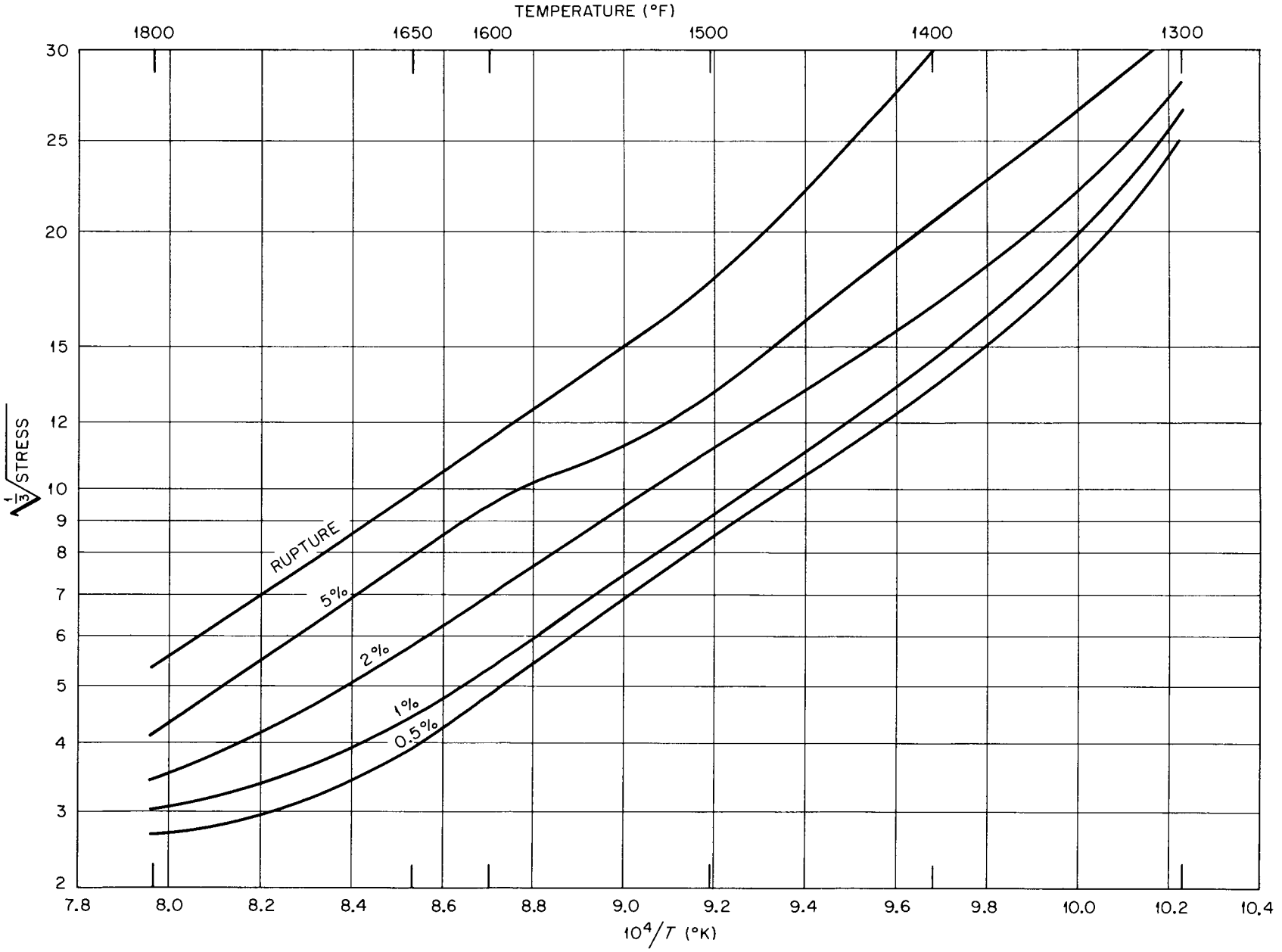

Fig. 26. 100 hr Isochronous Curves of Solution-Annealed Hastelloy W Sheet Tested in Argon.

UNCLASSIFIED
ORNL-LR-DWG 30531

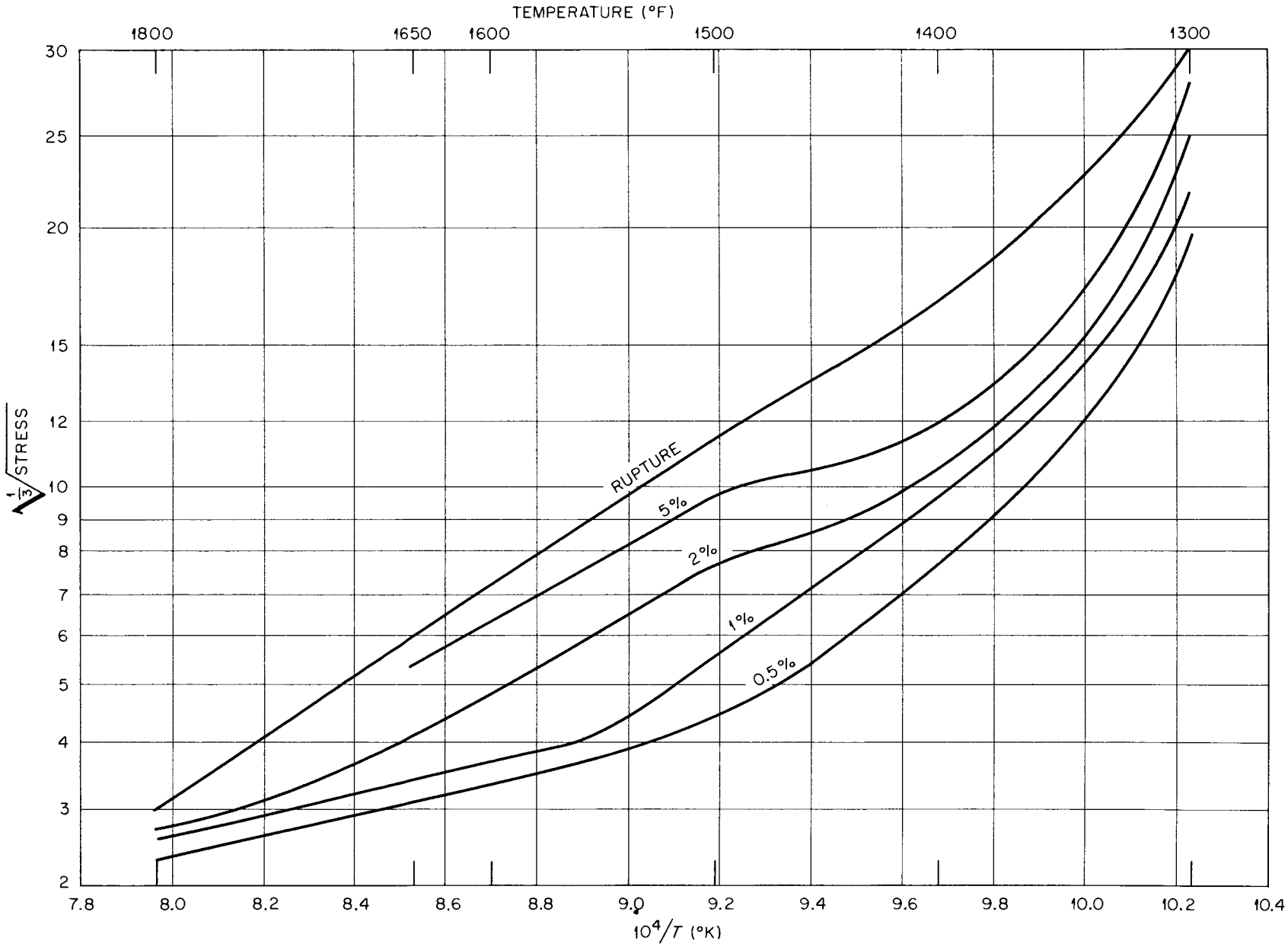

Fig. 27. 1000 hr Isochronous Curves of Solution-Annealed Hastelloy W Sheet Tested in Argon.

UNCLASSIFIED
ORNL-LR-DWG 30532

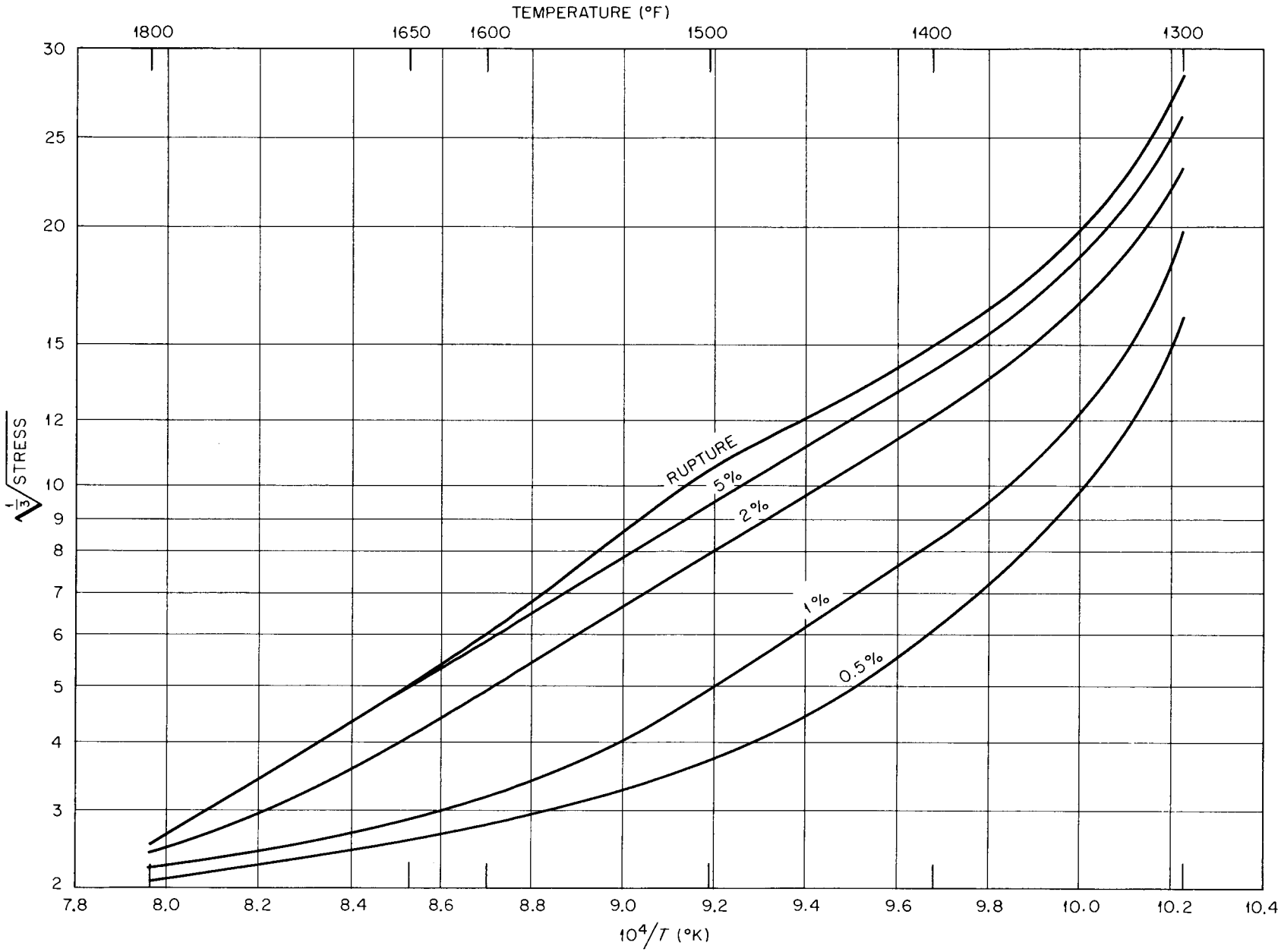

Fig. 28. 2000 hr Isochronous Curves of Solution–Annealed Hastelloy W Sheet Tested in Argon.

UNCLASSIFIED
ORNL-LR-DWG 30533

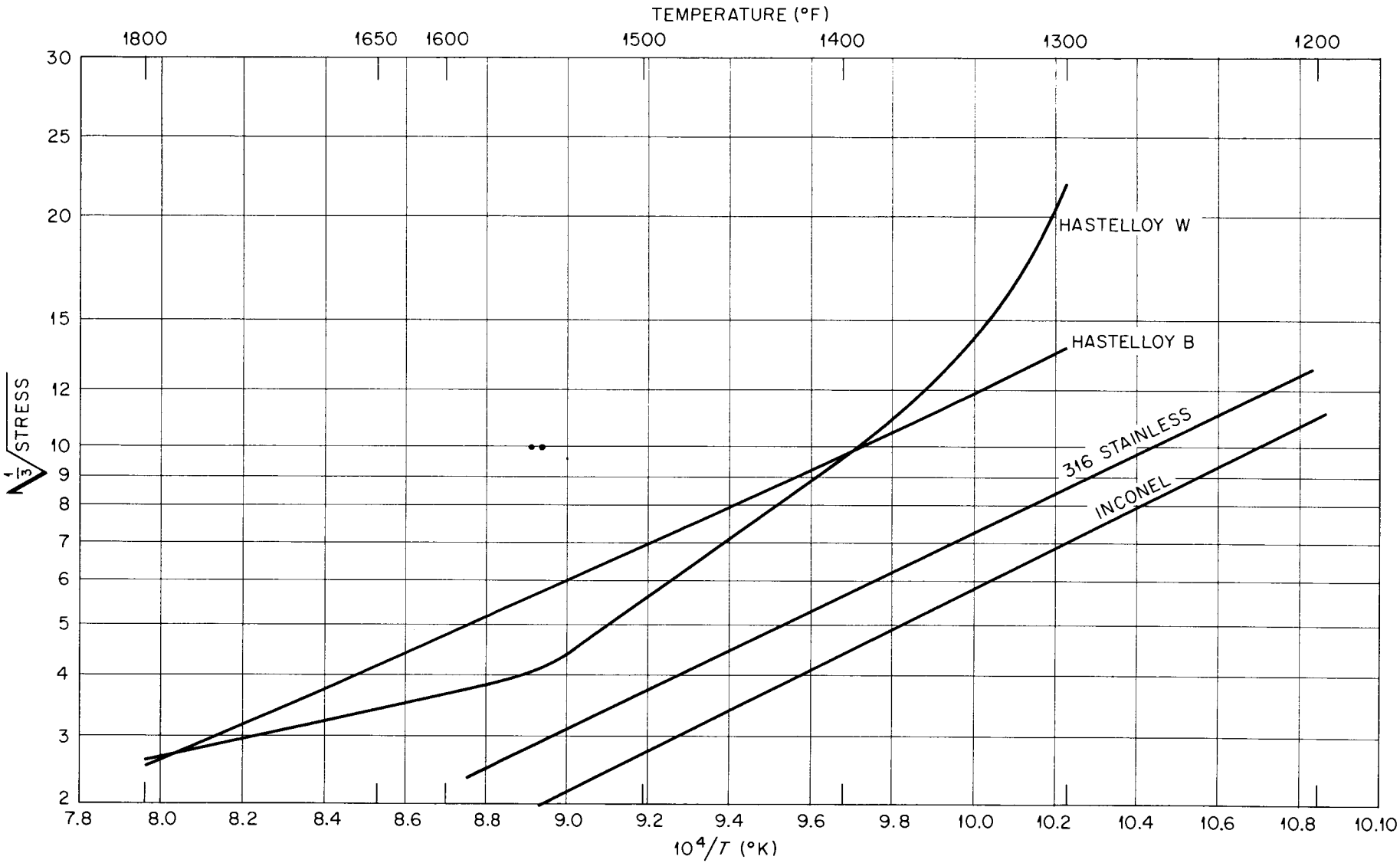

Fig. 29. Stress to Produce 1% Strain in 1000 hrs. for Several Alloys Tested in Argon.

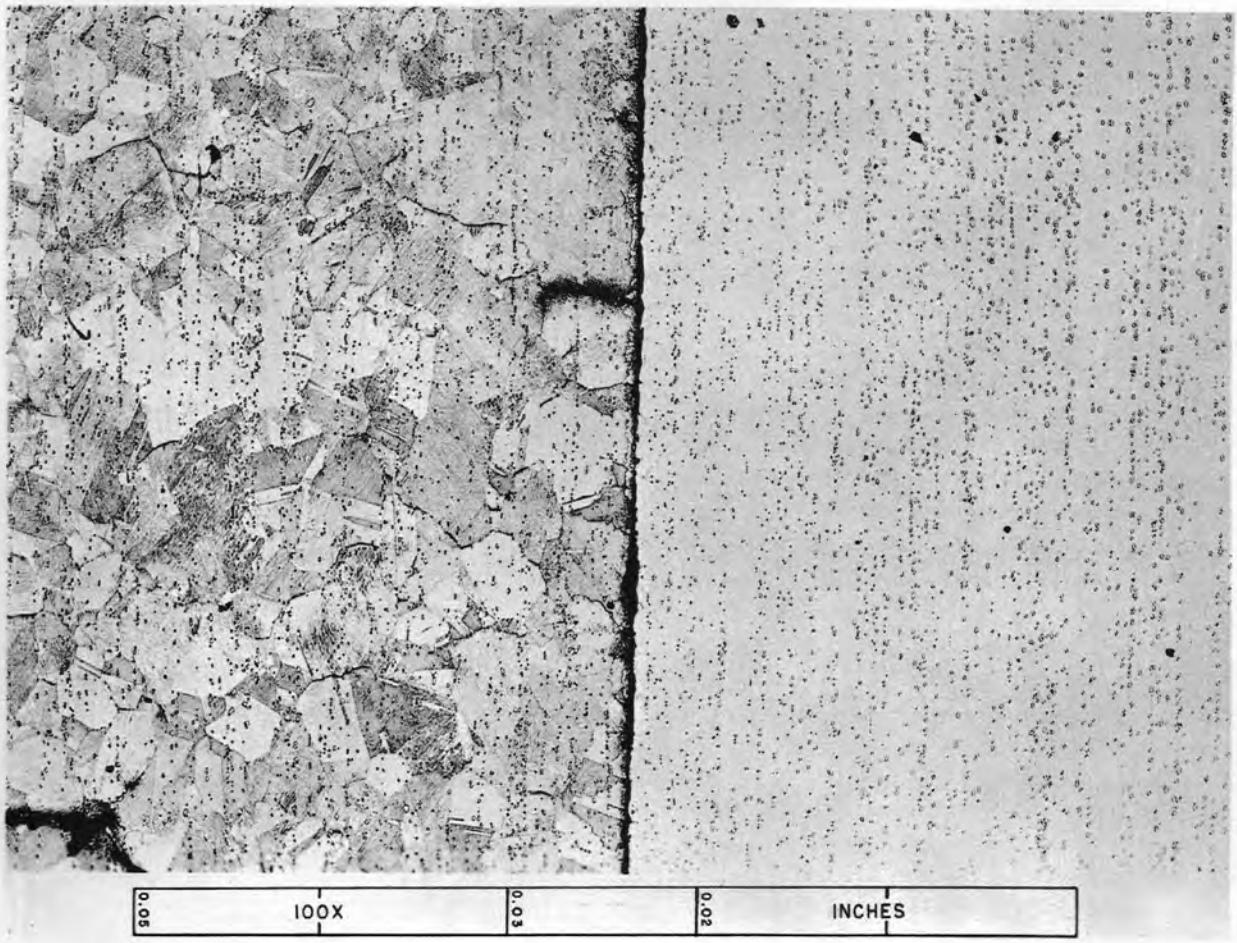

Fig. 30 (Y-19659) Hastelloy B Sheet Creep Tested in Argon at 45,000 PSI and 1300°F. Ruptured in 26 hr. 100X. Etchant: Chrome Regia.

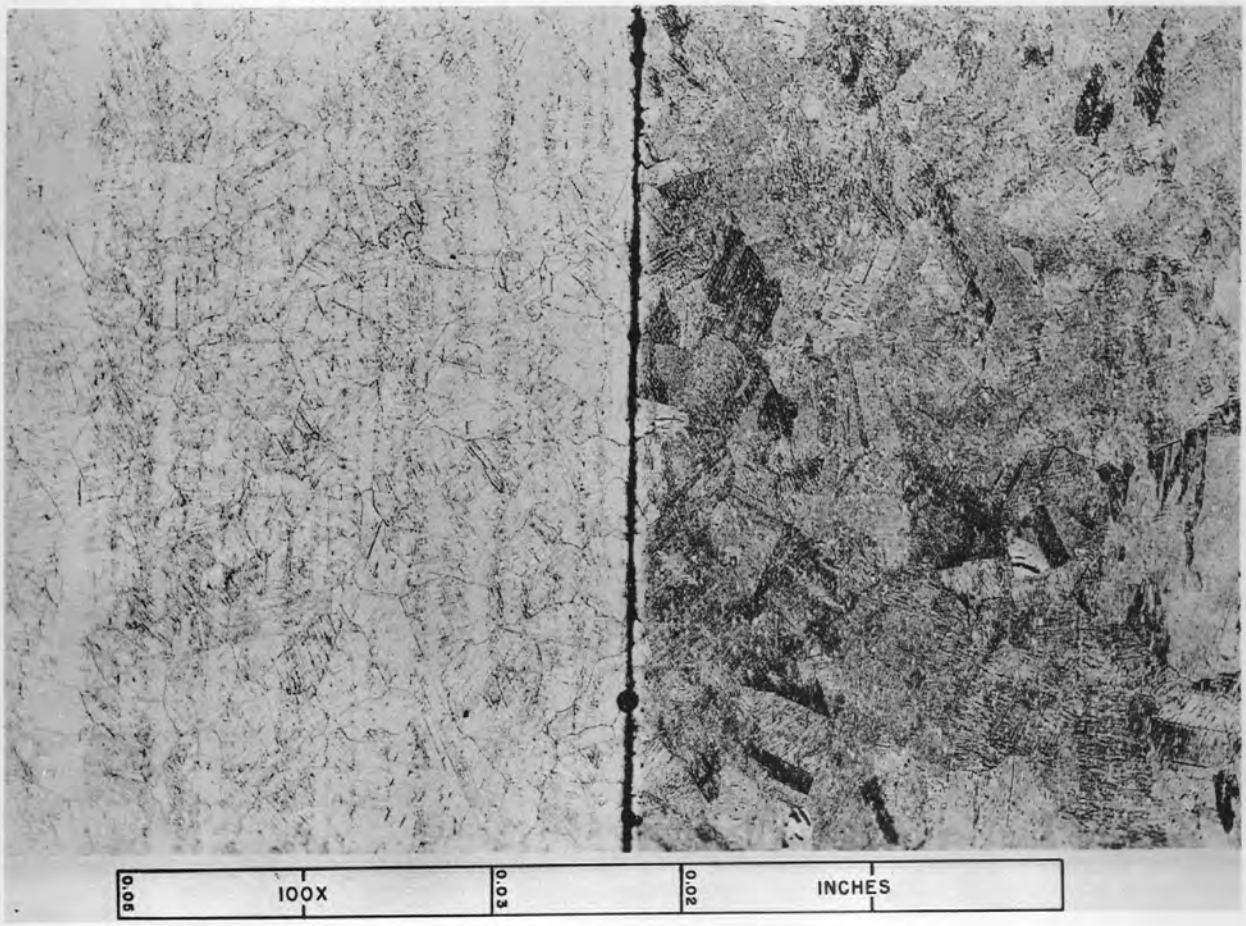

Fig. 31 (Y-15664) Hastelloy B Sheet Creep Tested in Argon at 30,000 PSI and 1300°F. Ruptured in 185 hr. 100X. Etchant: Chrome Regia.

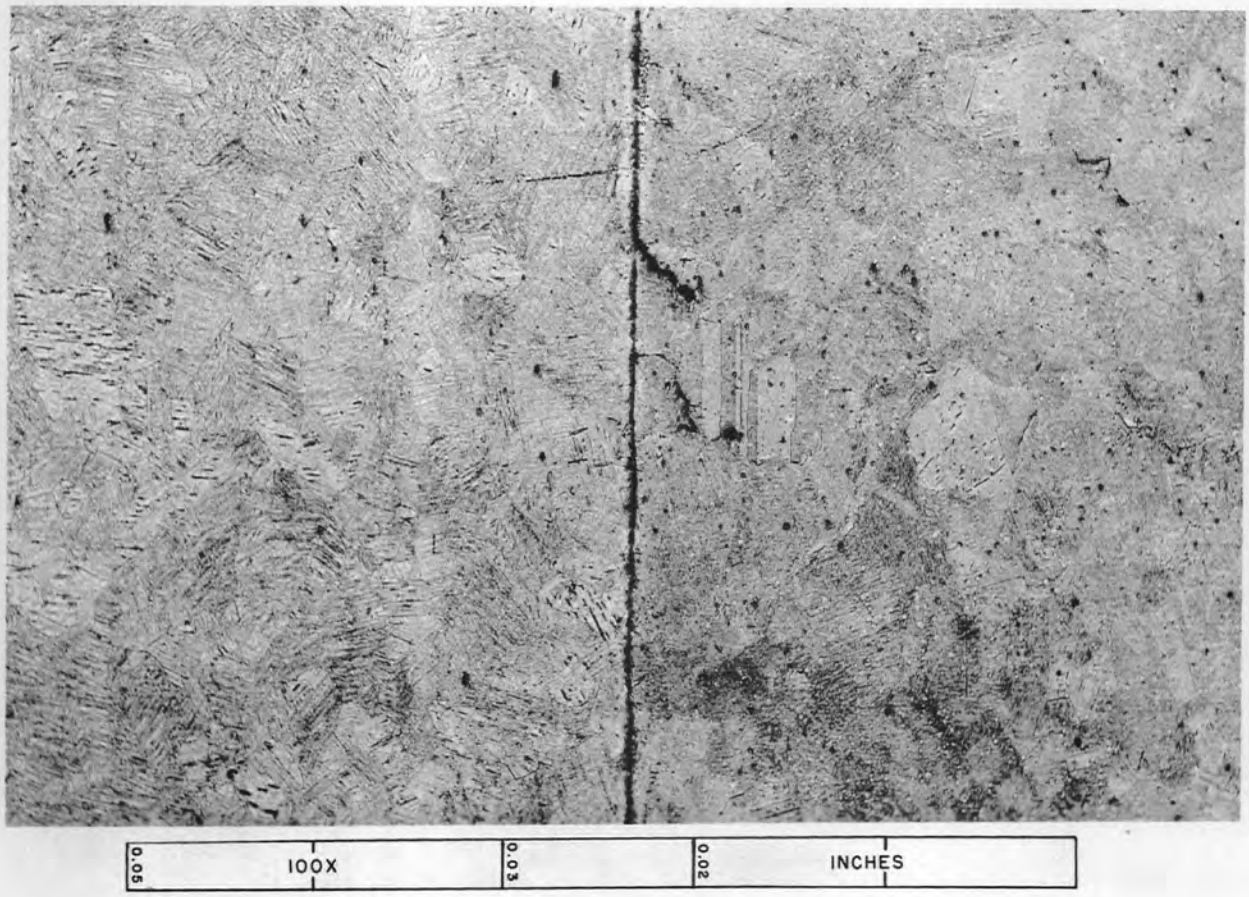

Fig. 32 (Y-15692) Hastelloy B Sheet Creep Tested in Argon at 25,000 PSI and 1300°F. Ruptured in 772 hr. 100X. Etchant: Chrome Regia.

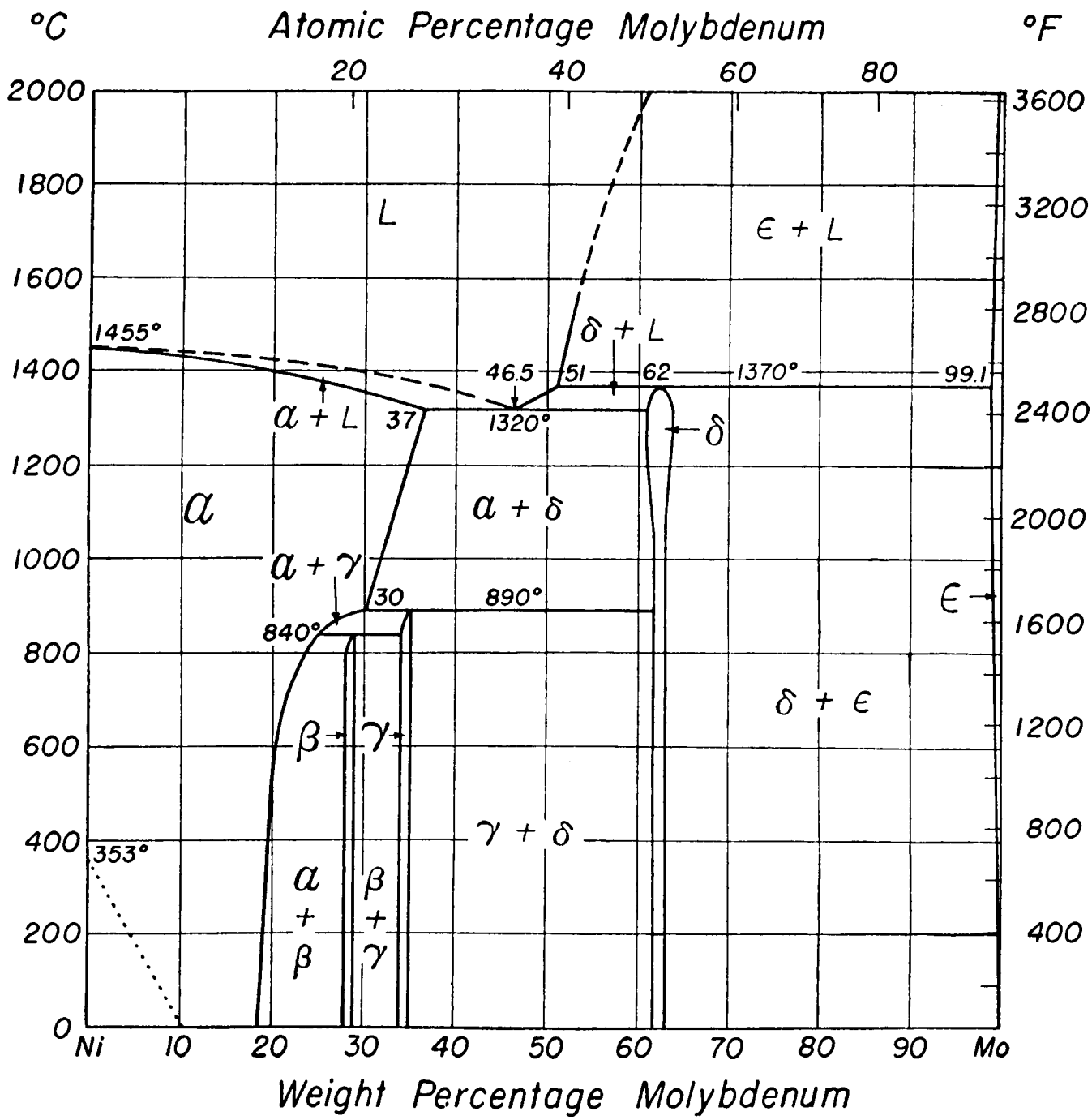

Fig. 33 (Y-21202) Nickel-Molybdenum Phase Diagram.

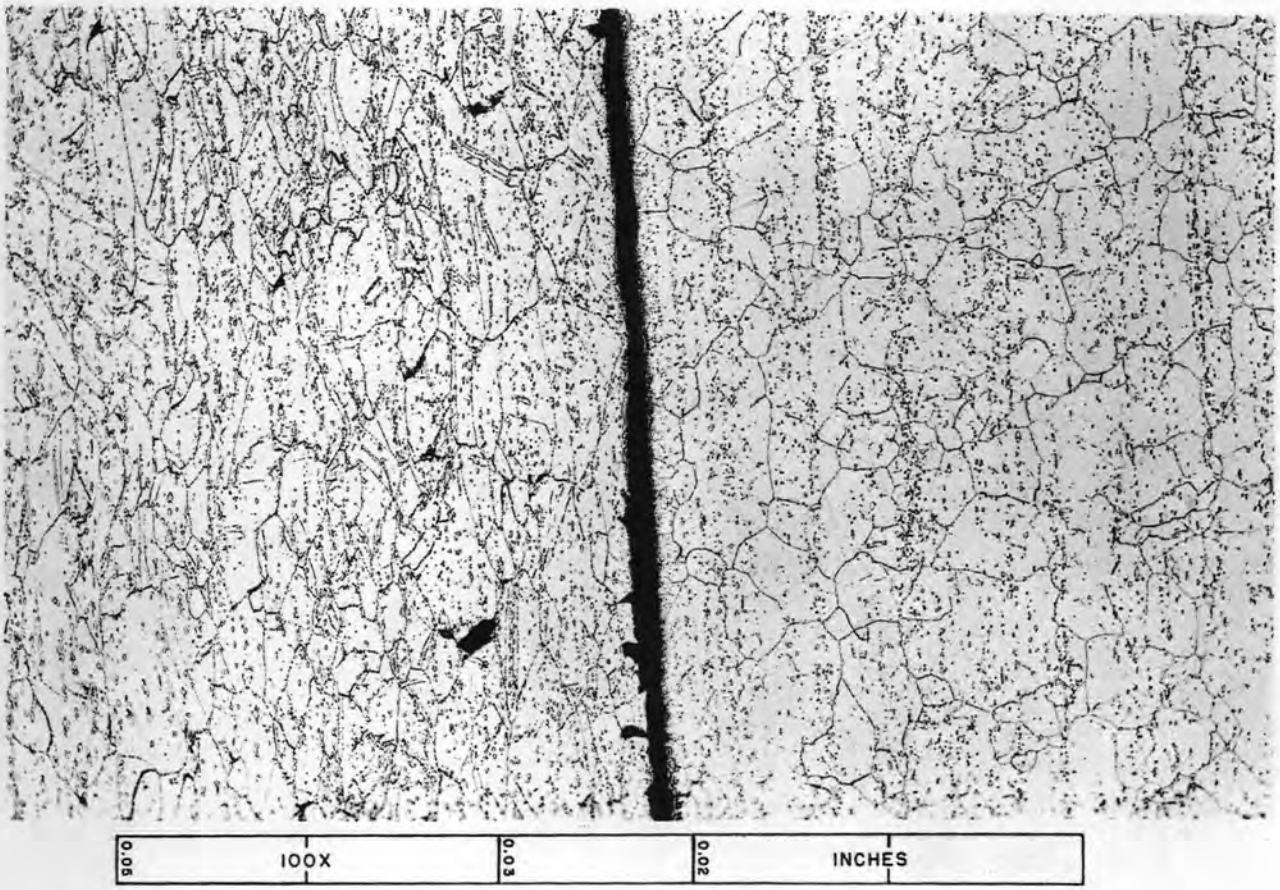

Fig. 34 (Y-19519) Hastelloy B Sheet Creep Tested in Argon at 18,000 PSI and 1500°F. Ruptured in 94 hr. 100X. Etchant: Chrome Regia.

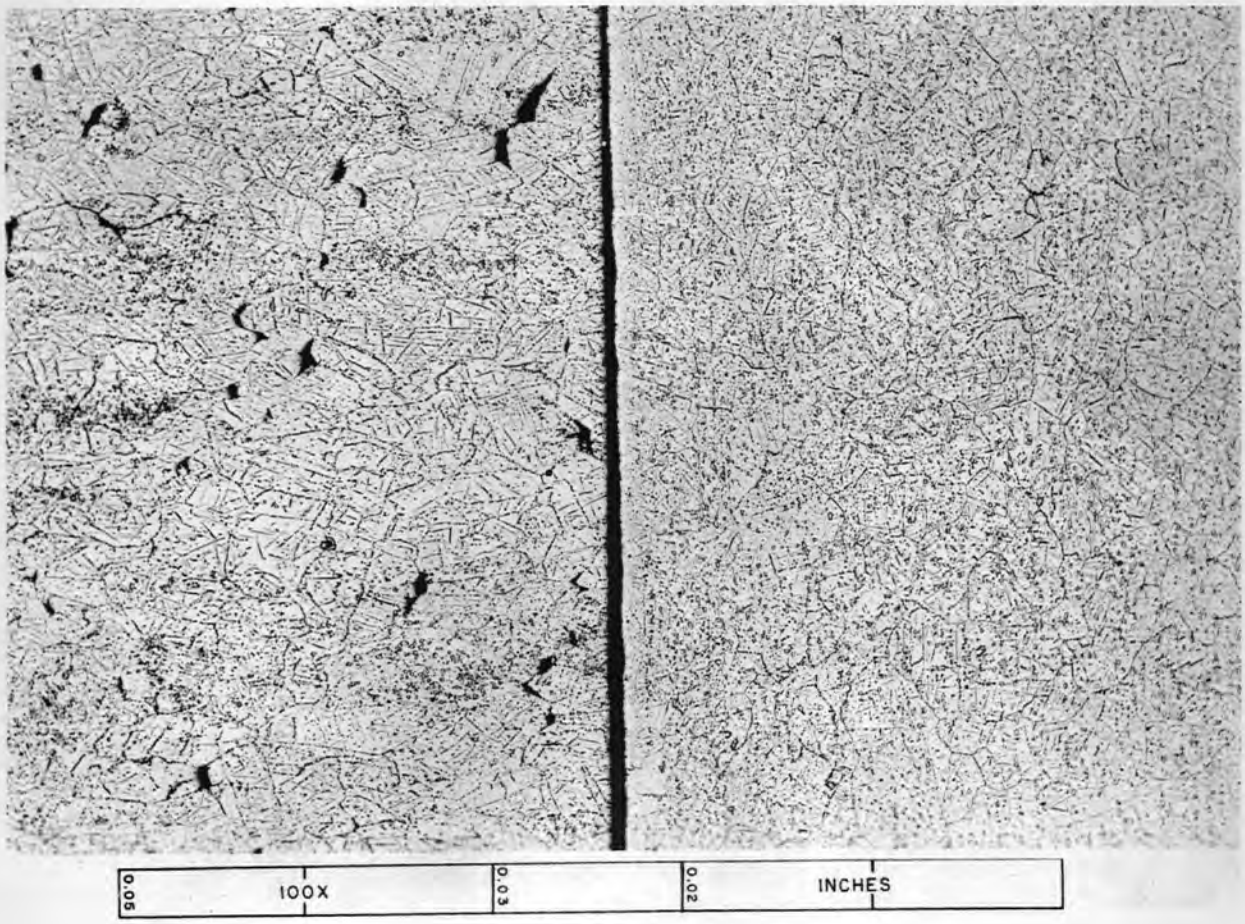

Fig. 35 (Y-17944) Hastelloy B Sheet Creep Tested in Argon at 12,000 PSI and 1500°F. Ruptured in 564 hr. 100X. Etchant: Chrome Regia.

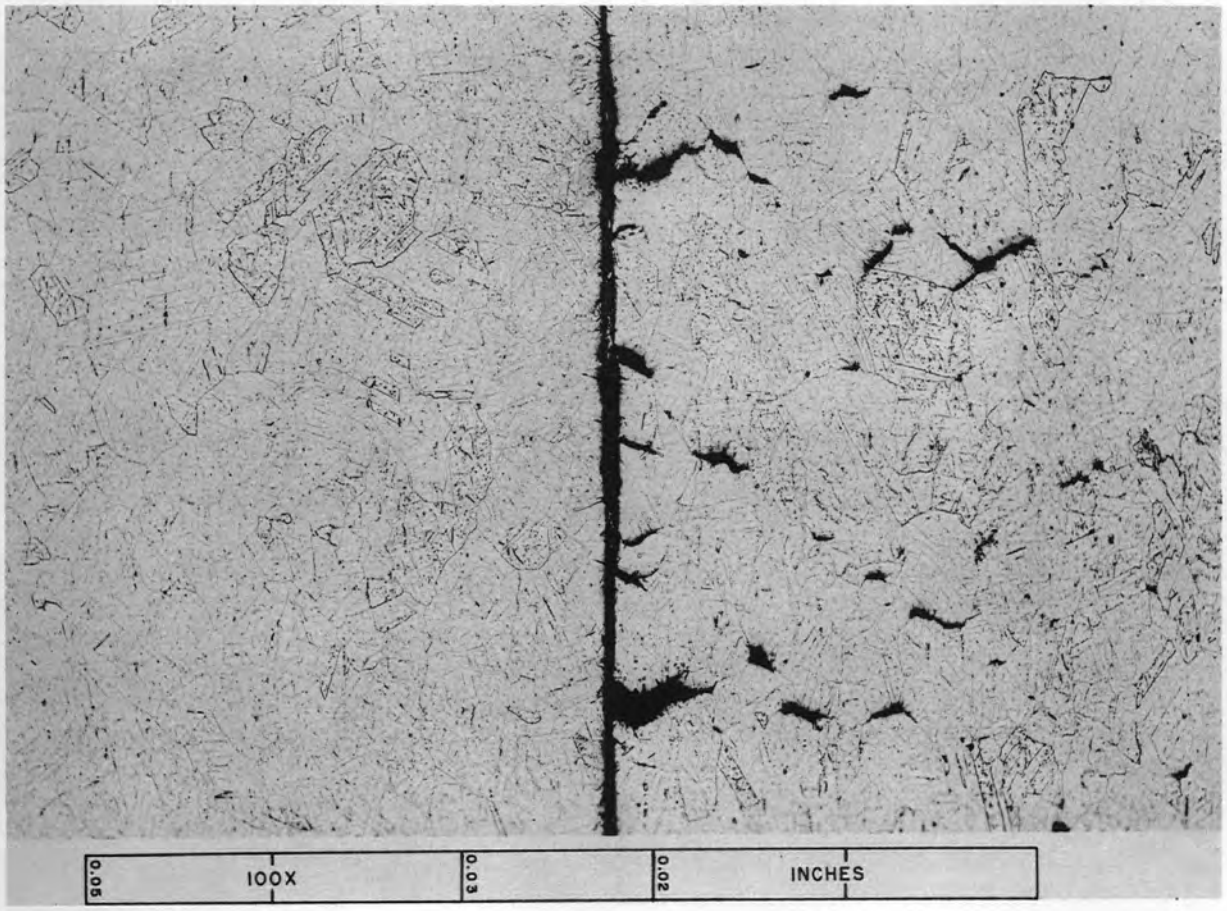

Fig. 36 (Y-15662) Hastelloy B Sheet Creep Tested in Argon at 11,000 PSI and 1500°F. Ruptured in 2,375 hr. 100X. Etchant: Chrome Regia.

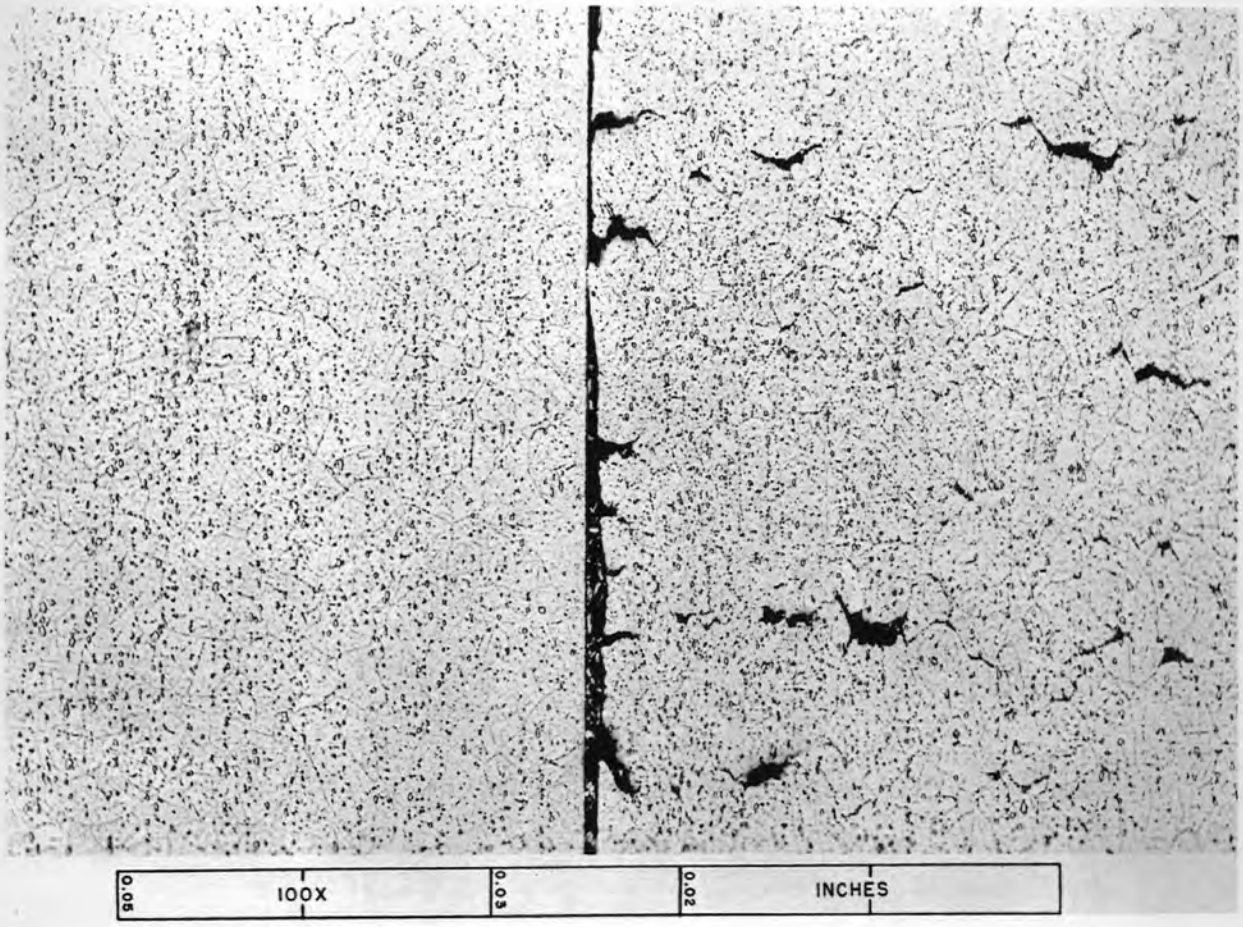

Fig. 37 (Y-17833) Hastelloy B Sheet Creep Tested in Argon at 10,000 PSI and 1650°F. Ruptured in 165 hr. 100X. Etchant: Chrome Regia.

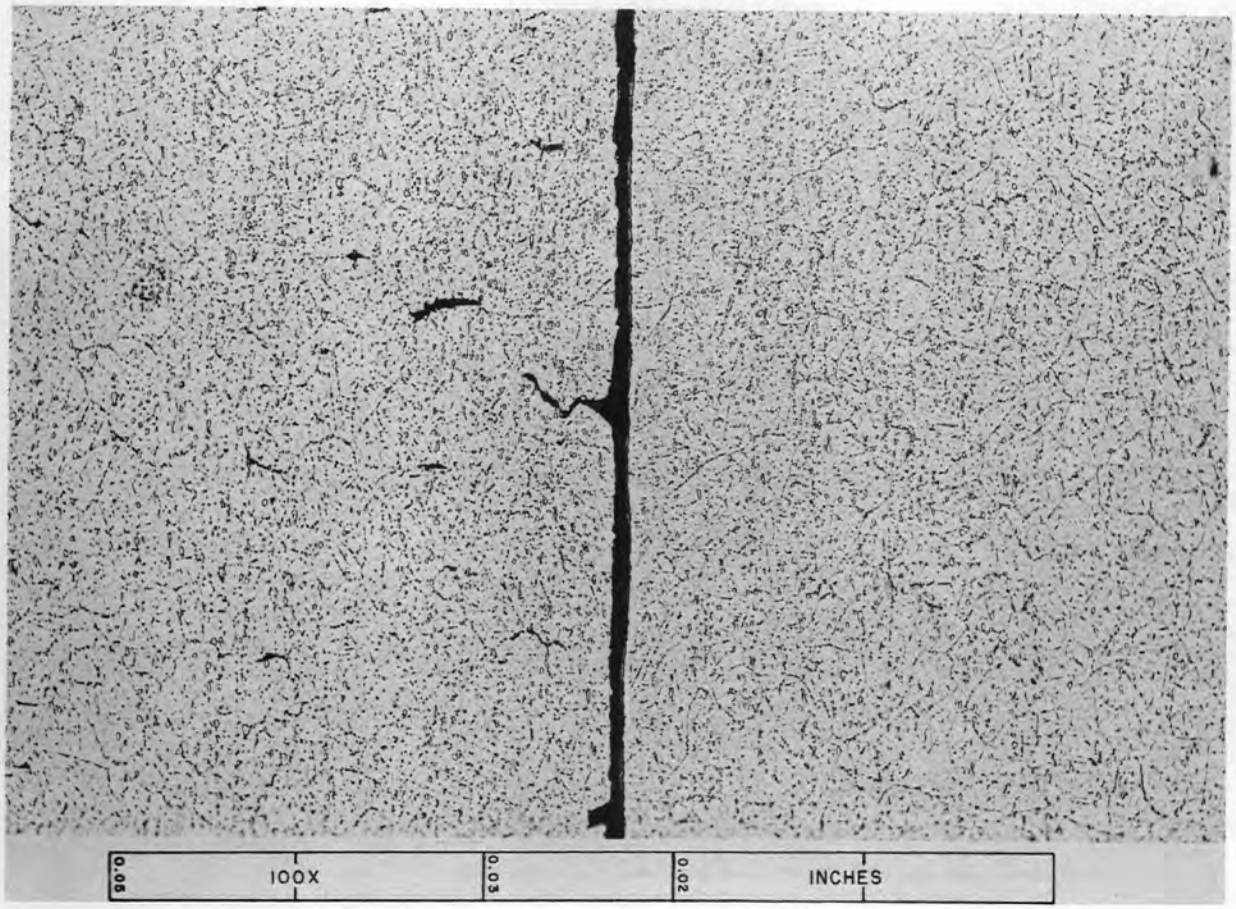

Fig. 38 (Y-17819) Hastelloy B Sheet Creep Tested in Argon at 7,500 PSI and 1650°F. Ruptured in 678 hr. 100X. Etchant: Chrome Regia.

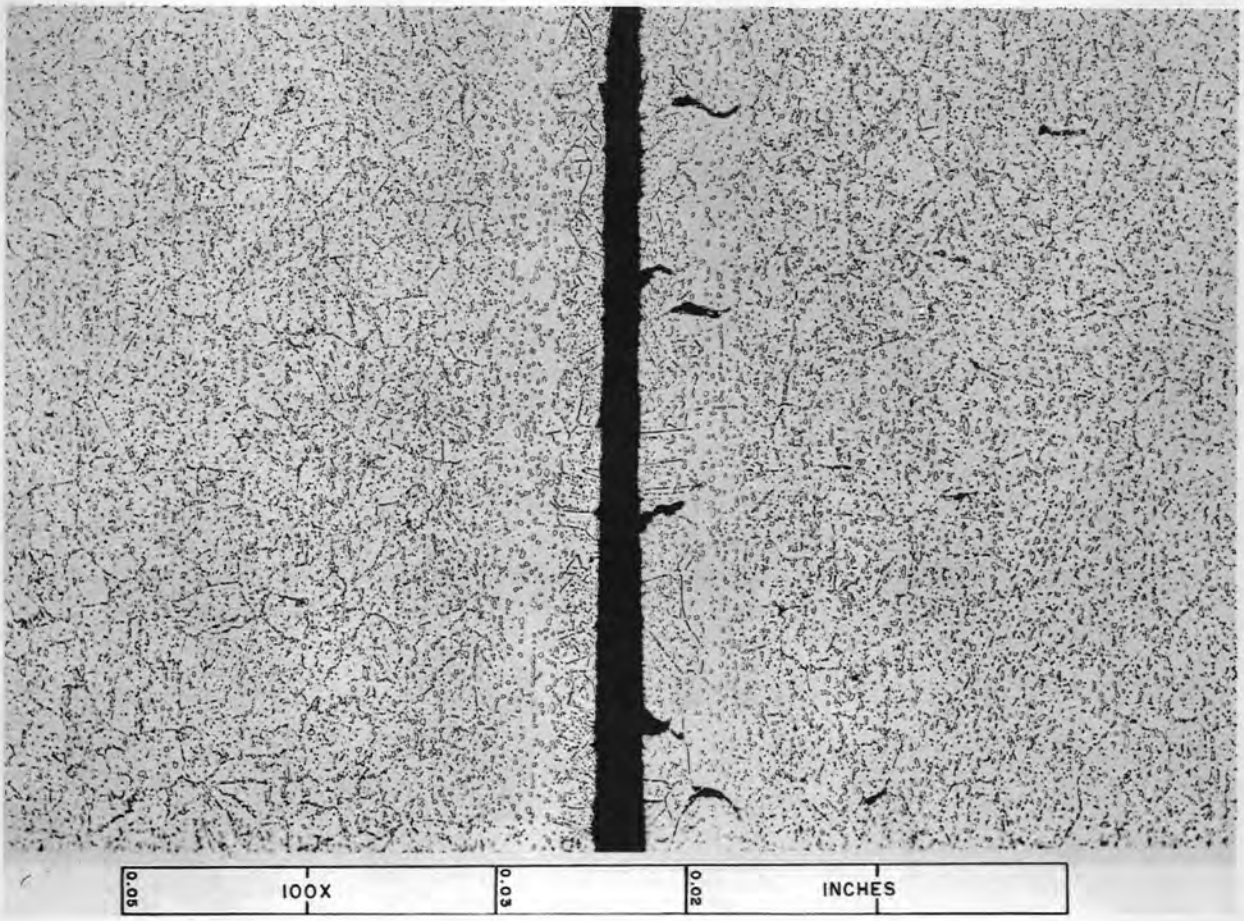

Fig. 39 (Y-20146) Hastelloy B Sheet Creep Tested in Argon at 5,000 PSI and 1650°F. Ruptured in 2,562 hr. 100X. Etchant: Chrome Regia.

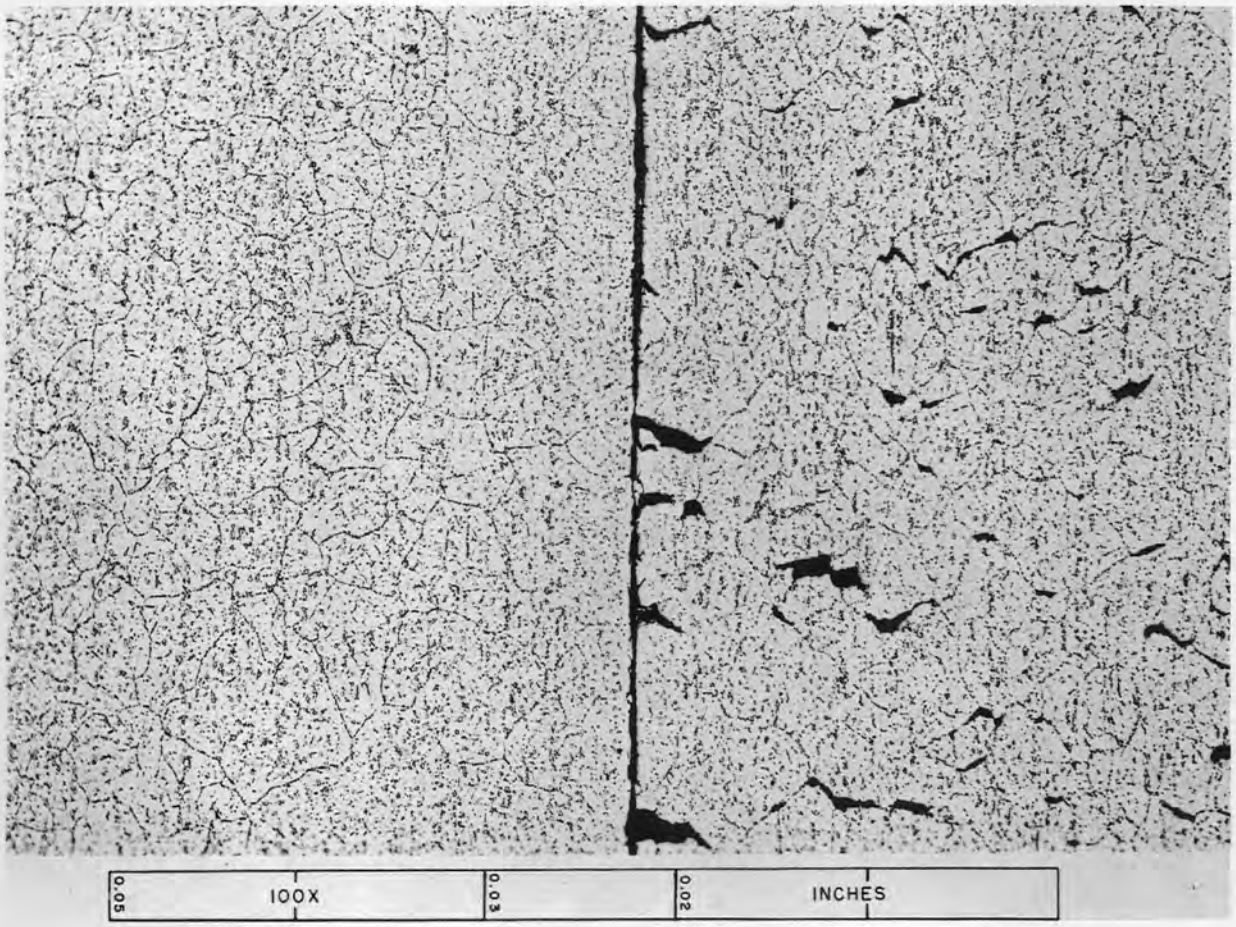

Fig. 40 (Y-19452) Hastelloy B Sheet Creep Tested in Argon at 7,000 PSI and 1800°F. Ruptured in 43 hr. 100X. Etchant: Chrome Regia.

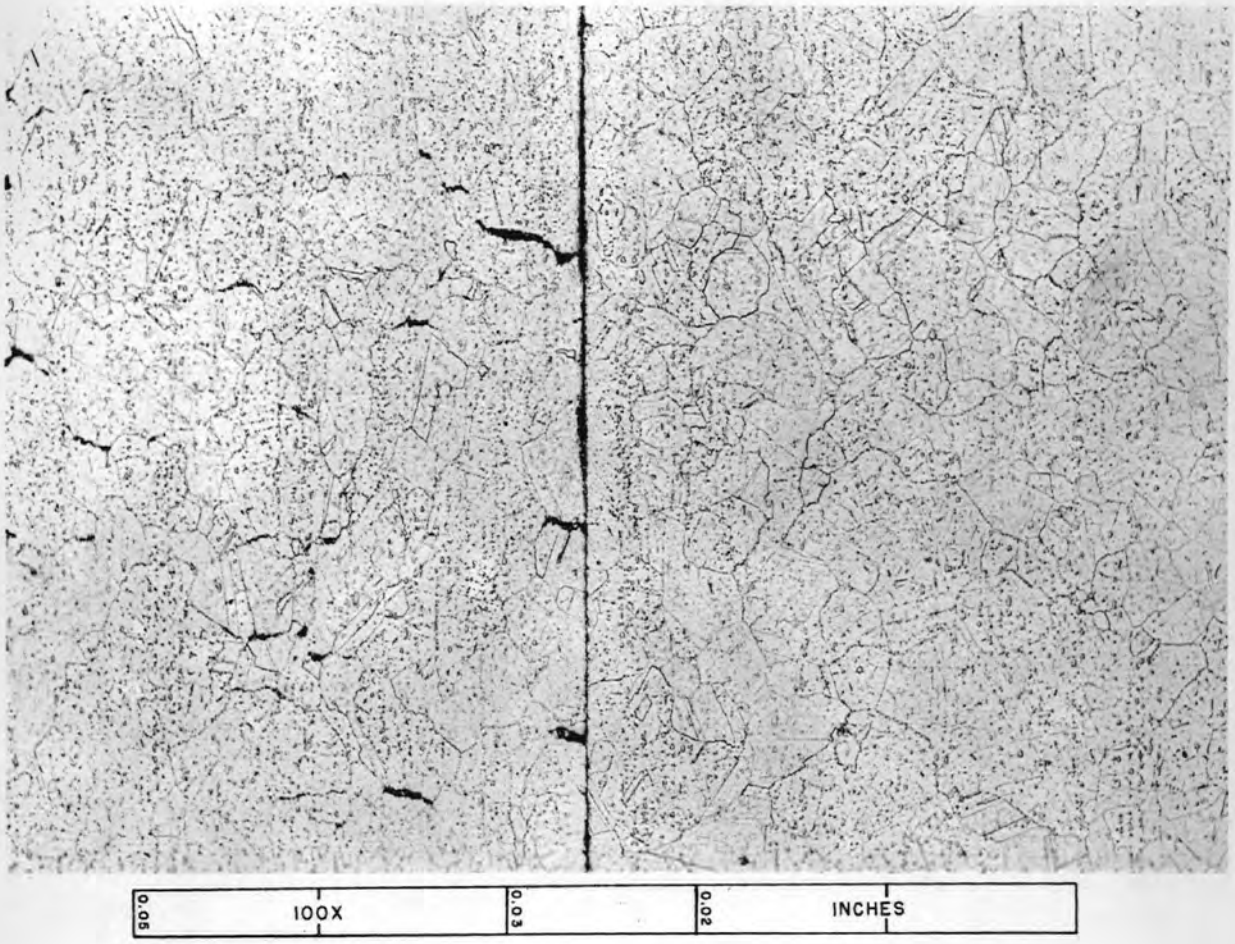

Fig. 41 (Y-15714) Hastelloy B Sheet Creep Tested in Argon at 5,000 PSI and 1800°F. Ruptured in 115 hr. 100X. Etchant: Chrome Regia.

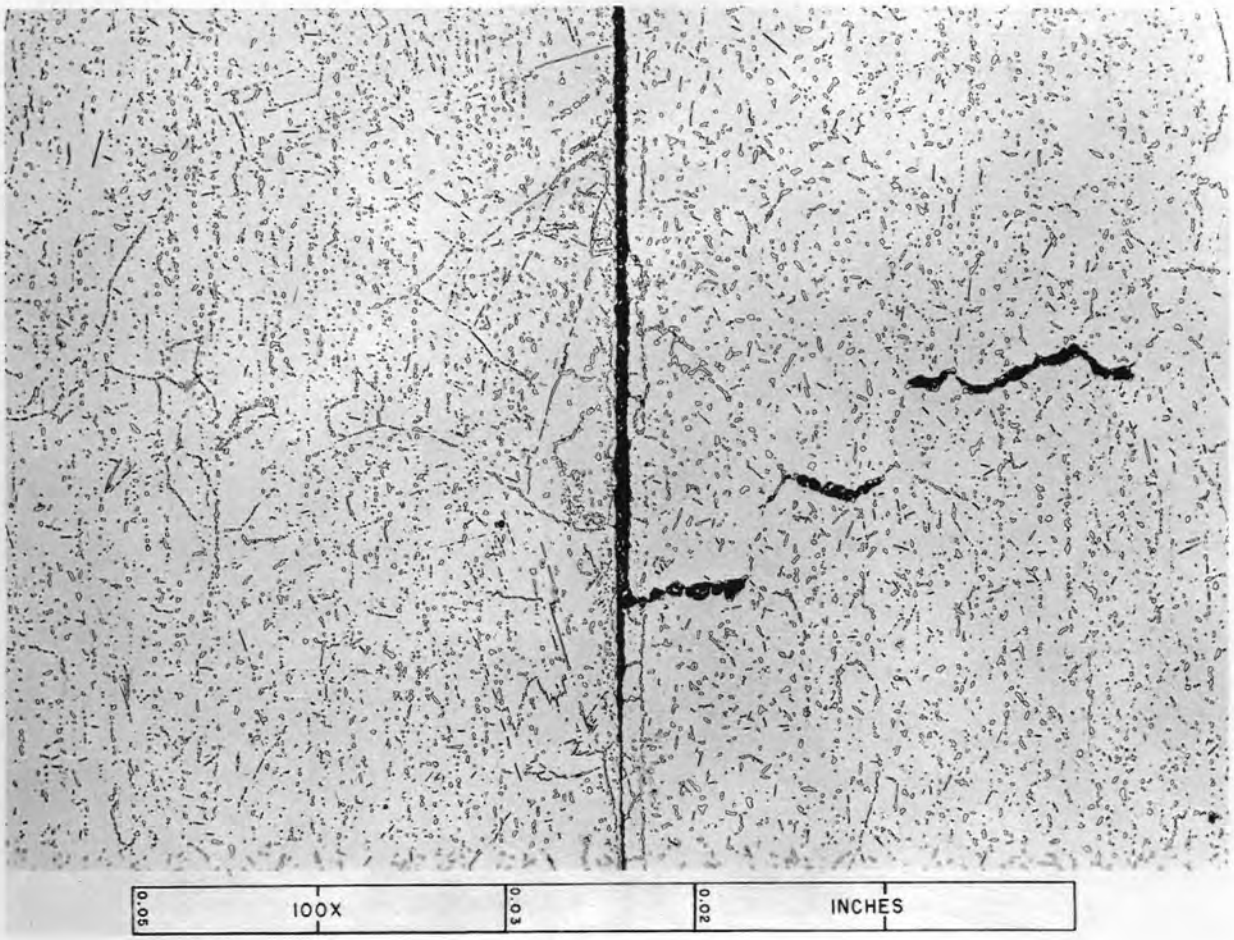

Fig. 42 (Y-17939) Hastelloy B Sheet Creep Tested in Argon at 2,500 PSI and 1800°F. Ruptured in 2,000 hr. 100X. Etchant: Chrome Regia.

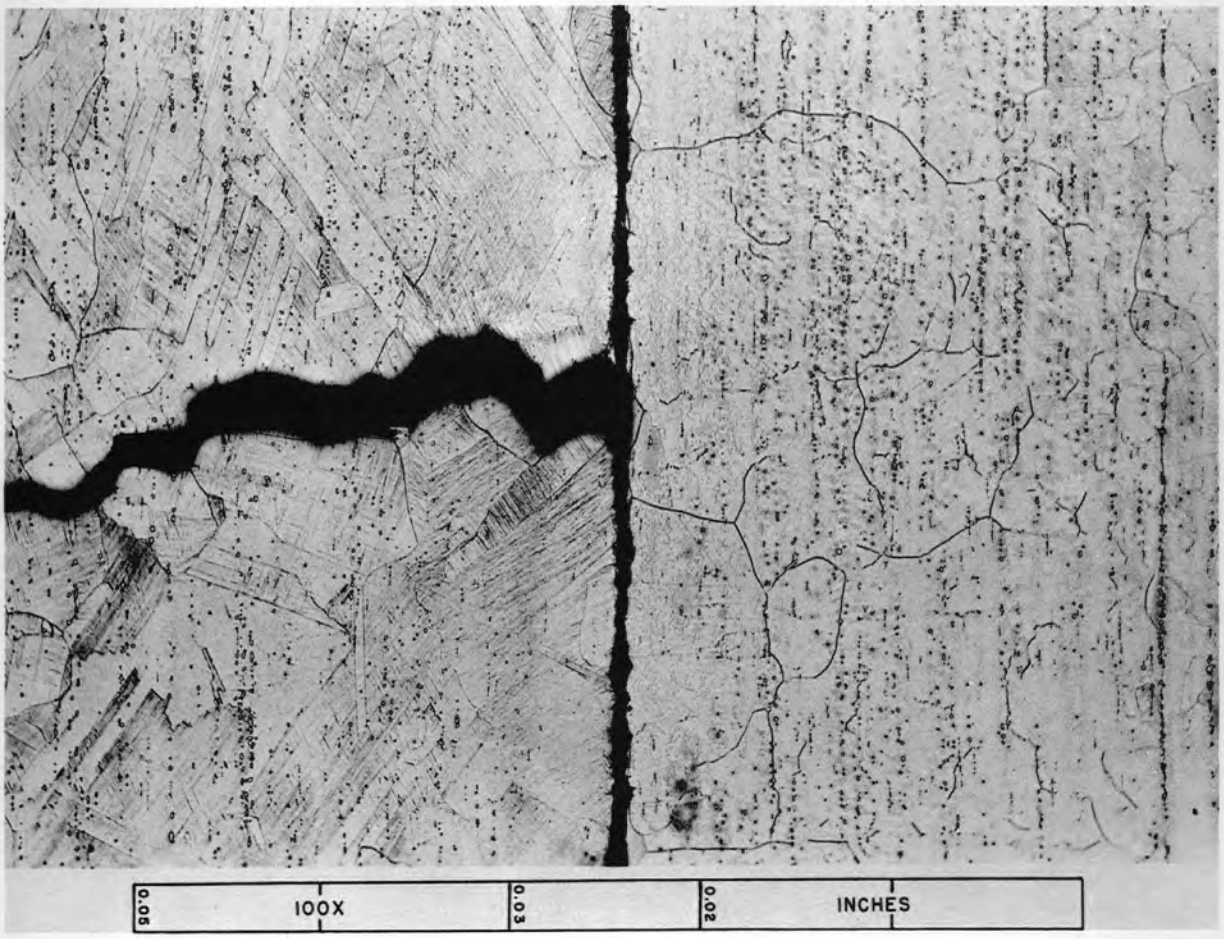

Fig. 43 (Y-16893) Hastelloy W Sheet Creep Tested in Argon at 35,000 PSI and 1300°F. Ruptured in 450 hr. 100X. Etchant: Chrome Regia.

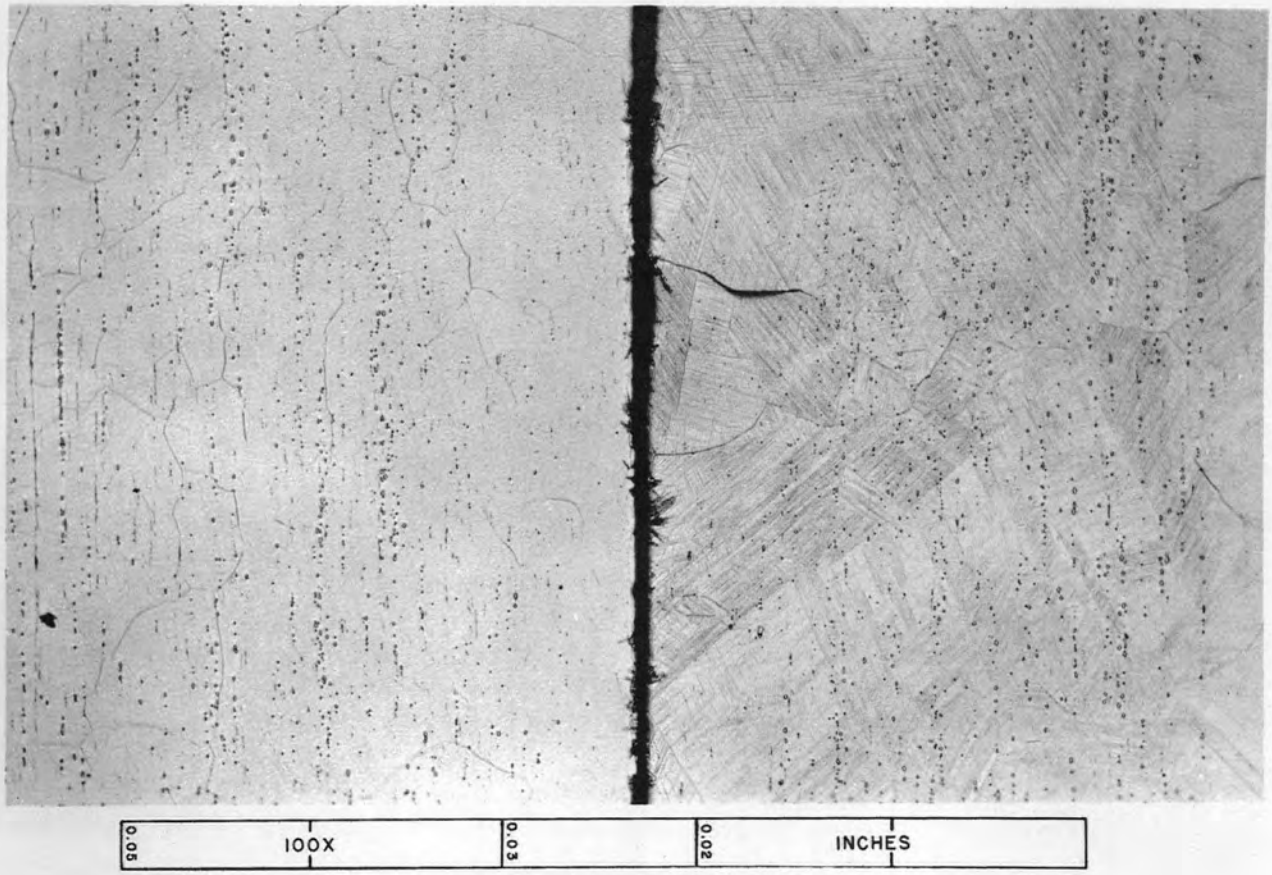

Fig. 44 (Y-18012) Hastelloy W Sheet Creep Tested in Argon at 30,000 PSI and 1300°F. Ruptured in 971 hr. 100X. Etchant: Chrome Regia.

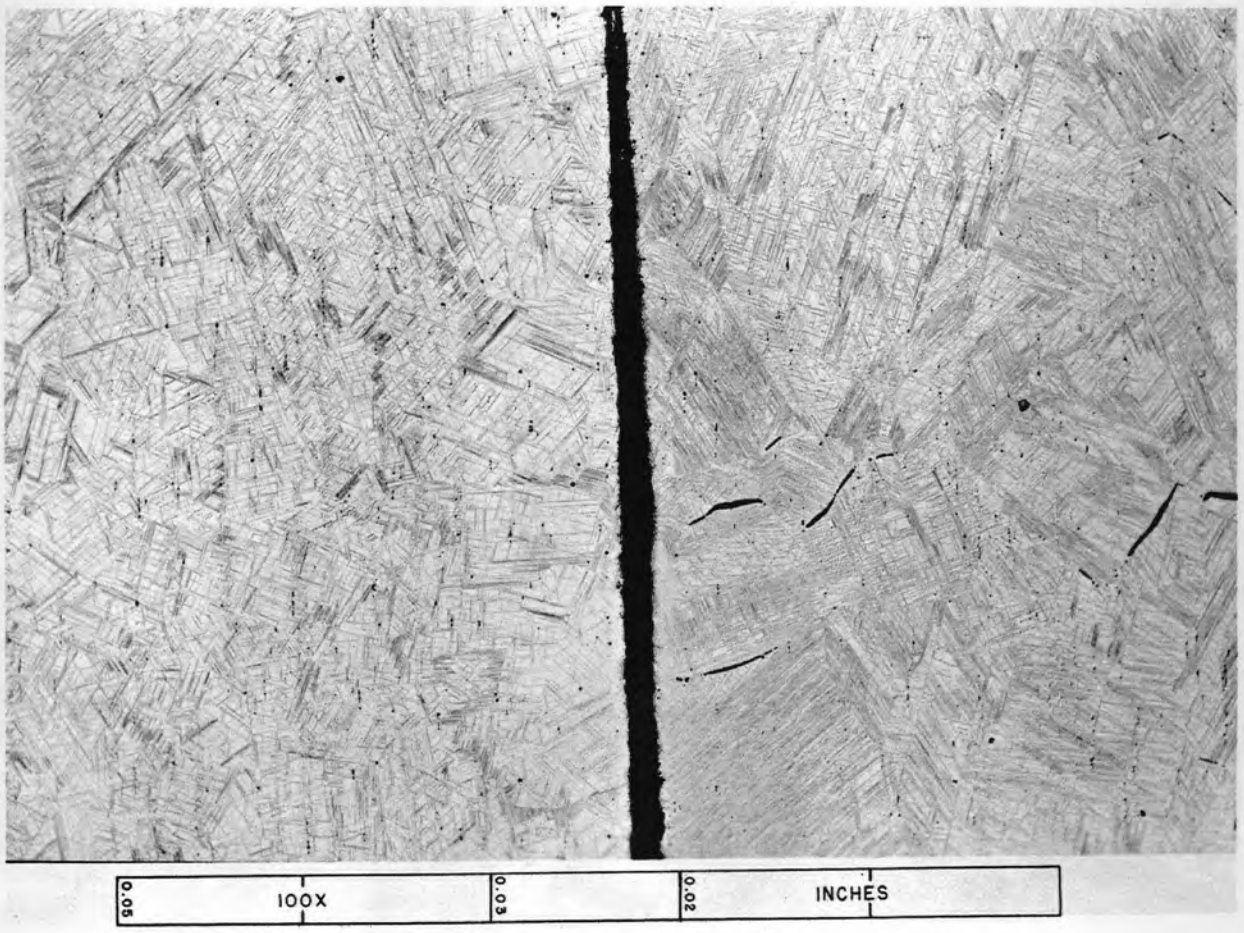

Fig. 45 (Y-18543) Hastelloy W Sheet Creep Tested in Argon at 25,000 PSI and 1300°F. Ruptured in 3,399 hr. 100X. Etchant: Chrome Regia.

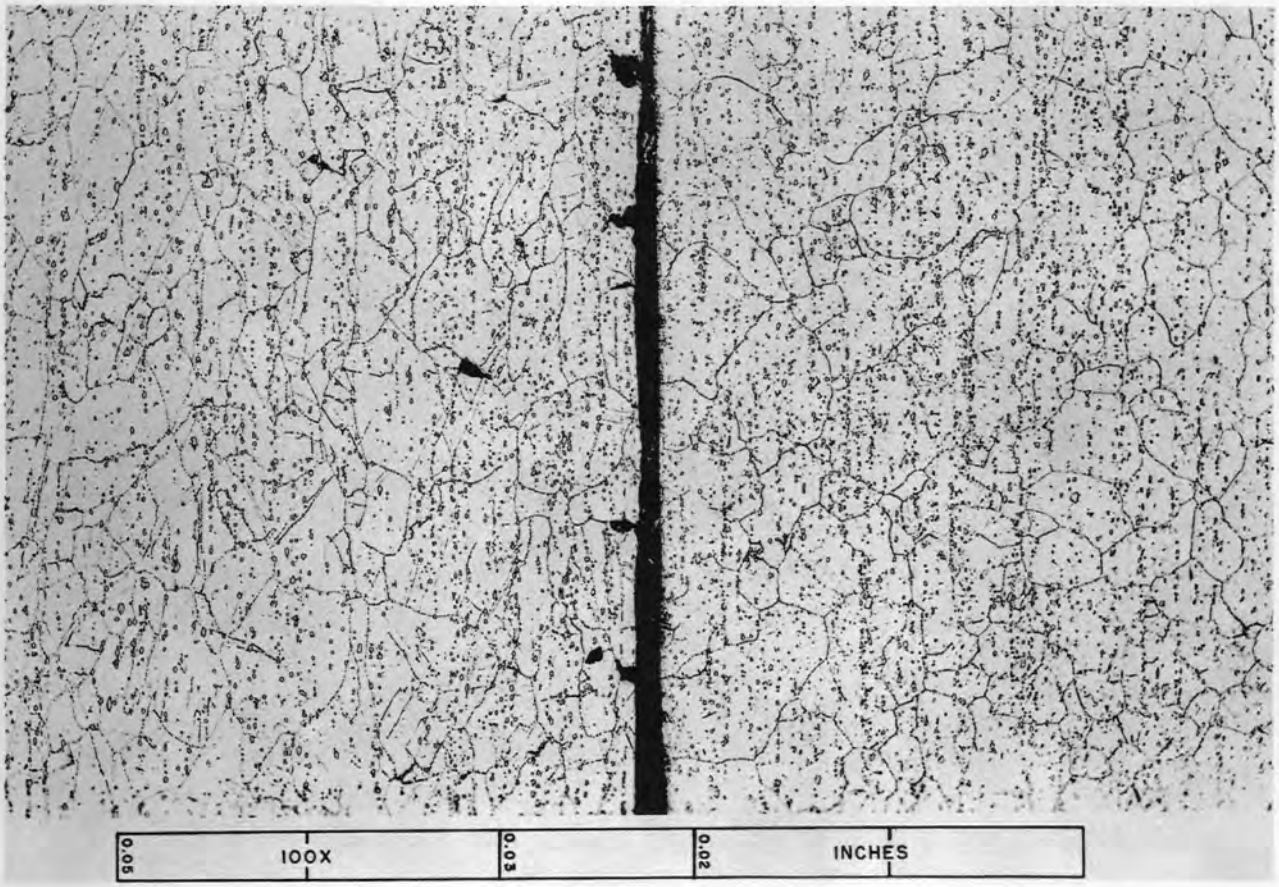

Fig. 46 (Y-19525) Hastelloy W Sheet Creep Tested in Argon at 25,000 PSI and 1400°F. Ruptured in 227 hr. 100X. Etchant: Chrome Regia.

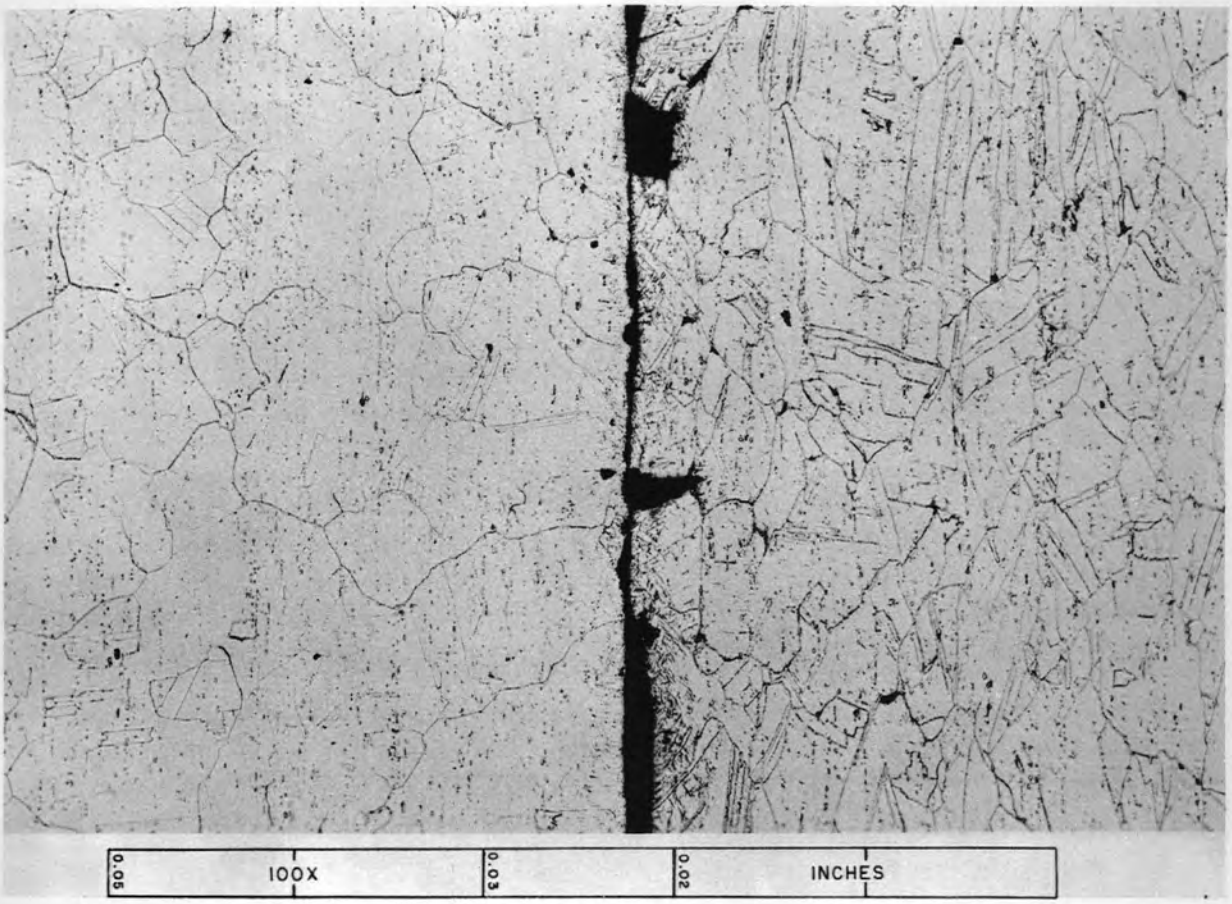

Fig. 47 (Y-19765) Hastelloy W Sheet Creep Tested in Argon at 20,000 PSI and 1400°F. Ruptured in 451 hr. 100X. Etchant: Chrome Regia.

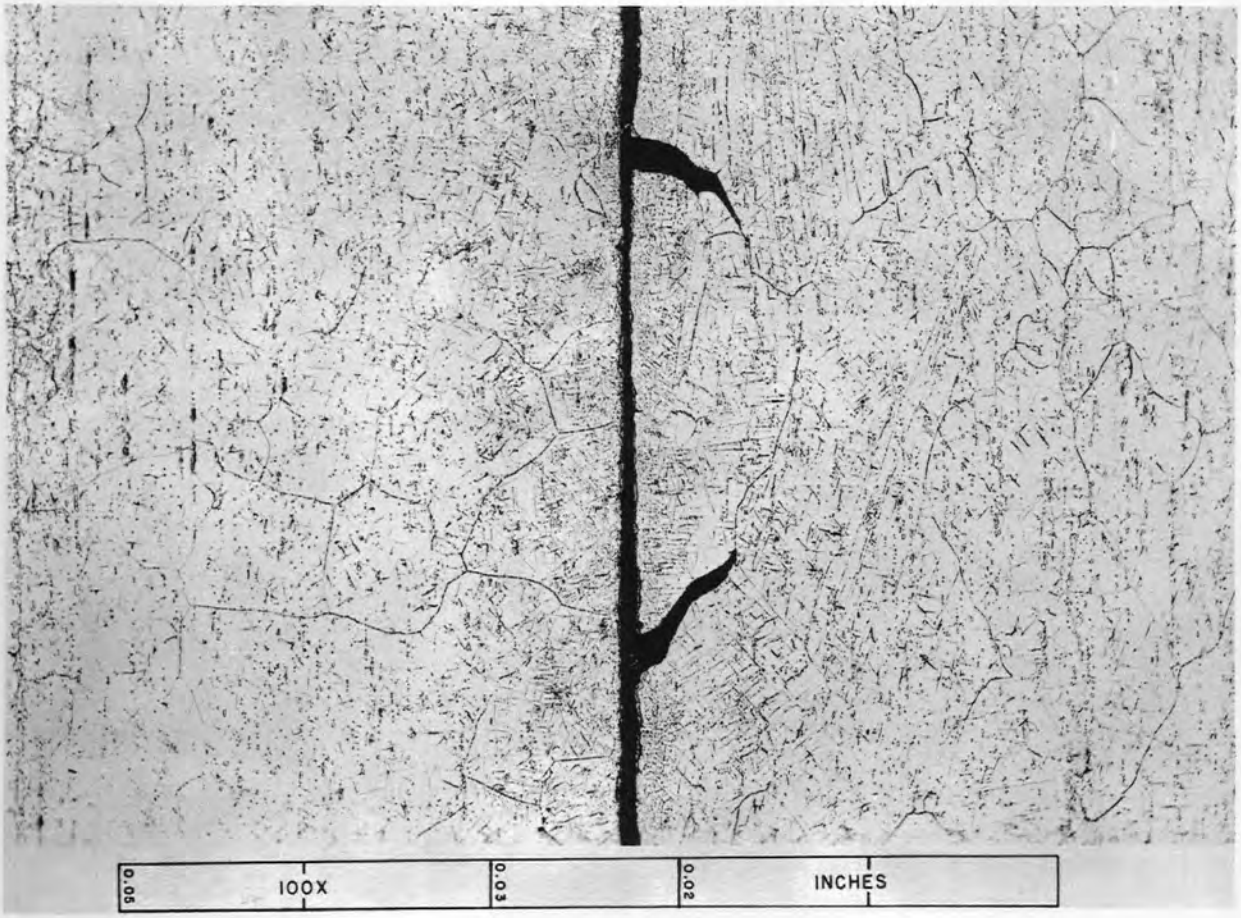

Fig. 48 (Y-17968) Hastelloy W Sheet Creep Tested in Argon at 12,000 PSI and 1500°F. Ruptured in 520 hr. 100X. Etchant: Chrome Regia.

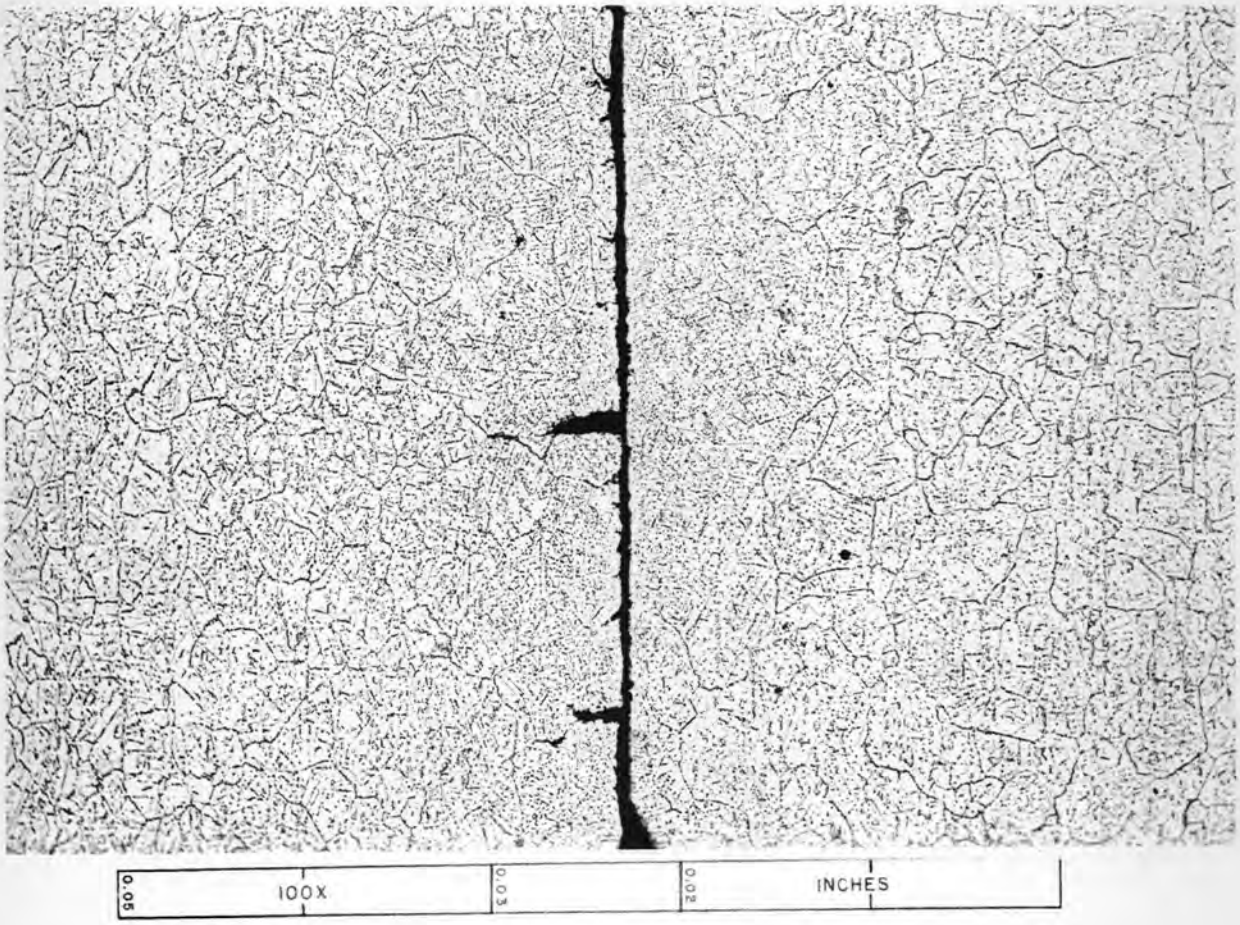

Fig. 49 (Y-19450) Hastelloy W Sheet Creep Tested in Argon at 10,000 PSI and 1500°F. Ruptured in 3,112 hr. 100X. Etchant: Chrome Regia.

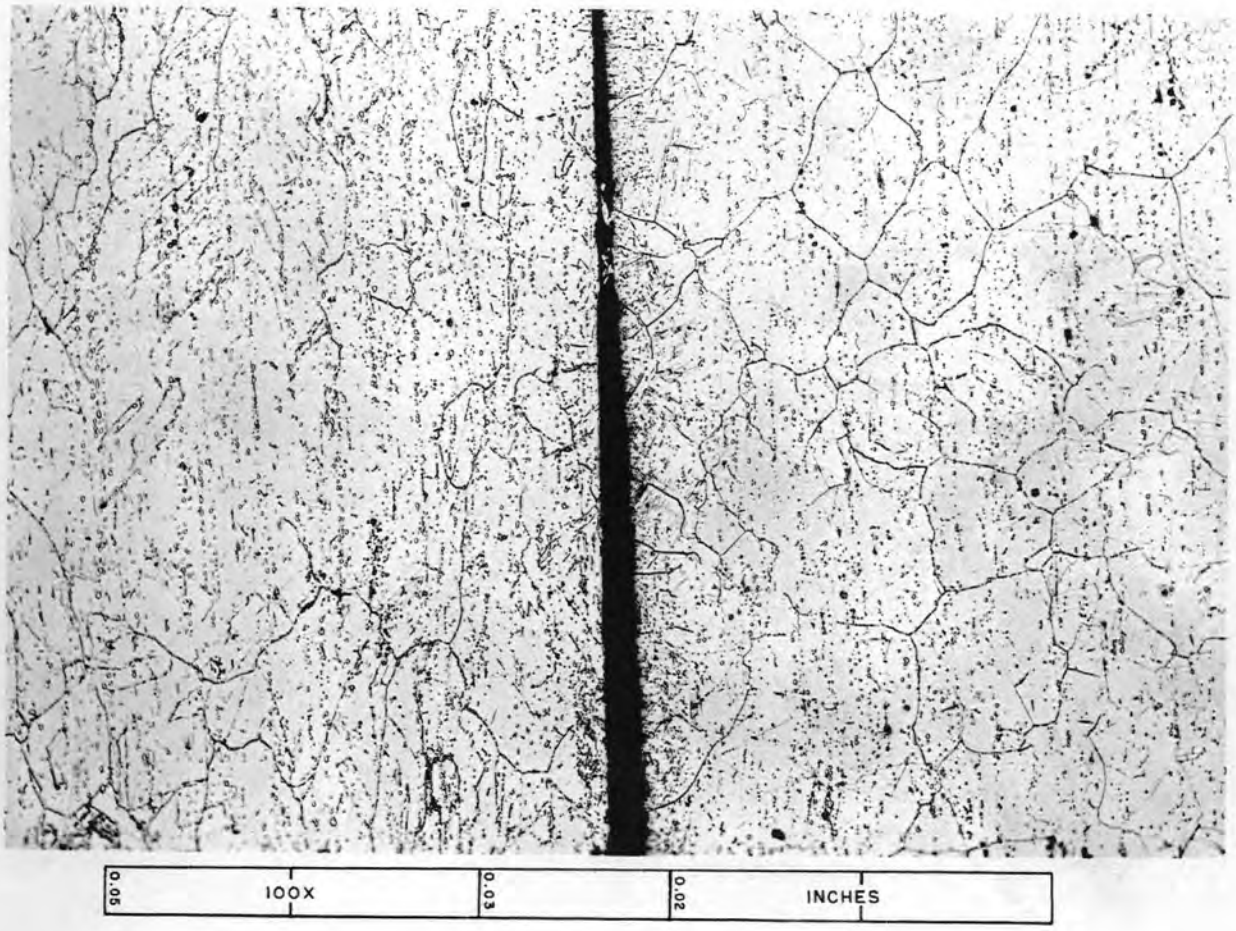

Fig. 50 (Y-19455) Hastelloy W Sheet Creep Tested in Argon at 12,000 PSI and 1650°F. Ruptured in 107 hr. 100X. Etchant: Chrome Regia.

Fig. 51 (Y-17946) Hastelloy W Sheet Creep Tested in Argon at 6,500 PSI and 1650°F. Ruptured in 1,098 hr. 100X. Etchant: Chrome Regia.

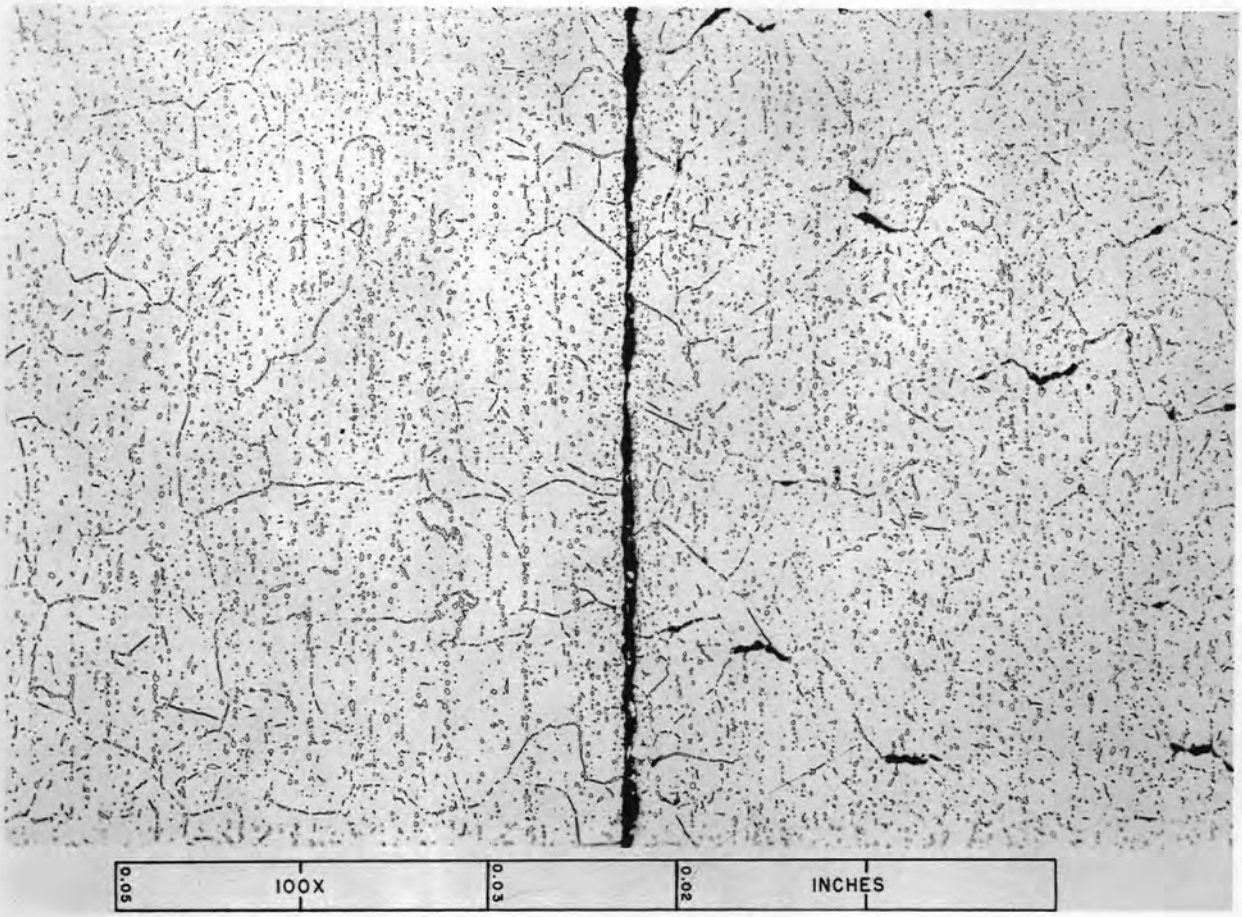

Fig. 52 (Y-19762) Hastelloy W Sheet Creep Tested in Argon at 4,000 PSI and 1800°F. Ruptured in 363 hr. 100X. Etchant: Chrome Regia.

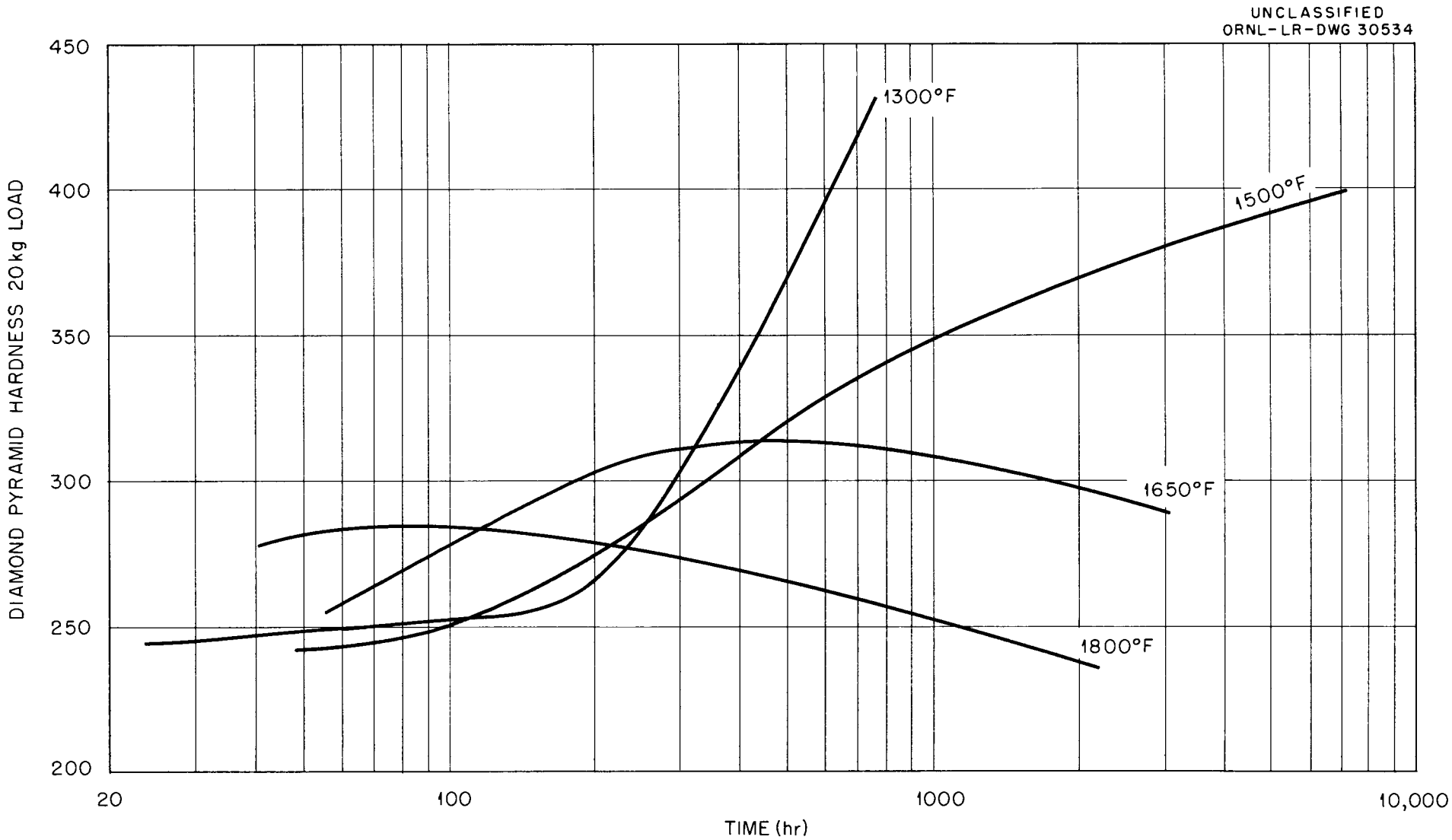

Fig. 53. Room Temperature Hardness of Hastelloy B vs. Aging Time at Temperatures of 1300, 1500, 1650, and 1800°F.

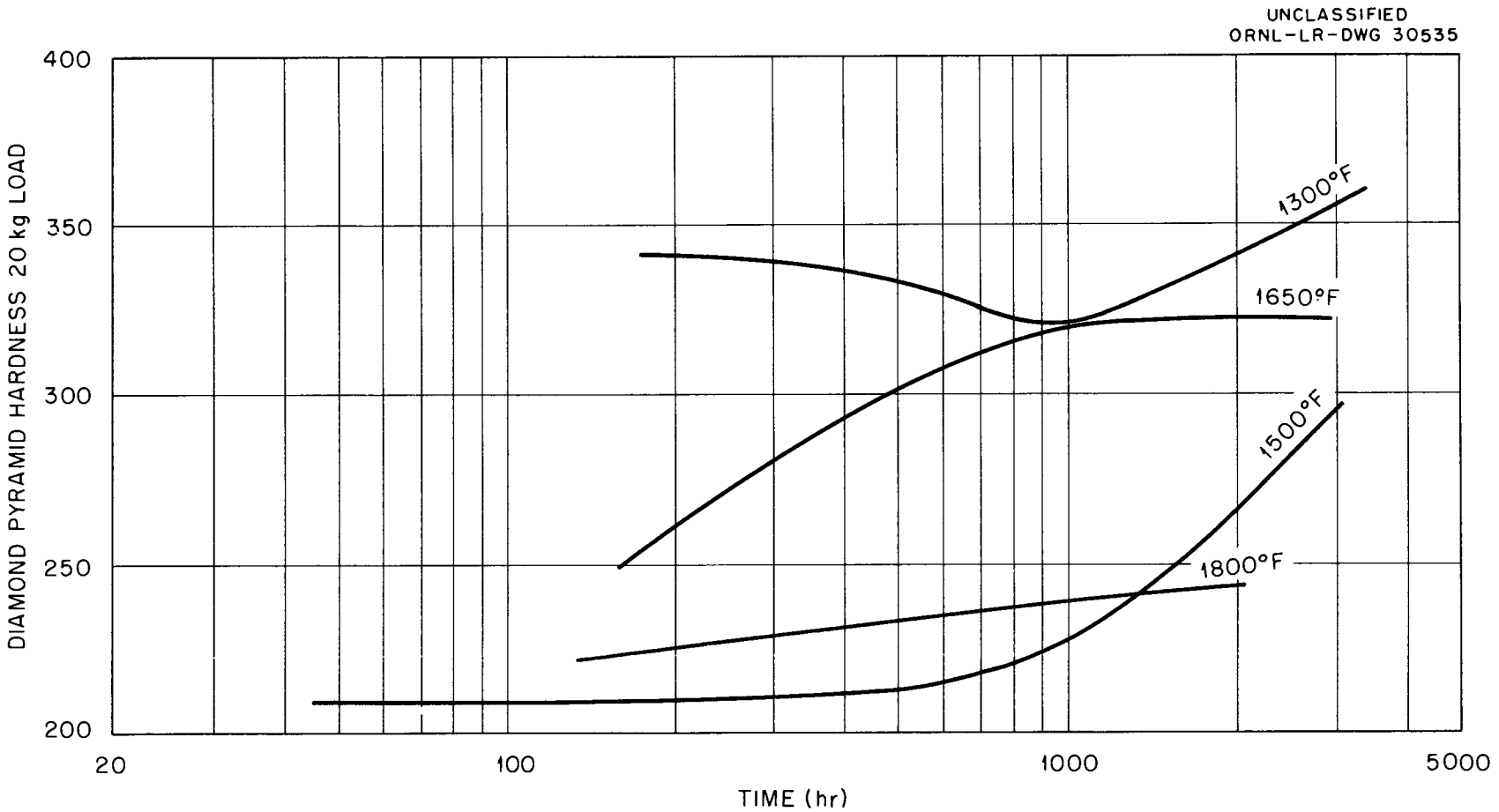

Fig. 54. Room Temperature Hardness of Hastelloy W vs. Aging Time at Temperatures of 1300, 1500, 1650, and 1800°F.

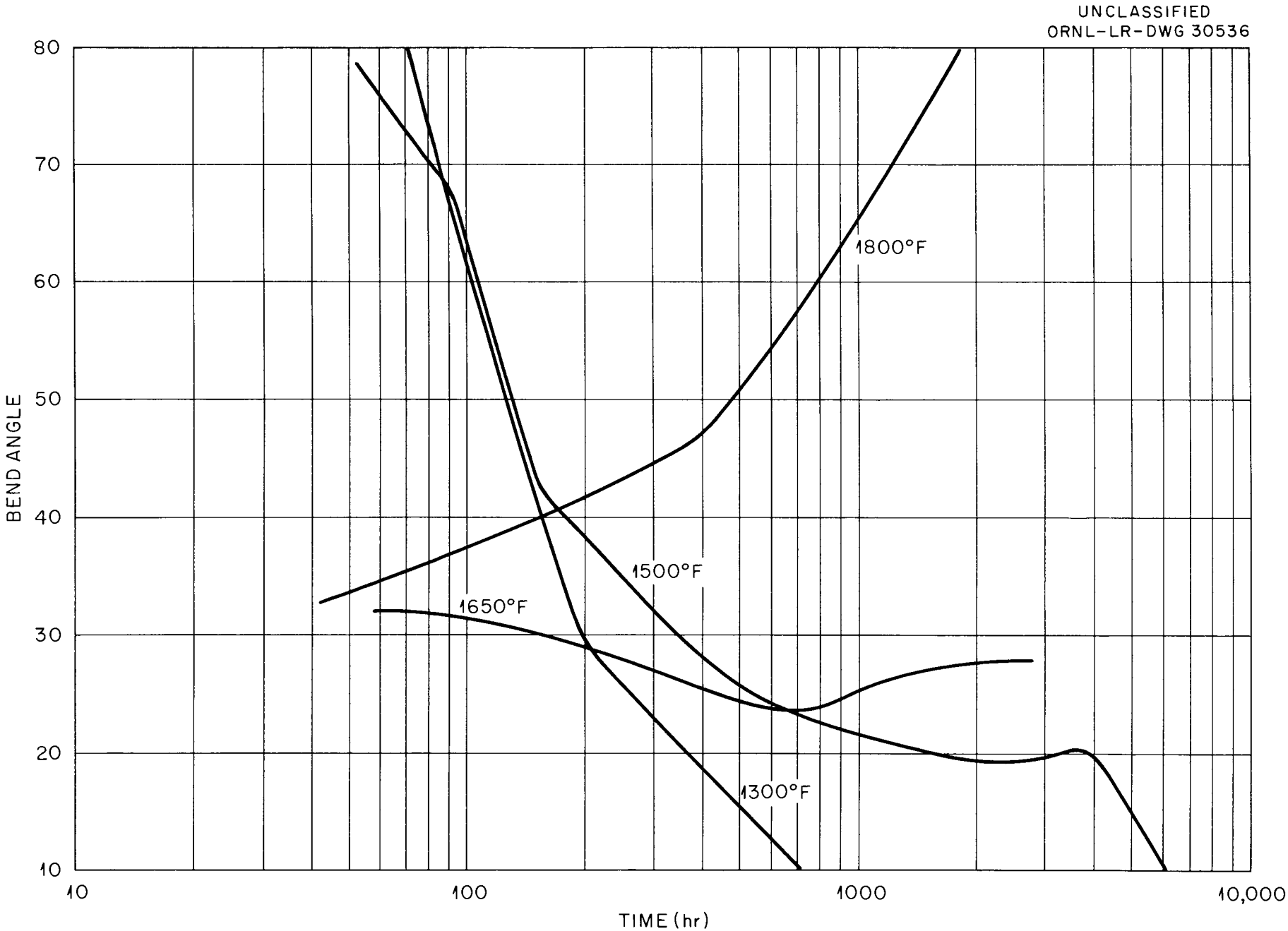

Fig. 55. Bend Angle of Hastelloy B vs. Aging Time at Temperatures of 1300, 1500, 1650 and 1800°F.

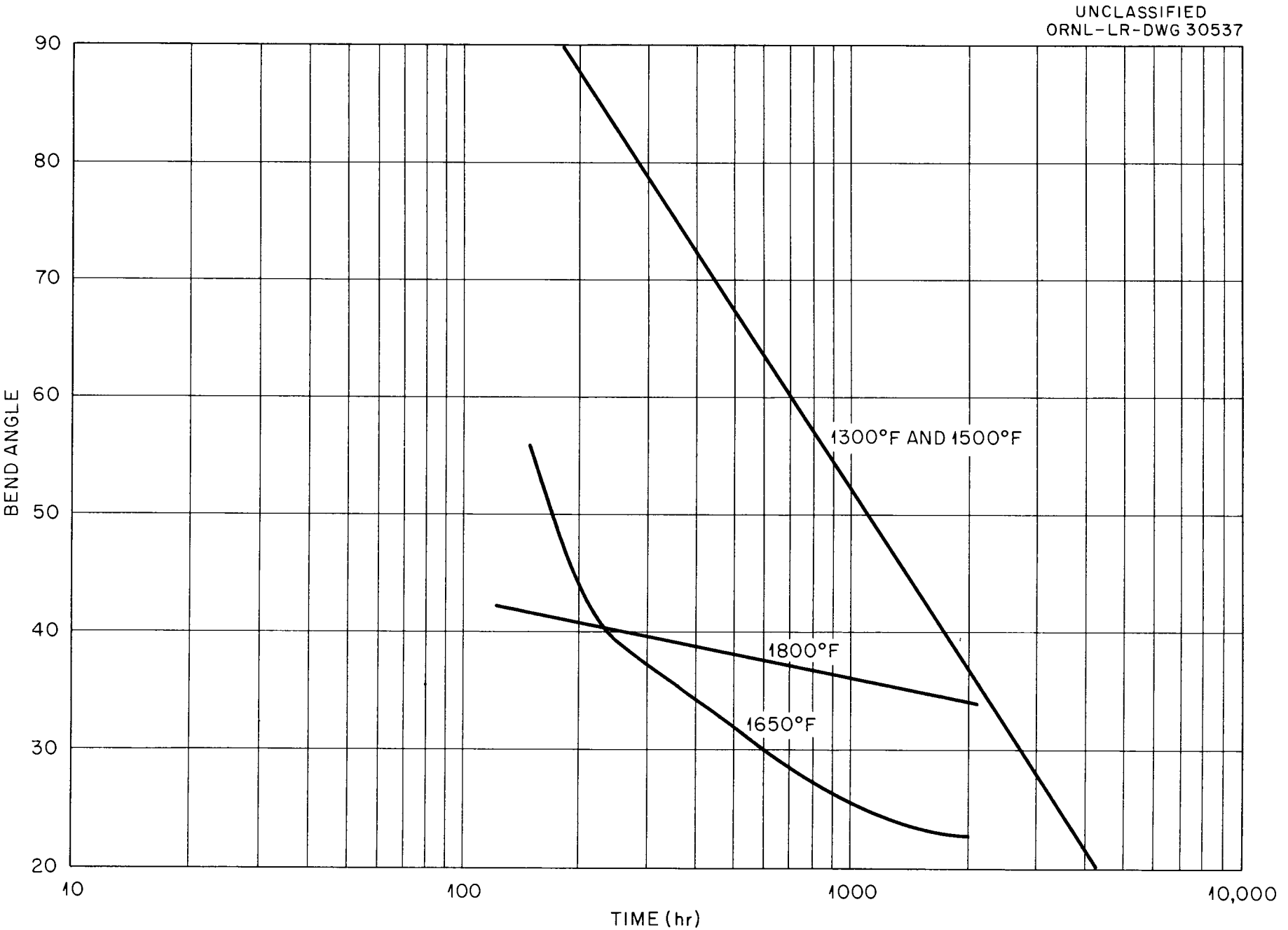

Fig. 56. Bend Angle of Hastelloy W vs. Aging Time at Temperatures of 1300, 1500, 1650 and 1800°F.

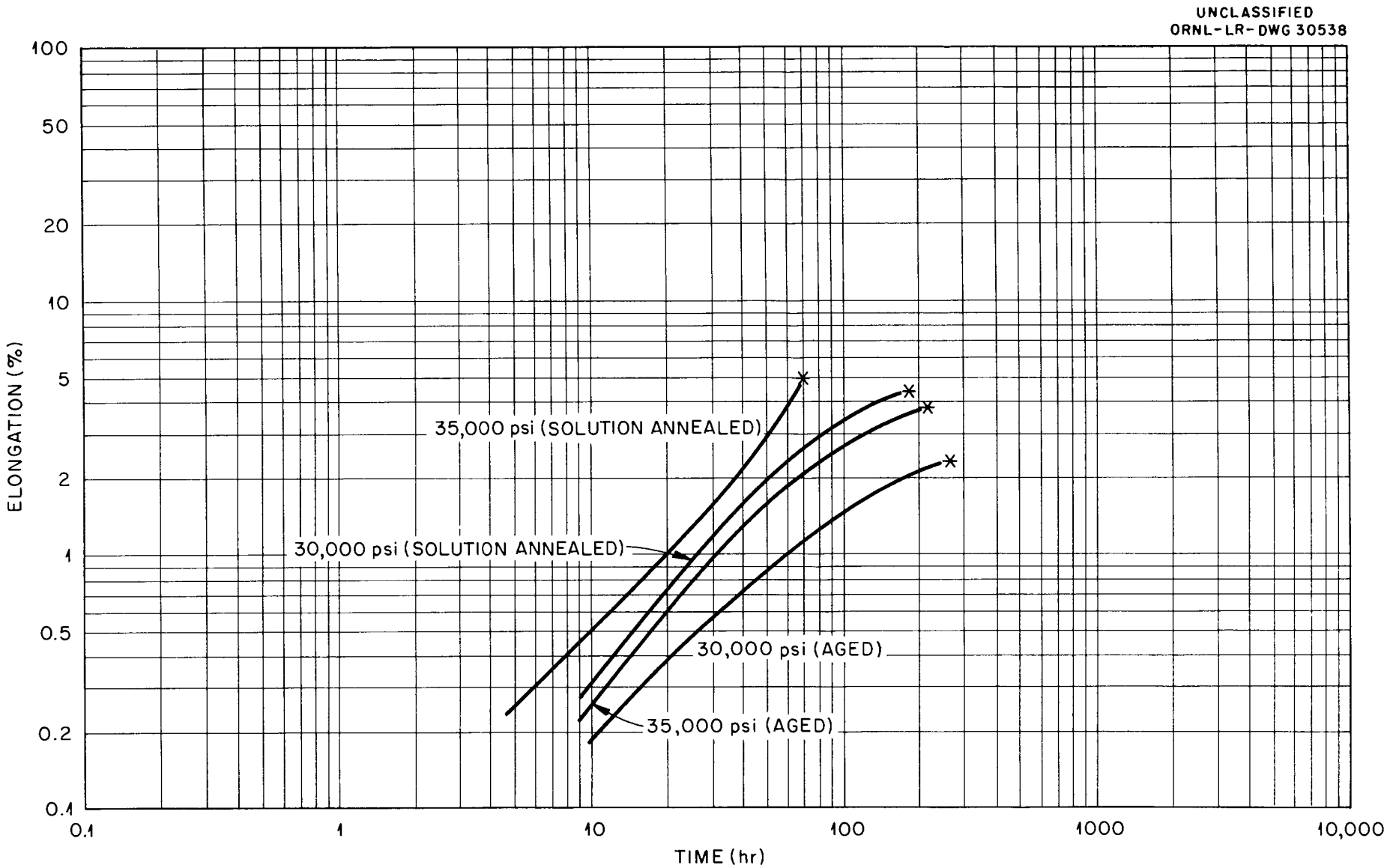

Fig. 57. Creep-Rupture Curves of Solution-Annealed and Aged Hastelloy B Sheet Tested in Argon at 1300°F, Aging Time 100 hr at 1300°F.

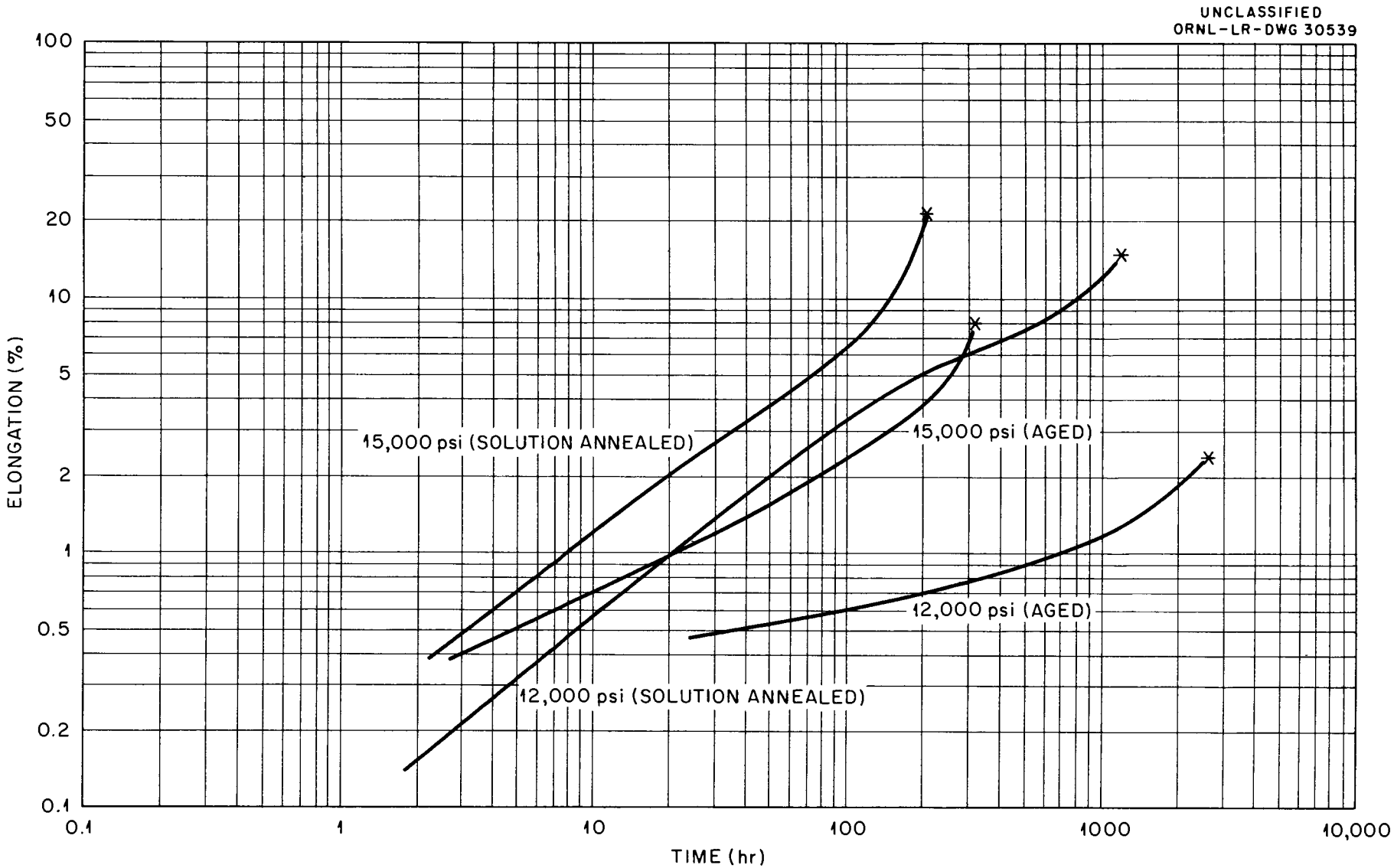

Fig. 58. Creep-Rupture Curves of Solution-Annealed and Aged Hastelloy B Sheet Tested in Argon at 1500°F, Aging Time 100 hr at 1300°F.

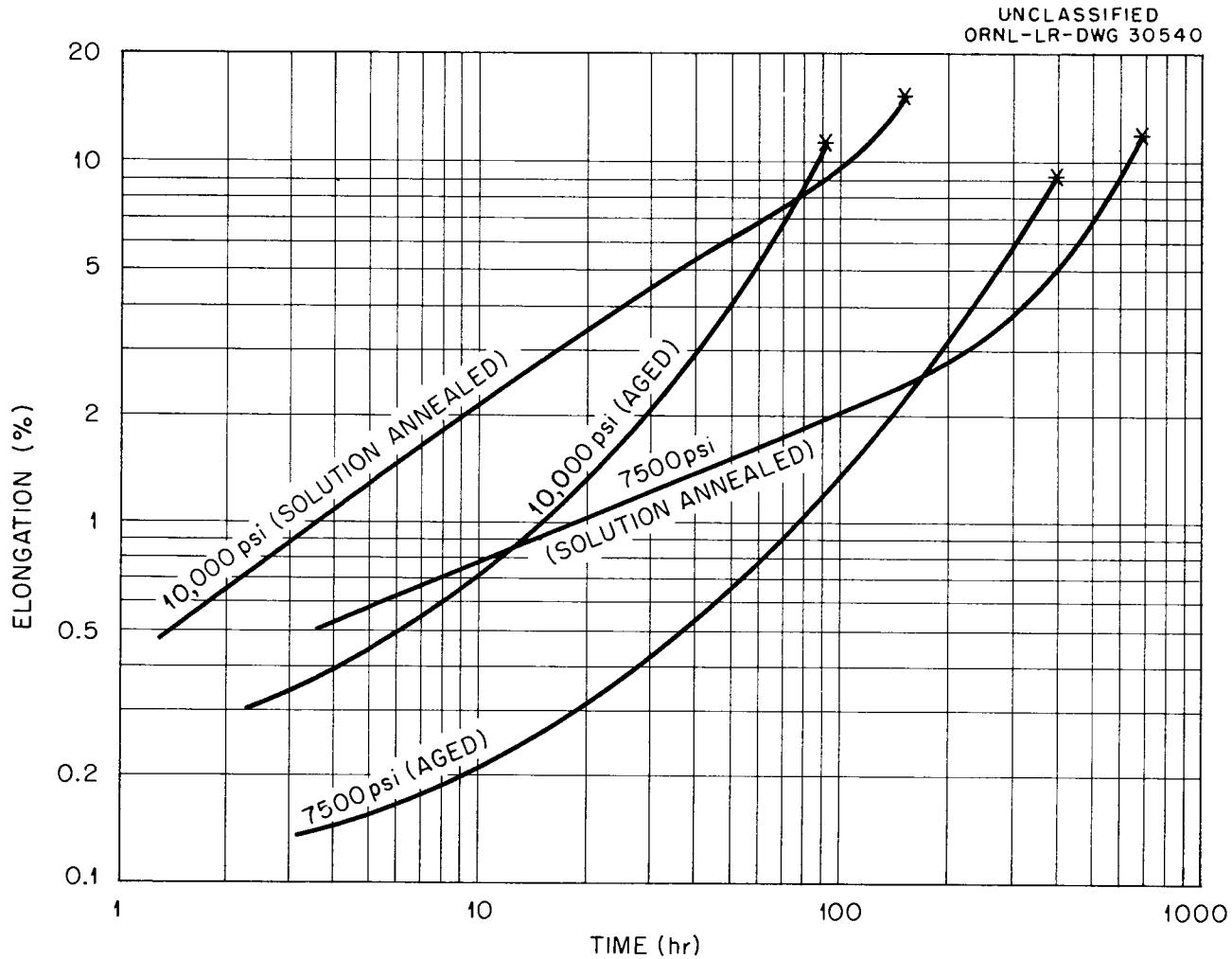

Fig. 59. Creep-Rupture Curves of Solution-Annealed and Aged Hastelloy B Sheet Tested in Argon at 1650°F. Aging Time 100 hr at 1300°F.

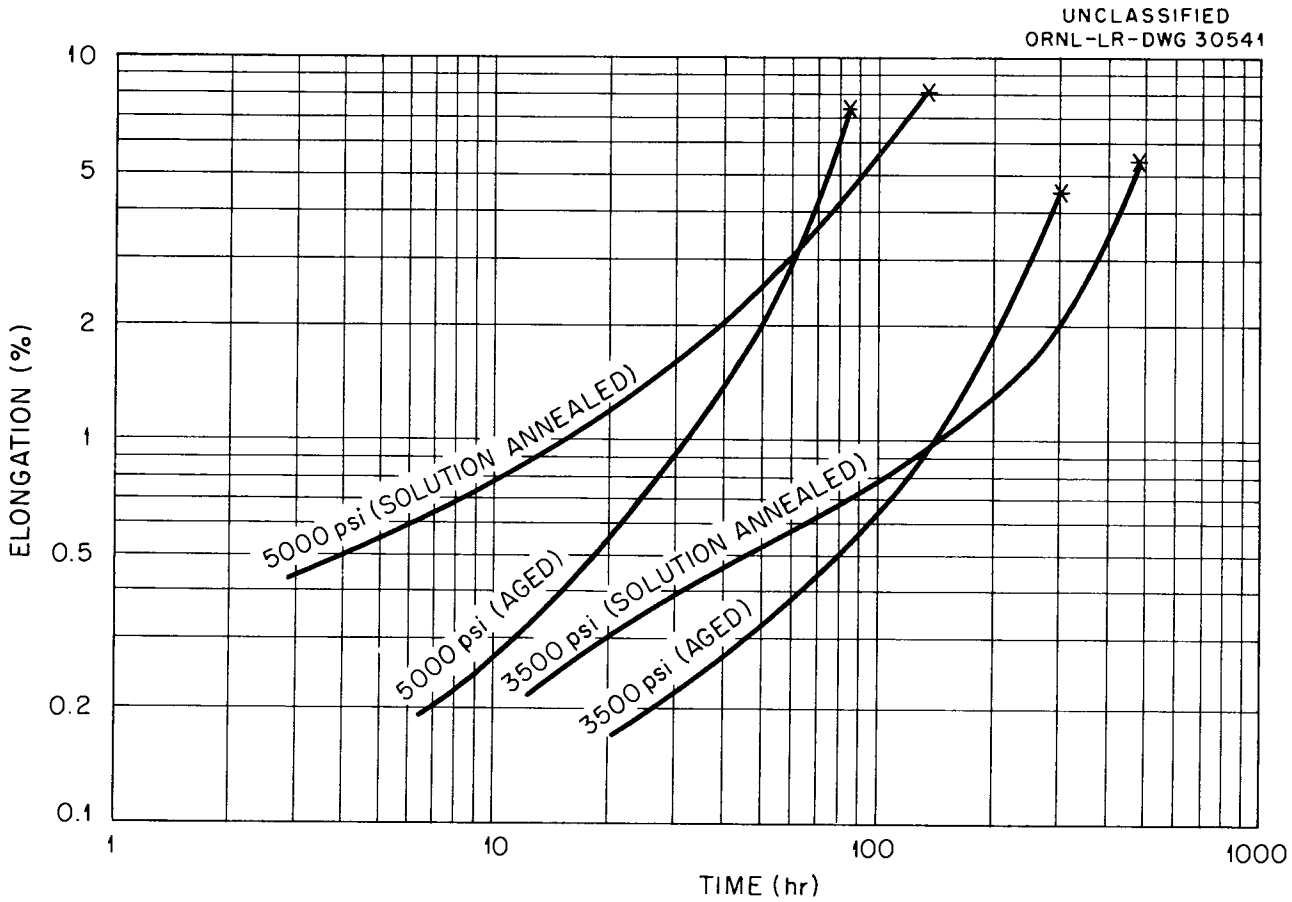

Fig. 60. Creep–Rupture Curves of Solution–Annealed and Aged Hastelloy B Sheet Tested in Argon at 1800°F. Aging Time 100 hrs at 1300°F.

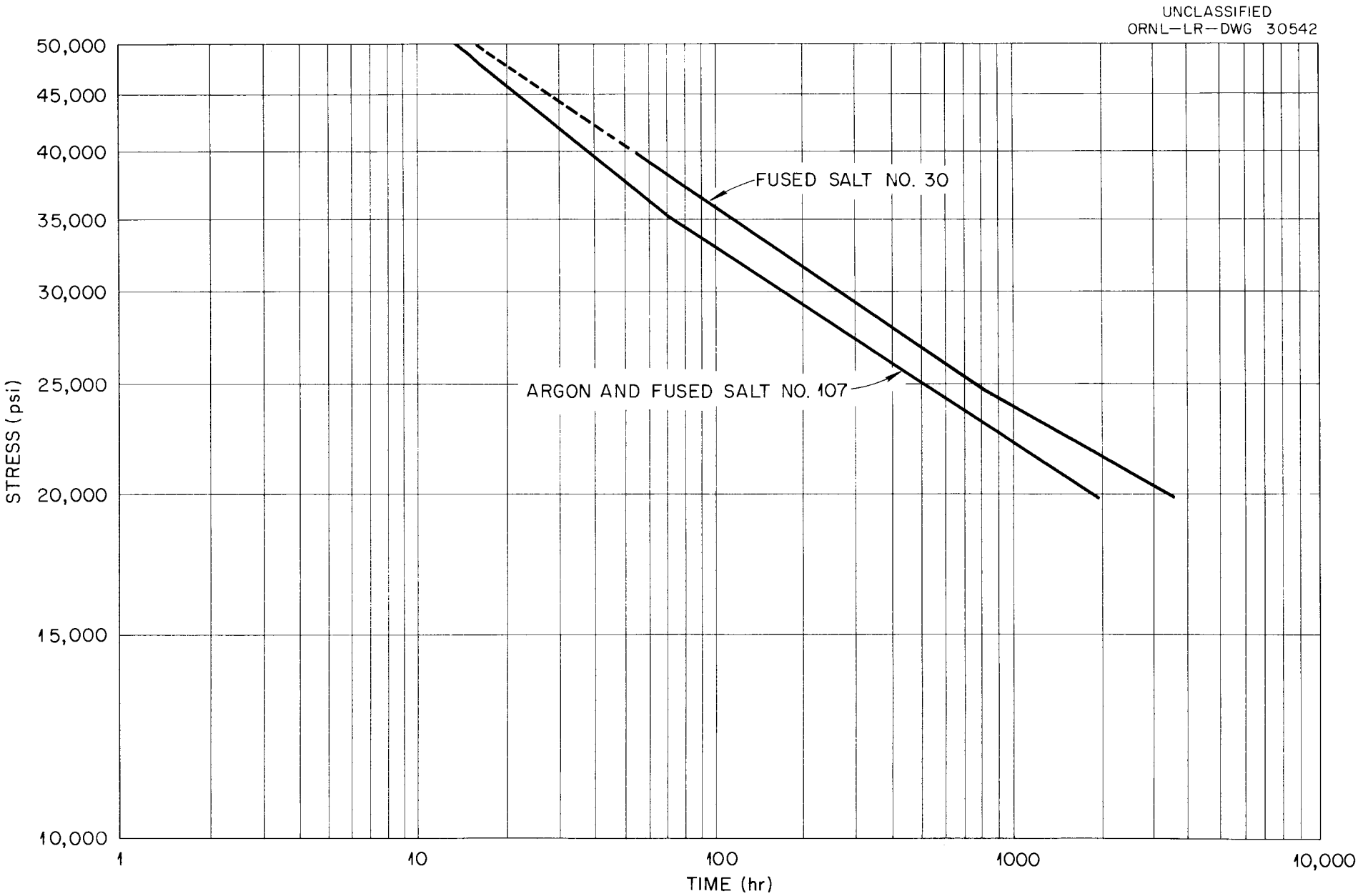

Fig. 61. Stress-Rupture Curves of Solution-Annealed Hastelloy B Sheet Tested in Various Environments at 1300°F.

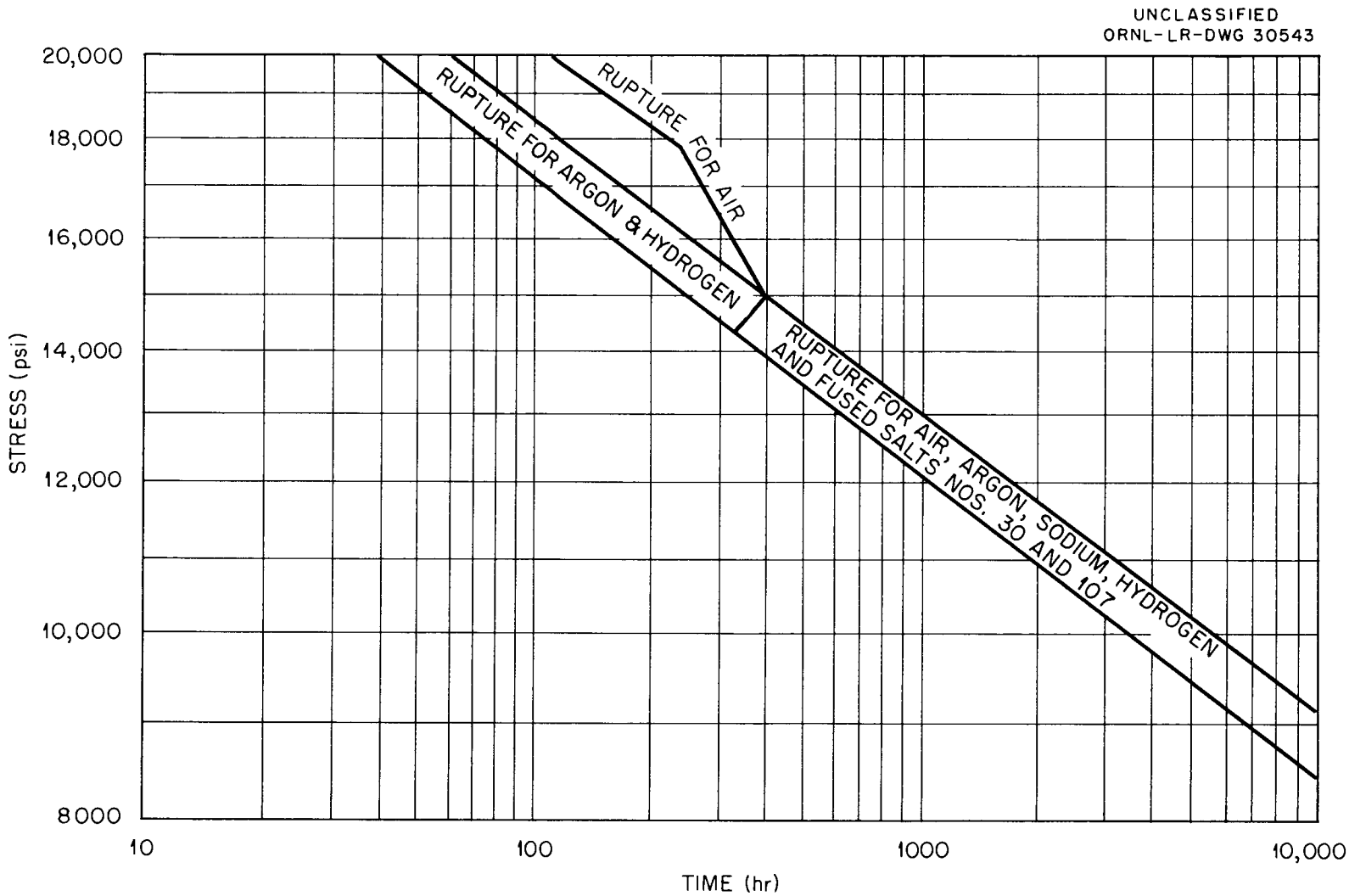

Fig. 62. Stress-Rupture Curves of Solution-Annealed Hastelloy B Sheet Tested in Various Environments at 1500°F.

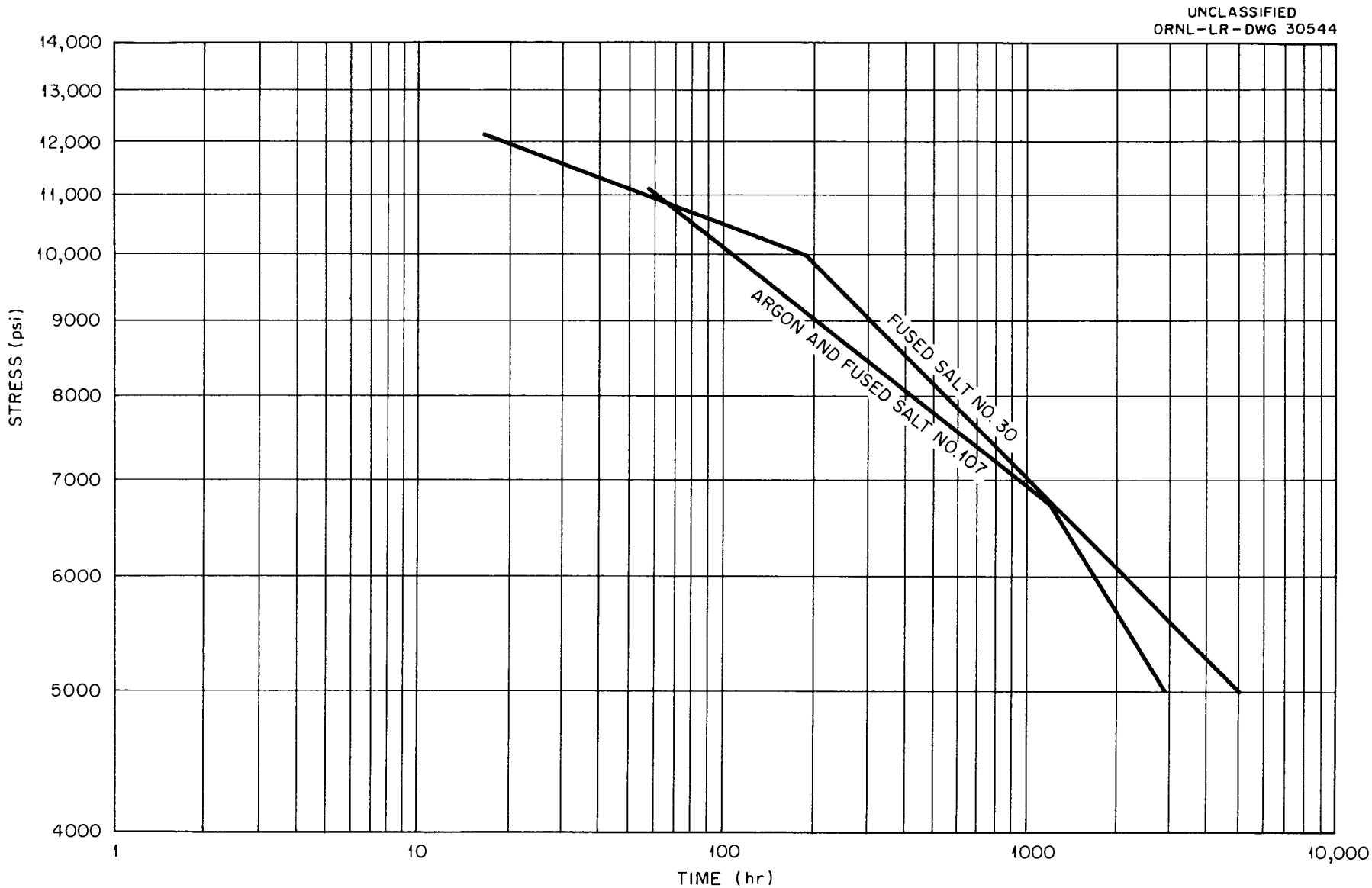

Fig. 63. Stress-Rupture Curves of Solution-Annealed Hastelloy B Sheet Tested in Various Environments at 1650°F.

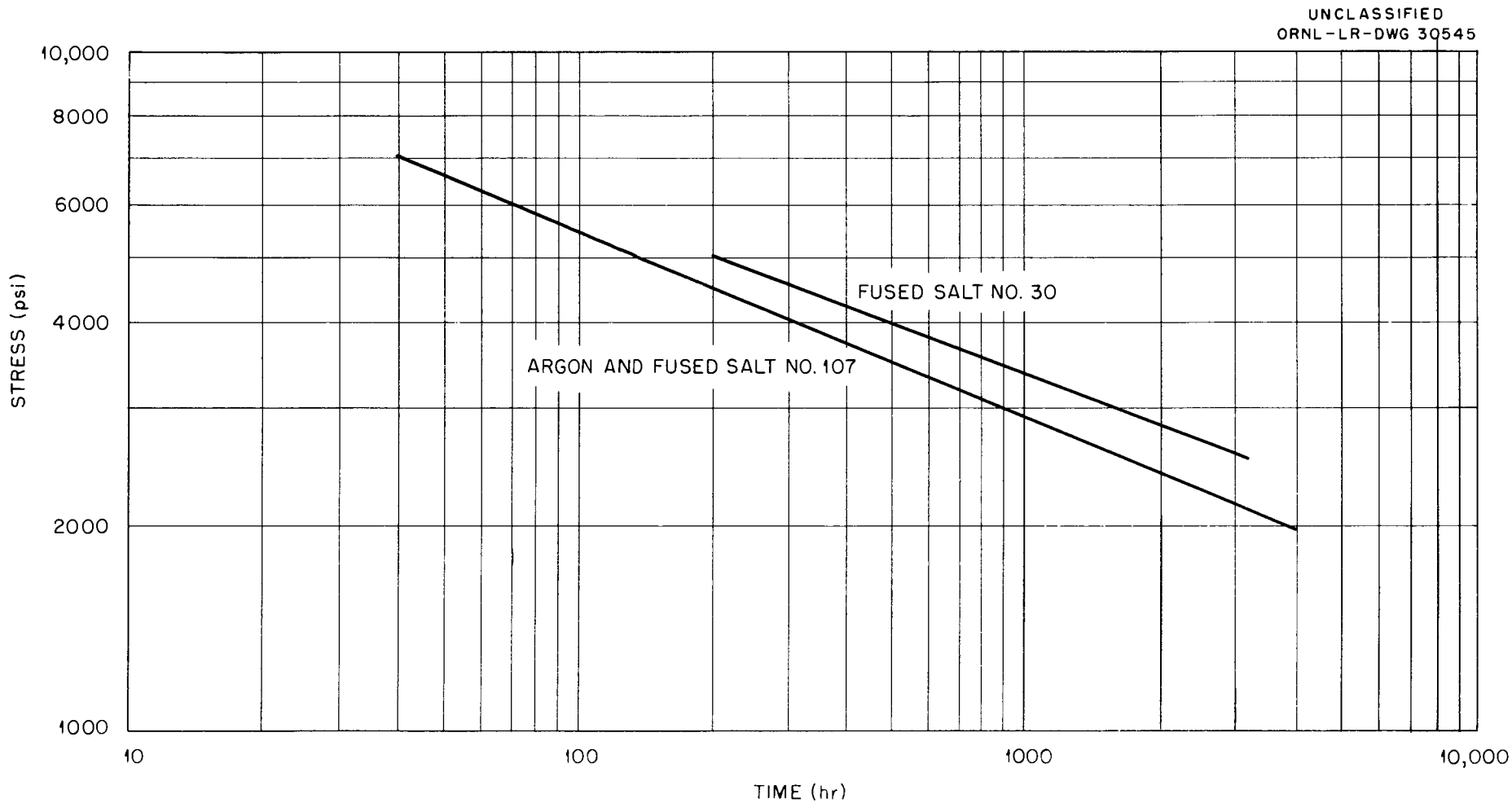

Fig. 64. Stress-Rupture Curves of Solution-Annealed Hastelloy B Sheet Tested in Various Environments at 1800°F.

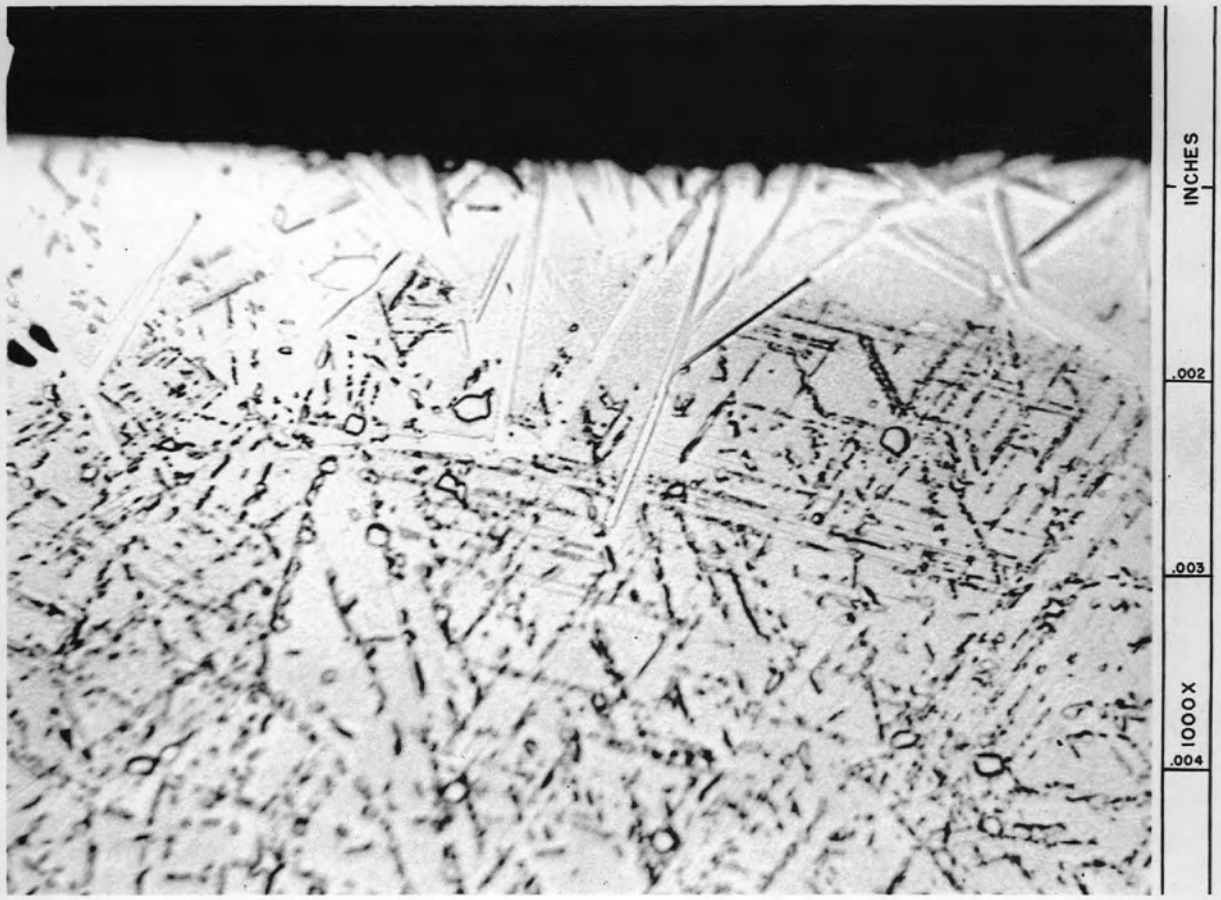

Fig. 65 (Y-18417) Surface Effect of the Stressed Portion of a Hastelloy B Specimen after Exposure to Fused Salt No. 30 for 1700 Hr with 13,500 psi Stress at 1500°F. 1000X. Etchant: Chrome Regia.

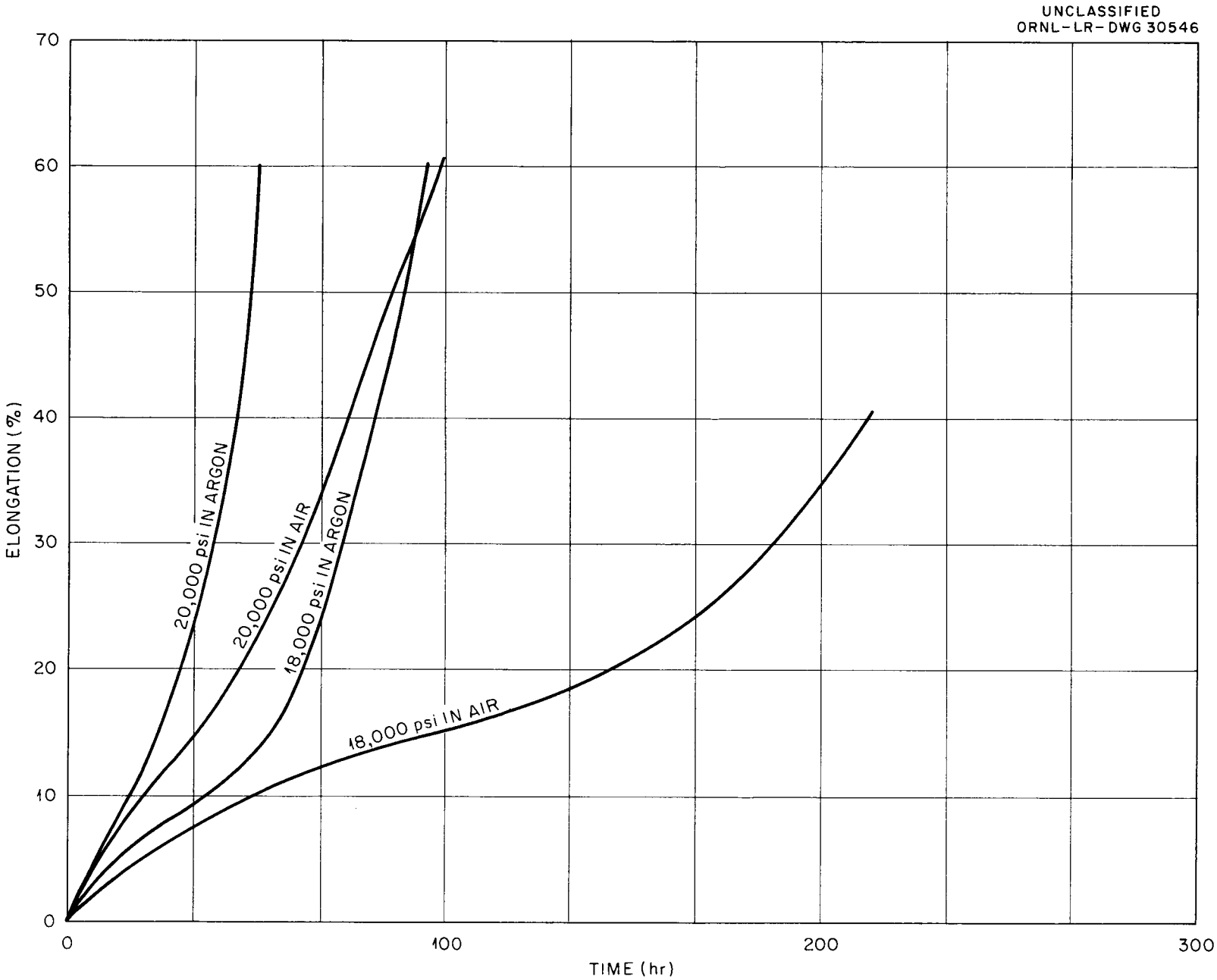

Fig. 66. Creep-Rupture Curves of Solution-Annealed Hastelloy B Sheet Tested in Argon and Air at 1500°F.

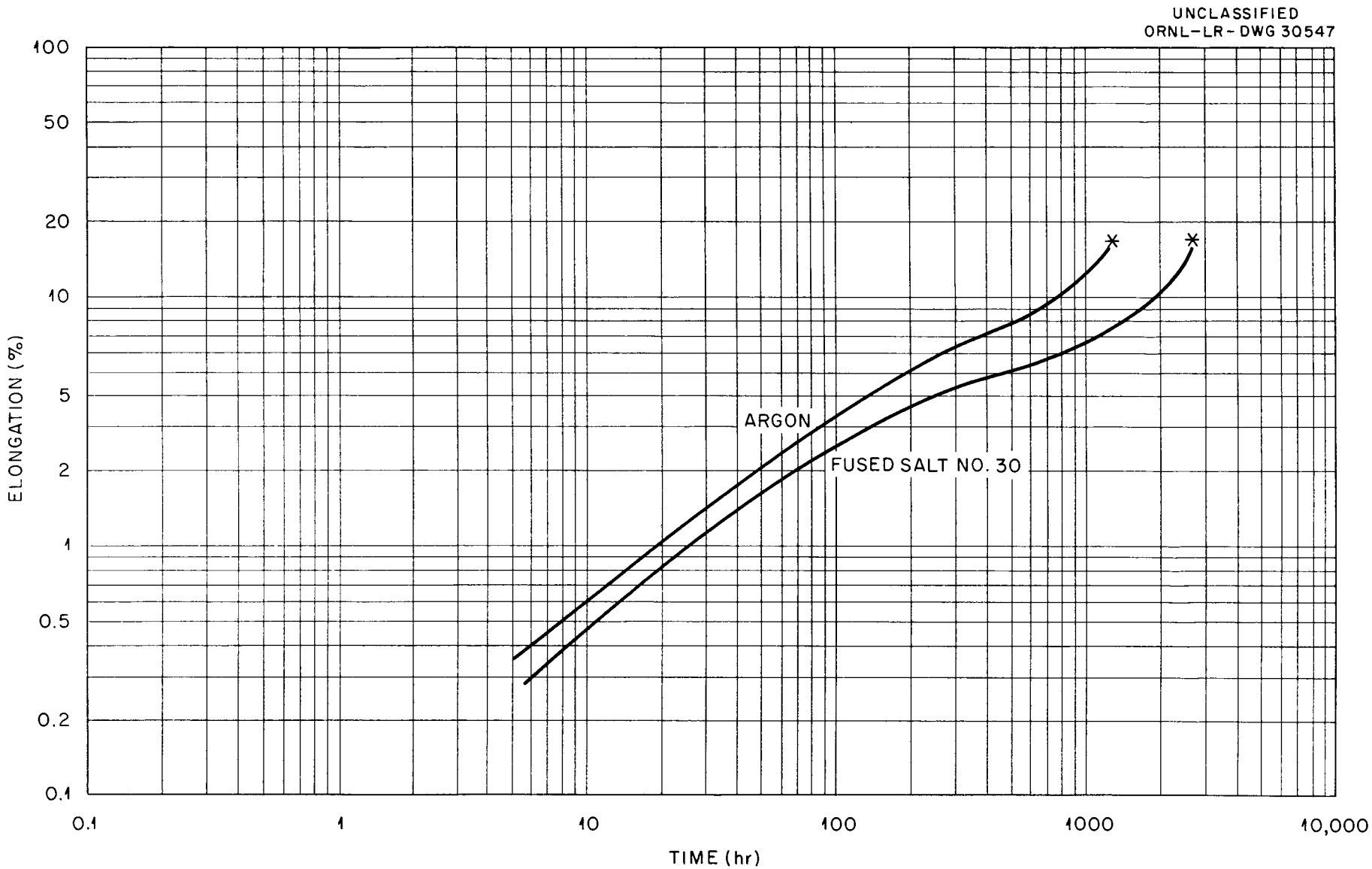

Fig. 67. Creep-Rupture Curves of Solution-Annealed Hastelloy B Sheet Tested in Argon and Fused Salt No. 30 at 1500°F and 12,000 psi.

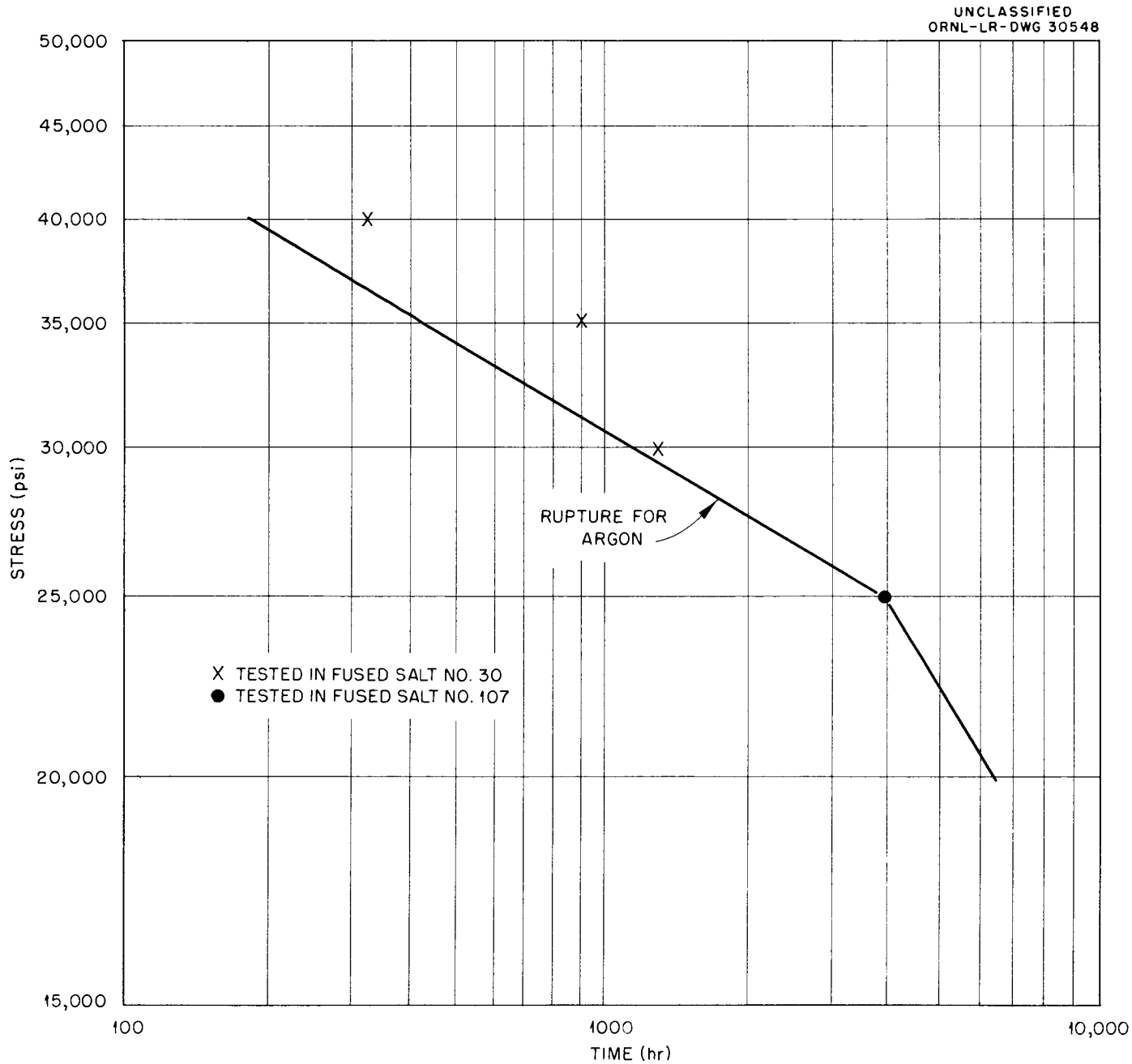

Fig. 68. Stress-Rupture Plot of Solution-Annealed Hastelloy W Sheet Tested in Various Environments at 1300°F.

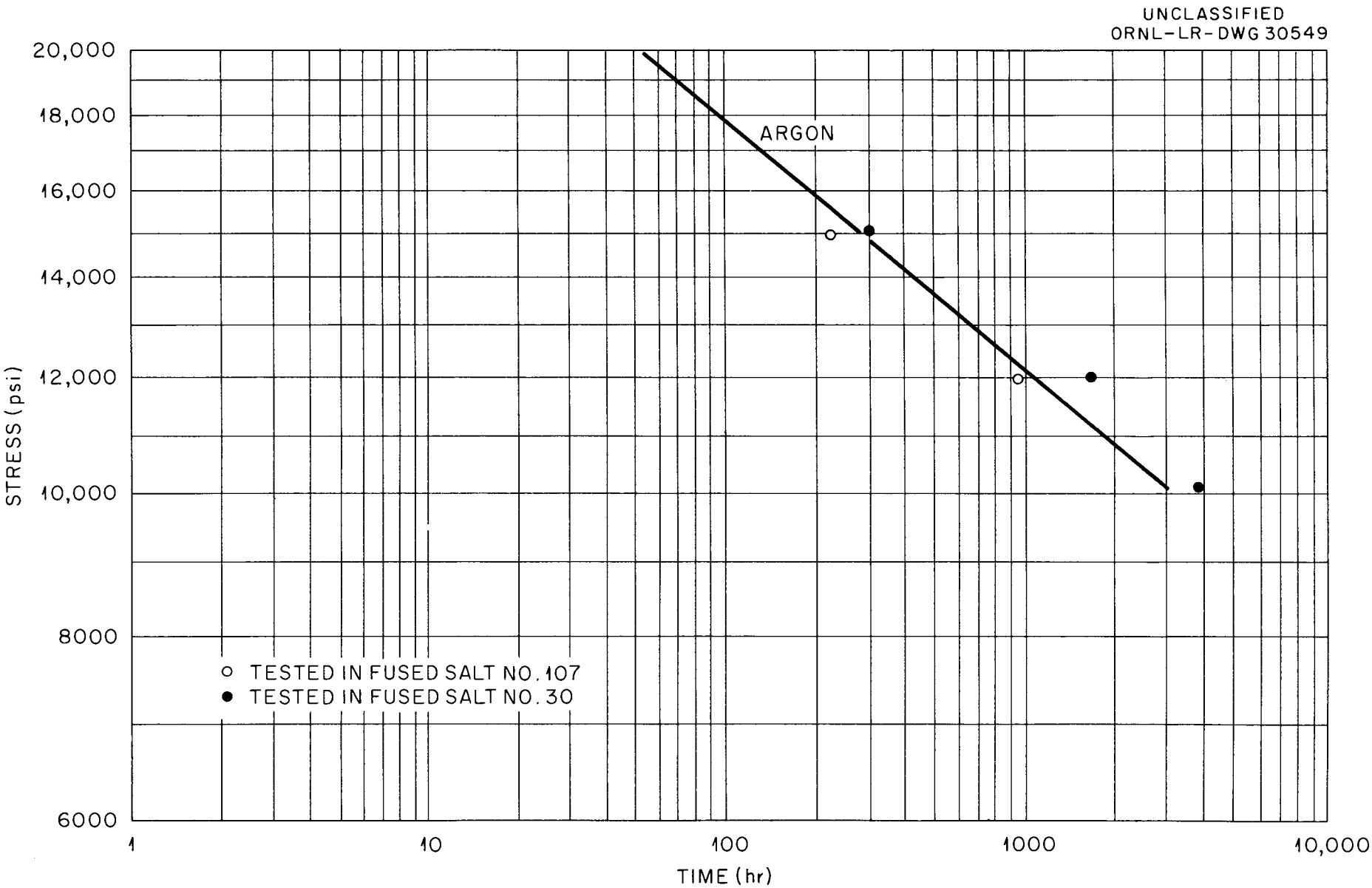

Fig. 69. Stress-Rupture Curves of Solution-Annealed Hastelloy W Sheet Tested in Various Environments at 1500°F.

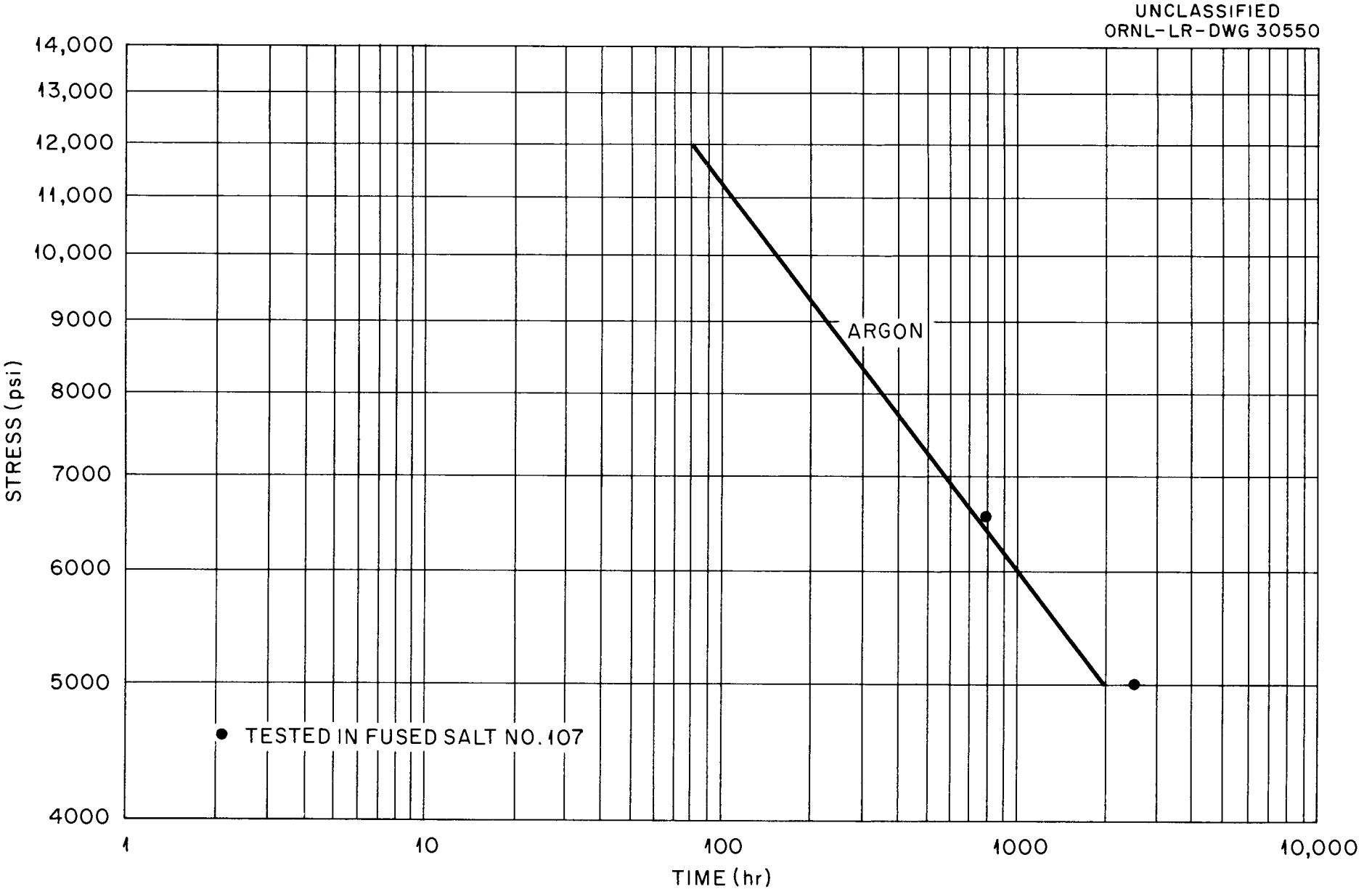

Fig. 70. Stress-Rupture Plot of Solution Annealed Hastelloy W Sheet Tested in Argon and Fused Salt No. 107 at 1650°F.

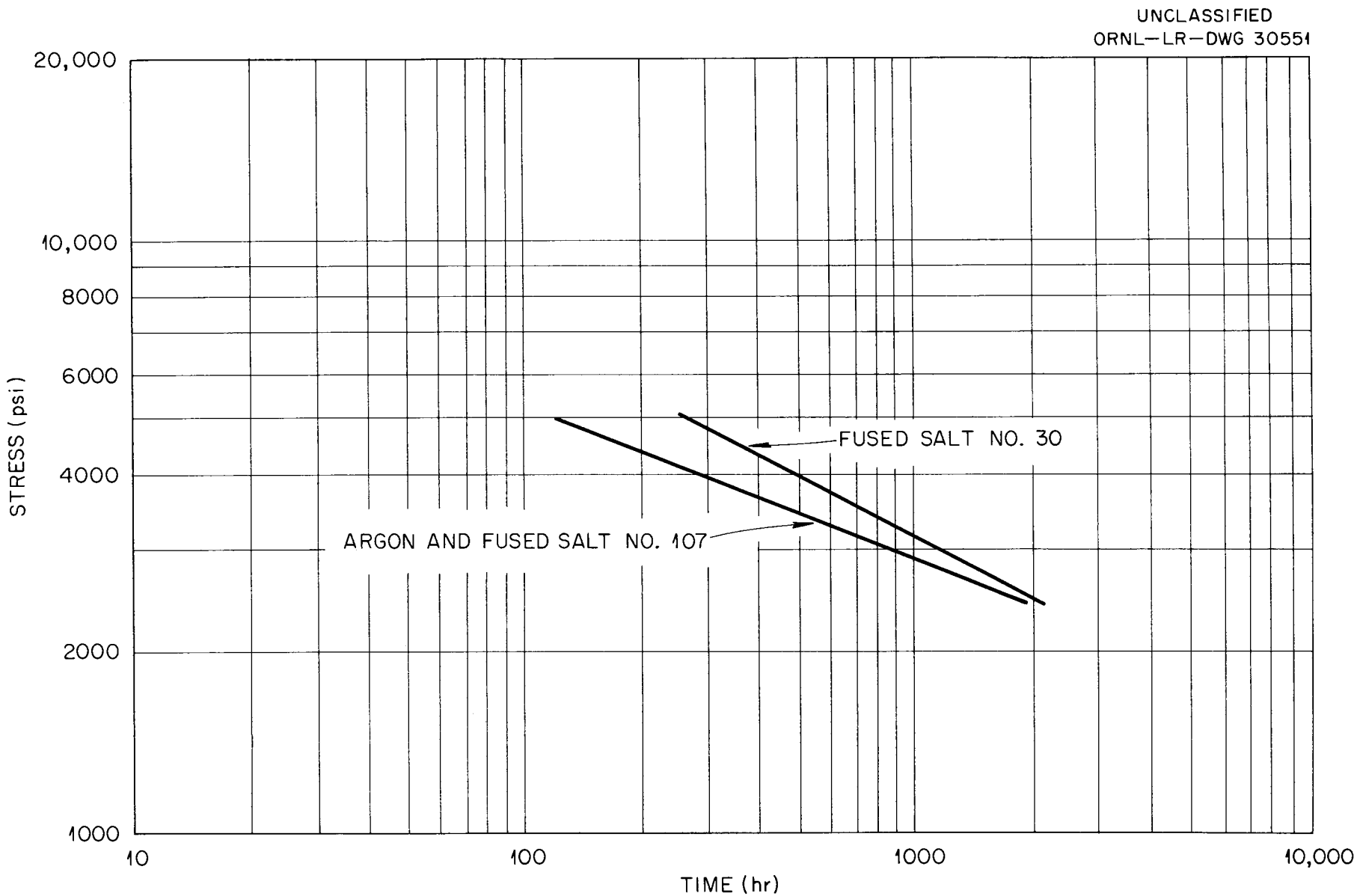

Fig. 71. Stress-Rupture Curves of Solution-Annealed Hastelloy W Sheet Tested in Various Environments at 1800°F.

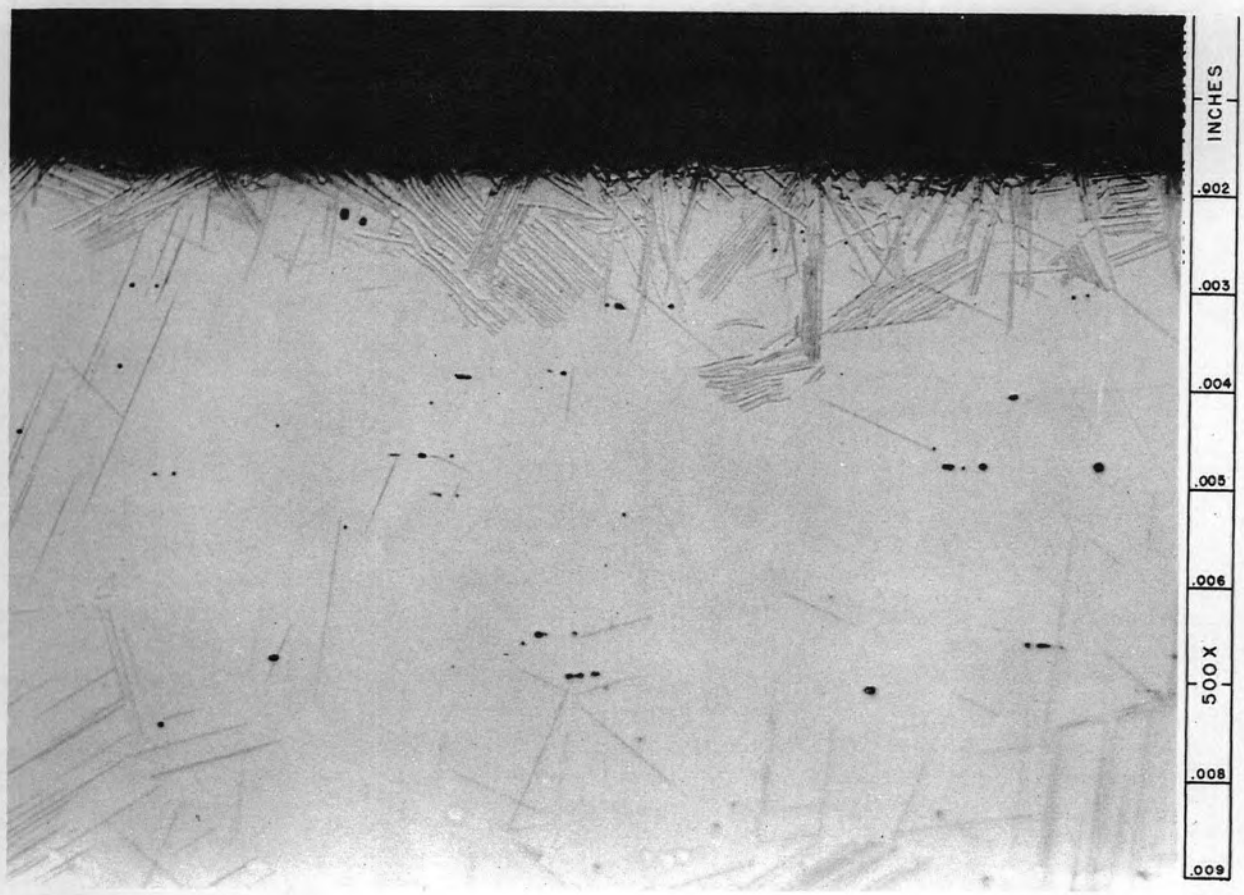

Fig. 72 (Y-18415) Surface Effect of the Unstressed Portion of a Hastelloy W Specimen after Exposure to Fused Salt No. 30 for 1,473 hr at 1300°F. 500X. Etchant: Chrome Regia.

INTERNAL DISTRIBUTION

1. C. E. Center
2. Biology Library
3. Health Physics Library
4-5. Central Research Library
6. Metallurgy Library
7. Reactor Experimental Engineering Library
8-27. Laboratory Records Department
28. Laboratory Records, ORNL R.C.
29. A. M. Weinberg
30. L. B. Emlet (K-25)
31. J. P. Murray (Y-12)
32. J. A. Swartout
33. E. D. Shipley
34. M. L. Nelson
35. W. H. Jordan
36. C. P. Keim
37. J. A. Lane
38. C. E. Winters
39. D. S. Billington
40. A. J. Miller
41. R. A. Charpie
42. M. J. Skinner
43. C. O. Smith
44. J. H. Frye, Jr.
45. W. D. Manly
46. J. E. Cunningham
47. A. P. Fraas
48. F. C. VonderLage
49. G. D. Whitman
50. J. Zasler
51. J. L. Scott
52. E. H. Taylor
53. G. M. Adamson
54. E. S. Bomar, Jr.
55. R. E. Clausing
56. J. H. Coobs
57. J. H. DeVan
58-60. D. A. Douglas
61. J. P. Hammond
62. T. Hikido
63. J. L. Gregg
64-98. M. R. Hill
99. E. E. Hoffman
100. H. Inouye
101. L. K. Jetter
102-104. C. R. Kennedy
105. C. F. Leitten, Jr.
106. C. J. McHargue
107. P. Patriarca
108. M. L. Picklesimer
109. T. K. Roche
110. G. P. Smith
111-113. R. W. Swindeman
114. A. Taboada
115. R. C. Waugh
116. J. W. Woods
117. A. L. Boch
118. W. C. Thurber
119. H. E. Seagren
120. H. G. MacPherson
121. F. J. Stanek
122. B. L. Greenstreet
123. L. A. Mann
124. M. E. Lackey
125. B. W. Kinyon
126. W. R. Gall
127. W. F. Boudreau
128. M. Bender
129. M. M. Yarosh
130-132. H. E. McCoy
133. J. H. Koenig (consultant)
134. H. Leidheiser, Jr. (consultant)
135. C. S. Smith (consultant)
136. H. A. Wilhelm (consultant)
137. ORNL - Y-12 Technical Library, Document Reference Section

EXTERNAL DISTRIBUTION

138. Division of Research and Development, AEC, ORO
139-140. University of Tennessee (W. O. Harms and R. L. Maxwell)
141-142. AEC Reactors Branch, Washington (M. J. Whitman and J. M. Simmons)
143-701. Given distribution as shown in TID-4500 (14th ed.) under Metallurgy and Ceramics category (75 copies - OTS)